CHALMERS
UNIVERSITY OF TECHNOLOGY

Upgrading of triglycerides, pyrolysis oil, and lignin over metal sulfide catalysts: A review on the reaction mechanism, kinetics, and catalyst

Downloaded from: https://research.chalmers.se, 2025-07-01 18:38 UTC

Citation for the original published paper (version of record):
Cheah, Y., Salam, M., Sebastian, J. et al (2023). Upgrading of triglycerides, pyrolysis oil, and lignin over metal sulfide catalysts: A review on
the reaction mechanism, kinetics, and catalyst deactivation. Journal of Environmental Chemical Engineering, 11(3). http://dx.doi.org/10.1016/j.jece.2023.109614

N.B. When citing this work, cite the original published paper.

research.chalmers.se offers the possibility of retrieving research publications produced at Chalmers University of Technology. It covers all kind of research output: articles, dissertations, conference papers, reports etc. since 2004. research.chalmers.se is administrated and maintained by Chalmers Library

(article starts on next page)

Journal of Environmental Chemical Engineering 11 (2023) 109614

Contents lists available at ScienceDirect

Journal of Environmental Chemical Engineering

journal homepage: www.elsevier.com/locate/jece

Upgrading of triglycerides, pyrolysis oil, and lignin over metal sulfide catalysts: A review on the reaction mechanism, kinetics, and catalyst deactivation

You Wayne Cheah [a,1], Muhammad Abdus Salam [a,1], Joby Sebastian [a], Sreetama Ghosh [a], Prakhar Arora [b], Olov Öhrman [b], Louise Olsson [a,*], Derek Creaser [a,*]

[a] Department of Chemical Engineering, Competence Centre for Catalysis, Chalmers University of Technology, SE-412 96 Gothenburg, Sweden
[b] Preem AB, Sweden

ARTICLE INFO

Keywords:
Sulfided catalysts
Hydrotreated vegetable oil (HVO)
Triglycerides
Pyrolysis oil
Lignin
Reaction kinetics
Catalysts deactivation

ABSTRACT

Human activities such as burning fossil fuels for energy production have contributed to the rising global atmospheric CO_2 concentration. The search for alternative renewable and sustainable energy sources to replace fossil fuels is crucial to meet the global energy demand. Bio-feedstocks are abundant, carbon-rich, and renewable bioresources that can be transformed into value-added chemicals, biofuels, and biomaterials. The conversion of solid biomass into liquid fuel and their further hydroprocessing over solid catalysts has gained vast interest in industry and academic research in the last few decades. Metal sulfide catalysts, a common type of catalyst being used in the hydroprocessing of fossil feedstocks, have gained great interest due to their low cost, industrial relevance, and easy implementation into the current refining infrastructures. In this review, we aim to provide a comprehensive overview that covers the hydrotreating of various bio-feedstocks like fatty acids, phenolic compounds, pyrolysis oil, and lignin feed using sulfided catalysts. The main objectives are to highlight the reaction mechanism/networks, types of sulfided catalysts, catalyst deactivation, and reaction kinetics involved in the hydrotreating of various viable renewable feedstocks to biofuels. The computational approaches to understand the application of metal sulfides in deoxygenation are also presented. The challenges and needs for future research related to the valorization of different bio-feedstocks into liquid fuels, employing sulfided catalysts, are also discussed in the current work.

1. Introduction

The global climate is facing two main challenges: first, the increased energy demand due to the growing world population, and second, growing anthropogenic CO_2 emissions due to the use of non-renewable fossil fuels in major economic sectors. Ambitious targets like limiting the rise of global temperature to stay below 2 °C in the Paris Agreement and achieving net-zero CO_2 emissions by 2050 in the European Green Deal will drive the current energy transition towards a low or neutral renewable carbon energy system. In line with this, the United Nations (UN) Sustainability Development Goals (SDGs) adopted by all UN members also provided a blueprint to tackle detrimental climate change and achieve a better sustainable society for all. Thus, the use of renewable energy in tackling climate change is inevitable. Renewable liquid biofuels fall under this category and provide an immediate solution for sectors like transportation.

Biomass feedstock can be divided into three main categories: (1) sugar-based feedstocks such as sugar beet, sugar cane, and corn, (2) triglyceride feedstocks like animal fats, vegetable oil, and waste cooking oil, and (3) lignocellulosic feedstocks like wood and forestry residues, bagasse, grass, and leaves. The types of biofuels depend largely on the biomass source. Renewable liquid fuels, also known as advanced biofuels, produced from the non-crop and waste-based bio-feedstocks, represent an excellent option as an alternative fuel and also serve the role of bridging the transition period for existing conventional combustion engine-based fleets. For instance, hydroprocessed esters and fatty acids (HEFA) as hydrotreated vegetable oils (HVO), are the only drop-in biofuels that are commercially produced in refineries. Several

* Corresponding authors.
E-mail addresses: louise.olsson@chalmers.se (L. Olsson), derek.creaser@chalmers.se (D. Creaser).
[1] Both authors contributed equally to the manuscript.

https://doi.org/10.1016/j.jece.2023.109614
Received 16 June 2022; Received in revised form 18 February 2023; Accepted 28 February 2023
Available online 3 March 2023
2213-3437/© 2023 The Author(s). Published by Elsevier Ltd. This is an open access article under the CC BY license (http://creativecommons.org/licenses/by/4.0/).

examples of such commercial technologies are NEXBTL™, Ecofining™, Vegan™, and Hydroflex which produce these advanced biofuels. Apart from these commercially available examples, the next-generation biofuels such as those derived from pyrolysis oil also possess advantages in reducing greenhouse gas (GHG) emissions and fossil fuel dependency. Pyrolysis oil can be produced using different processes, one of which is fast pyrolysis or thermal liquefaction of biomass feedstocks [1,2]. The conversion of solid biomass via a thermochemical process like fast pyrolysis results in bio-oils that can be subsequently upgraded via catalytic hydrotreating into biofuels and high-value platform chemicals. Another potential advanced feedstock like lignin can also be used to substitute fossil-based feeds. Lignin is a biopolymer consisting of phenylpropane units (coniferyl, sinapyl, and p-coumaryl alcohol) [3]. It is an important renewable carbon source and accounts for 20–30% of the major mass of lignocellulosic biomass. Due to the large utilization of cellulosic and hemicellulosic materials in the existing biorefineries, the remaining lignin fraction is considered a byproduct and is often burnt to produce heat and power for the mill. Thus, lignin can serve as a sustainable feed for liquid fuel production or value-added fine and platform chemicals.

However, there are a few common undesired properties of the bio-feedstocks such as high oxygen content depending on the biomass (Table 1) and acidic nature caused by the presence of carboxylic acids. The high oxygen content contributes to detrimental properties of bio-oils like high viscosity and low heating value as compared to fossil-derived fuels [4]. Owing to the various negative characteristics of the bio-oils from these feedstocks, it is difficult to use these bio-liquids directly as engine fuel. Therefore, a refining process is required to improve the quality of the products so that the produced liquid fuel is compatible with the existing fuel grades. This process involves conventional hydrotreating technology such as hydrodesulfurization (HDS), hydrodenitrogenation (HDN), hydrodeoxygenation (HDO), and hydrodemetallization (HDM) processes. These processes serve to remove or reduce the sulfurous, nitrogenous compounds, oxygenates, and metals from fossil feeds. Catalytic hydrodeoxygenation (HDO) has been implemented in the refineries to remove excess oxygen in the form of H_2O, CO, and CO_2 at various temperatures and pressure with hydrogen as a co-reactant. Moreover, the reaction is catalyzed by a selective hydrotreating catalyst. The key elements in such a process are the choice of catalyst material, reaction conditions, type of reactors, and feedstocks that are upgraded. Over the past few decades, transition metal sulfides/noble metals and non-sulfided catalysts have been studied extensively for valorizing bio-based feedstocks (Triglycerides/Fatty acids/pyrolysis oil/ lignin-derived bio-oil, etc.). In this review, we focus on the application of metal sulfides as catalysts for advanced biofuel production.

Krauch and Pier discovered the transition metal sulfides (TMS) at the former Badische Anilin und Sodafabrik (BASF) in 1924 [8]. Their early findings showed that MoS_2 and WS_2 were effective hydrogenation catalysts, and this led to the future development of hydrotreating catalysts. The traditional industrial metal sulfides are Ni or Co-promoted Mo/W disulfides. The Ni or Co promotion in a fully sulfided catalyst gives the so-called active Ni/CoMoS phase [9]. It is postulated that the promotion weakens the Mo-S bonds via d-electron donation by Ni/Co producing a sulfur vacancy or so-called co-ordinately unsaturated sites (CUS), indicated by the green dotted oval in Fig. 1 [4,10]. In terms of deoxygenation, the electrophilicity of Mo thus attracts oxygen-bearing molecules [10,11]. On the other hand, the presence of H_2 generates metal hydrides and sulfhydryl groups that play additional roles [12]. In other words, the catalytic activity of metal sulfides is thus governed by the type and composition of sites available to the substrate molecule which can be engineered by parameters such as promoters, support, additives, and activating conditions. The morphologies of the evolved catalyst also play a dominant role in determining the activity of the catalysts [13]. These Ni or Co-promoted MoS_2 catalysts are depleted of sulfur during oxygen removal from bio-oils and require constant addition of sulfur sources like DMDS or H_2S to maintain them in their active sulfide state [14]. Due to this fact, these sulfided catalyst systems are criticized in literature since they nullify the advantage of bio-oils which inherently contain no or low sulfur [15]. However, these sulfided catalysts have excellent hydrotreating selectivity and are low cost which makes them viable for commercial refinery operations. Metal sulfide catalysts will continue to have a significant role in the refining industries owing to the versatility of this type of catalytic material and also the transition toward cleaner and sustainable fuel production. This can be evident from the scientific publications regarding HDO which have increased by 10-fold since 2010 because of the escalating need for alternative sources of energy and also the increasing application of sulfided catalysts in deoxygenation applications (Fig. 2). Existing review articles related to the application of sulfided catalysts focused on the understanding of the fundamental principles of the materials [16], and their applications in electrocatalysis [17,18], photocatalysis [18], and as supercapacitors [19].

Although there are various reviews in the last decade focused on the upgrading of renewable feedstocks in the form of model compounds and/or real feedstocks over various types of catalysts (see Table 2); a comprehensive review solely dedicated to sulfided catalysts is still lacking. Given the significance of hydrotreating catalysts in the emerging field of advanced biofuel production, a comprehensive review of the use of sulfided catalysts for biomass conversion is needed. In this work, we have reviewed the catalytic upgrading of different important bio-feedstocks such as triglycerides, monomeric and dimeric phenolic compounds that are present in pyrolysis oil, biomass-derived pyrolysis oil, woody feedstocks, and waste lignin using metal sulfide catalysts. The reaction routes of the biomass-derived feed during the hydrotreatment have been emphasized. Furthermore, kinetics studies of upgrading the various feedstocks using sulfided catalysts and also the deactivation of catalysts are highlighted. Insights of the deoxygenation reaction and deactivation mode over metal sulfides from theoretical studies and computational approaches are also presented. Finally, the challenges and future possible research related to the valorization of different bio-feedstocks into liquid fuels employing the sulfided catalysts, and hurdles utilizing bio-feeds in the industry are also discussed in the current work.

Table 1
Elemental composition in wt% of different bio-feedstocks.

	Triglycerides/fatty acids/waste cooking oil [5]	Phenolics from pyrolysis [6]	Kraft lignin [7]
Carbon	75.6	39.2	62.1
Oxygen	9.8	52.82	29.5
Hydrogen	13.3	7.88	5.8
Sulfur	0.09	0.0081	2.2
Nitrogen	0.12	< 0.15	0.4

2. Hydrodeoxygenation (HDO) of natural triglyceride-based and vegetable oil-like feedstocks

Out of all advanced biofuel technologies like – Hydrotreated Vegetable Oil (HVO), fast pyrolysis, catalytic pyrolysis, hydro pyrolysis, lignin depolymerization, and hydrothermal liquefaction (HTL), it is only HVO process that has been commercialized so far. There are already several companies like Neste, Preem, Diamond diesel, REG producing HVO biofuels at a commercial scale. The only other biofuel process which is close to commercialization is fast pyrolysis bio-oil (FPBO), where commercial fluid catalytic cracking (FCC) trials of FPBO are underway [45].

HEFA/HVO (Hydroprocessed Esters and Fatty Acids) fuels are compatible with fossil-based diesel fuels due to their chemical resemblance. As a result, existing refinery facilities, and infrastructure can be used for production, transportation, and distribution for further use. Fig. 3 shows a parametric comparison between ultra-low sulfur diesel and HVO/HEFA fuels. Thus, standalone, or blended forms of HVO/HEFA

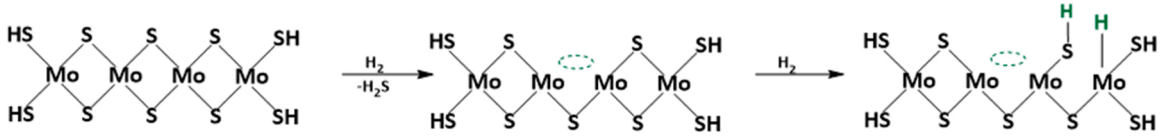

Fig. 1. Sulfur vacancy, metal hydrides, and sulfhydryl group.

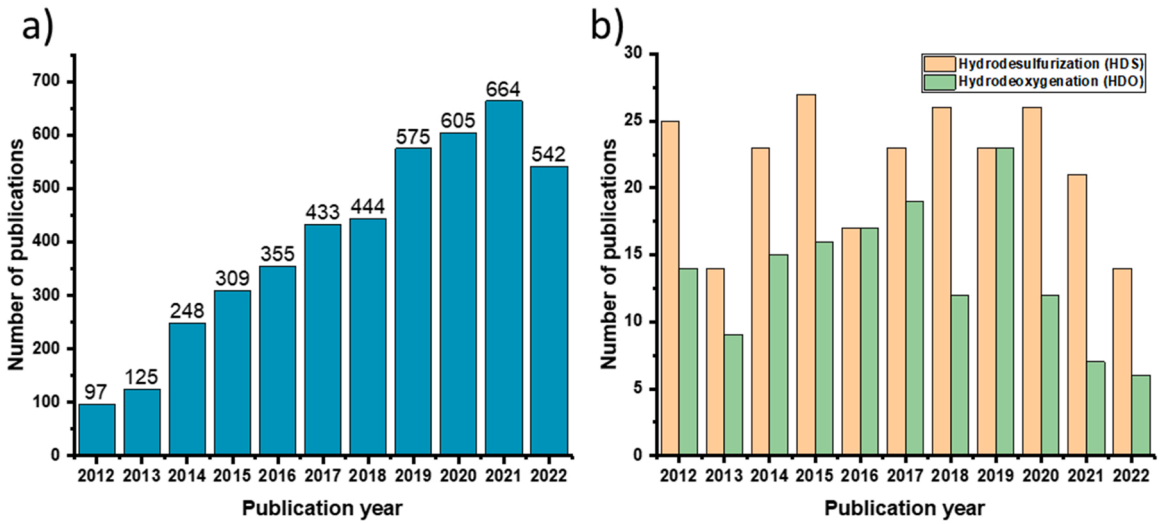

Fig. 2. The publications related to a) hydrodeoxygenation (HDO) and b) the use of sulfided catalysts for hydrodesulfurization (HDS) and HDO in the past decades. Data
Source: Web of Science (19 December 2022).

fuels contribute toward a significant reduction of GHG and particulate matter emissions. As a result, tremendous research focus has been devoted to understanding the mechanistic insights in the core upgrading process, HDO. Such renewables can be obtained from variable feedstocks like animal fat, waste cooking/vegetable oil, and tall oil from wood and forest biorefinering. It is expected that refineries will face scarcity of these feedstocks in the next few years as the demand for sustainable fuels from the heavy transport and aviation sectors accelerates. Thus, more research and technology developments are needed in pretreatment methods for low-value, ubiquitous, and high-contamination feedstocks such that they can be hydroprocessed in the refinery.

However, the turnover time of a hydrotreater is much shorter when renewable oils like used cooking oil, waste animal fat, tall oil, etc. are processed compared to a hydrotreater processing fossil feeds like vacuum gas oil (VGO), etc. There are three main reasons for the shorter lifetime of catalysts in hydrotreater processing HVO feedstocks. Firstly, since the oxygen content of renewable oils is higher than sulfur in VGO, larger quantities of hydrogen are required to remove oxygen as H_2O. The second reason is that hydrodeoxygenation reactions are more exothermic compared to hydrodesulfurization reactions as can be observed from the differences in the enthalpy of formation of $H_2O(g)$ and $H_2S(g)$ respectively (−242 kJ/mol vs −21 kJ/mol) [47]. Last but one of the most important reason which has not received enough attention in research studies is the contaminants present in renewable feeds like iron, phosphorus, alkali metals, etc. [48–50]. So these three factors – depletion of hydrogen, high temperature, and contamination, combined result in accelerated catalyst deactivation and pressure build-up [51]. In this section, we will focus on the studies that have used sulfided catalysts since they are the most industrially relevant catalysts. The literature studies can be categorized in two segments based on the feedstocks studied – Model compounds which include - Fatty acids (FAs), Fatty acids alkyl esters (FAAEs), Triglycerides (TGs), and commercial feedstocks like UCO (used cooking oils), tall oil, etc. It should be noted that the HDO reaction mechanism for fatty acids, fatty acid alkyl esters, triglycerides is quite similar. Renewable oils like UCO, tall oil, etc. primarily contain free fatty acids and triglycerides so their reaction chemistry is similar as well. Typically, fatty acid alkyl esters and triglycerides undergo hydrolysis to produce fatty acids as the common intermediate in the overall reaction scheme. Deoxygenation of fatty acids over sulfided catalysts occurs in the following three ways [48,52]:

a) A so-called direct-HDO in which oxygen is removed as a water (H_2O) molecule
b) Decarbonylation (DCO) in which oxygen is removed as carbon monoxide (CO)
c) Decarboxylation (DCO_2) in which oxygen is removed as carbon dioxide (CO_2)

In the direct-HDO route, there is no loss of carbon as oxygen is removed in the form of a H_2O molecule while in the two latter routes, oxygen is removed in the form of CO or CO_2 such that the hydrocarbon product is formed with one less carbon.

The term decarbonation (DCOx) will be used to refer to decarbonylation and decarboxylation together, otherwise, they will be separately specified in the following sections of this review. The hydrodeoxygenation or "HDO" is a broader term to define the removal of oxygen irrespective of the three routes. However, "direct-HDO" is referred to when deoxygenation occurs while producing water as the side product [48,52].

2.1. HDO of fatty acids

The catalytic cycle for hydrodeoxygenation of fatty acid molecules (here stearic acid) over sulfided molybdenum catalysts is presented in Fig. 4 [53]. The following steps of this catalytic cycle, initiated with the creation of a sulfur vacancy have been also reported for phenol-like molecules, so this is also relevant for later sections discussing the

Table 2
Reviews from the past decade (2012–2021) on different catalyst types used for hydrotreatment of bioresources.

Year	Catalyst types	Objective and scope of the review	Ref
2012	-Microporous and mesoporous zeolites -Metal oxide catalysts -Precious metal-based catalysts -Transition metal sulfides -Noble metals -Transition metal phosphides -Transition metal nitrides and carbides -Non-precious metal catalysts	-To discuss the catalytic deoxygenation of woody biomass, herbaceous biomass, algae, and triglycerides Scope: catalytic properties, reactor configurations, and process optimization -To review the hydrodeoxygenation (HDO) of pyrolysis bio-oil model compounds Scope: reaction mechanism and catalyst deactivation	[20] [21]
2013	-Zeolite HZSM-5	-To summarize the catalytic pyrolysis and cracking of woody biomass Scope: Upgrading methods and reaction mechanisms	[22]
	-Transition metal sulfides -Noble metals -Metal carbide, nitrides, and phosphide catalysts -Bifunctional catalysts	-To discuss the hydrodeoxygenation (HDO) of biomass pyrolysis focusing on the chemistry of model compounds over different catalysts related to the reaction pathways Scope: *ex-situ* catalytic pyrolysis conditions, catalyst supports, and stability	[23]
2014	-Metal carbide, nitride, and phosphide catalysts -Mesoporous-based and noble metals catalysts	-To discuss the preparation of metal carbides, nitrides, and phosphides and their general properties -To review the application of metal carbides, nitrides, and phosphides in HDO reactions -To present the potential of mesoporous and noble metal catalysts as hydrotreating catalysts Scope: hydrotreating technology, conventional catalysts, biomass utilization	[24]
2015	-Microporous zeolite catalysts -Mesoporous catalysts -Metal-based catalyst	-To summarize the cracking and deoxygenation of pyrolysis vapors producing fuel-like components and chemicals Scope: vapor phase upgrading and catalyst deactivation	[25]
	-Fluid catalytic cracking (FCC) catalysts -Hydrocracking catalysts -Hydrotreating catalysts	-To summarize and review solid catalysts used in refineries -To discuss the catalysts used for bio-oil upgrading through FCC and hydrotreating Scope: refining catalysts and biomass conversion to liquid fuels and chemicals	[26]
2016	-Fe-based catalysts	-To summarize the use of iron-based catalysts for biomass HDO and to discuss ways to improve the activity and stability of the catalysts Scope: *in-situ* and *ex-situ* catalytic fast pyrolysis	[27]
	-Zeolites -Oxides catalysts -Sulfided catalysts -Noble metals catalysts -Transition metals catalysts	-To address the application of heterogeneous catalysts in bio-oil upgrading Scope: catalytic cracking, HDO, catalyst deactivation, and regeneration	[28]
	-Metal supported and bimetallic catalysts -Transition-metal oxides, sulfides, carbides, nitrides, and phosphides	-To summarize HDO of pyrolysis oil and model compounds Scope: deoxygenation, catalyst structure-performance relations, bifunctional effects	[29]
	-Nickel based catalysts (non-sulfide)	-To critically review the support effect, nickel loading, promoter effects of Ni-based catalysts -To study selective deoxygenation pathways of triglycerides-based feedstocks -To review catalyst preparation methods and comparison with other catalysts -To review the development of nickel phosphide, NiMo, NiW non-sulfide catalysts and also catalyst stability Scope: triglyceride-based materials upgrading via transesterification, hydrotreatment, and selective deoxygenation	[30]
	-Noble metal catalysts -Transition metal catalysts -Zeolites	-To compare the methods for biomass pyrolysis upgrading such as fast pyrolysis, bio-oils, and vapor phase deoxygenation Scope: biomass pyrolysis, reaction conditions	[31]
2017	-Molecular sieves supported noble metal and/or transition metal catalysts	-To summarize the lignin-derived phenolic compound's HDO activities and reaction pathways using noble metal and transition metal catalysts that are supported on microporous molecular sieves, mesoporous molecular sieves, and porous molecular sieves Scope: molecular sieve-supported catalysts	[32]
	-Metal/zeolite bifunctional catalysts	-To summarize the hydroprocessing of bio-oil to transportation fuels (gasoline, diesel, and jet fuel) Scope: deoxygenation, catalytic properties, model, and real bio-oil upgrading	[33]
	-Solid acid and base catalysts	-To review the esterification of bio-oils and reaction pathways for individual model compounds such as carboxylic acids, aldehydes, furans, sugars, phenolics, terpenoids, N-containing organics, and metal species Scope: acid-catalyzed esterification, acid treatment of bio-oils	[34]
	-Noble metal catalysts	-To provide a comprehensive review of the use of noble metal catalysts in the hydroprocessing of fossil and bio-feedstocks Scope: catalyst deactivation, regeneration, and use of spent catalysts, environmental and safety issues	[35]
	-Metal-supported catalysts (alkali metals, alkaline earth metals, and post-transition metals)	-To present the use of solid metal catalysts for bio-oil model compound deoxygenation Scope: catalyst properties, proper reaction conditions, deactivation and regeneration of catalysts	[36]
2018	-Zeolites	-To discuss the bio-oil production routes via the use of zeolites -To study the effect of zeolite properties, biomass particle size, and catalyst loading Scope: catalytic fast pyrolysis, lumped kinetic models, technical difficulties; and challenges	[37]
2019	-Noble and non-noble metals catalysts	-To discuss the HDO of bio-oil to biodiesel over noble metal (Rh, Pt, Pd, and Ru) and non-noble metal (Co, Fe, and Ni) catalysts Scope: catalytic properties, catalyst supports and promoters, HDO mechanism, future development	[38]

(*continued on next page*)

Table 2 (*continued*)

Year	Catalyst types	Objective and scope of the review	Ref
2020	-Noble and non-noble metals supported catalysts	-To review and provide the selectivity and major products for the noble (Pt, Pd, and Ru) and non-noble metals (Ni, Co, Mo, and other metal-based) supported catalysts applied in HDO of pyrolysis oil -Scope: hydroprocessing, model pyrolysis compounds, reaction pathways	[39]
	-ZSM-5 catalyst	-To review the shape selectivity of ZSM-5 in improving quality of fast pyrolysis bio-oil -Scope: ZSM-5 physical and chemical properties, catalyst modification, influence factors	[40]
	-Metal-modified HZSM-5 catalyst	-To review the upgrading of pyrolysis vapors to BTX (benzene, toluene, and xylene) over metal-modified HZSM-5 -Scope: influence of metals, reaction parameters	[41]
	-Sulfides, base metals (oxides), noble-metal-based catalysts, and carbides/nitrides/phosphides	-To summarize the HDO of phenolics focusing on reaction mechanism Scope: catalyst properties, design of effective HDO catalysts	[42]
2021	-Sulfides, oxides, noble metals, phosphides, and other catalysts (carbides and nitrides)	-To outline the influence of reaction parameters on the HDO process, and discuss the HDO reaction mechanism and catalyst deactivation Scope: biomass pyrolysis, hydrothermal liquefaction, hydrotreatment, model compounds	[43]
	-Carbon supported catalysts, transition metal carbide catalysts, solid acid catalysts, porous metal oxides, metal-organic framework materials, metal sulfides	-To review progress in the preparation and fabrication of porous nano catalysts for catalytic hydrogenolysis of lignin and model compounds Scope: support effects, catalyst design, catalyst stability	[44]

phenolic models. Sulfur linked to Mo reacts with hydrogen to produce H_2S and a "sulfur vacancy" is created on the MoS_2 structure. It is postulated that there is always a dynamic equilibrium of such sulfur vacancies depending on H_2/H_2S partial pressure. Then a heterolytic dissociation of the hydrogen molecule occurs such that one hydrogen atom binds to sulfur to form a sulfhydryl (-SH) group while the other hydrogen atom forms a metal hydride bond with molybdenum. The carbonyl moiety of the fatty acid molecule binds at the sulfur vacancy. Then a proton from the acidic SH group attacks the hydroxy group of the stearic acid as an example. A water molecule is removed, and the charge is transferred to the neighboring carbon. This cation species extracts a hydride from the next Mo atom. In the final step of this catalytic cycle, a hydrogen molecule reacts to yield metal hydride (Mo-H) and sulfhydryl (-SH) species and results in the conversion of stearic acid to octadecanal. The patent literature has reported the use of Ni or Co-promoted molybdenum sulfided catalysts for the deoxygenation of fatty acid-based feedstocks for more than three decades now [54].

Several studies have been explored for HDO of fatty acid to green diesel employing supported and unsupported sulfided catalysts. The sulfidation temperature influences the formation of different Mo species (Mo^{4+}, Mo^{5+}, Mo^{6+}) catalyzing deoxygenation of palmitic acid to straight-chain hydrocarbons to varying degrees over $NiMo/Al_2O_3$-TiO_2 catalyst [55]. The role of unsupported MoS_2 and Ni-promoted MoS_2 has been studied using hexadecenoic acid by Wagenhofer et al. [56]. It is concluded that fatty acid deoxygenation over MoS_2 is primarily followed via C-O hydrogenolysis to an aldehyde, hydrogenation to a primary alcohol, dehydration, and hydrogenation to corresponding alkanes (C_n pathway). On the other hand, deoxygenation over unsupported Ni promoted MoS_2 mainly proceeds through a ketene intermediate, and decarbonylation via the scission of its C-C bond to yield saturated hydrocarbons (C_{n-1} pathway) via alkene intermediates. However, keto-enol tautomerism of intermediate aldehyde has also been demonstrated for the HDO of fatty acid over supported sulfided $NiMo/Al_2O_3$ catalysts [52,57]. Ni or Co promotion to base MoS_2 typically promotes the decarbonation pathway [53]. Surfactant-modified and magnetically reusable unpromoted and Ni(Co) promoted MoS_2 over greigite (G) have been evaluated for stearic acid HDO and the deoxygenation activity was ranked in the order of NiMo/G > CoMo/G > Mo/G [58]. Interestingly, an inhibiting effect of fatty acid which preferentially occupies the active site and hinders access for the intermediate aldehydes/alcohols has also been explained via experimental and DFT studies [10,59]. Hydrogen donor solvents and acidity imparted by BEA zeolite were found to enhance the conversion/deoxygenation of stearic acid at low pressure (0.8 MPa H_2 and 350 °C) and give a high yield of alkanes (C17 being the major one) for NiMo supported over mixed oxide (γ-Al_2O_3-BEA-zeolite) [60].

2.2. HDO of fatty acid alkyl esters

Alkyl esters like – fatty acid methyl esters (FAMEs) and fatty acid ethyl esters (FAEEs) have different decomposition pathways. As shown in Fig. 5, β-elimination occurs only in FAEEs (or esters with alkyl groups >C1) to produce free fatty acids [61]. The FAEEs are expected to have a similar reaction mechanism like TGs via β-elimination. This reaction is not possible for FAME molecules due to the absence of the β hydrogen.

Another route through which such alkyl esters can produce fatty acids is hydrolysis. There is not a significant difference in the reaction mechanism for the hydrolysis of methyl and ethyl esters with a similar

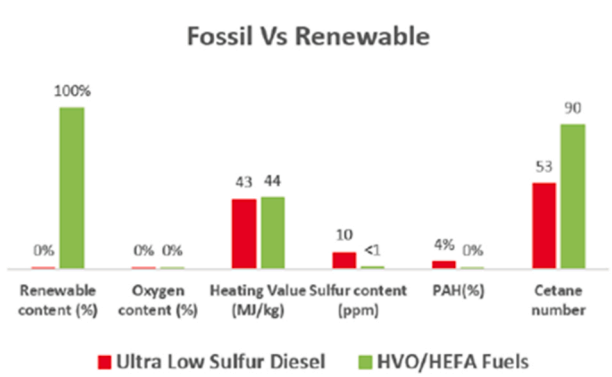

	Ultra Low Sulfur Diesel	HVO/HEFA Fuels
Renewable content (%)	0	100
Oxygen content (%)	0	0
Heating Value (MJ/kg)	43	44
Sulfur content (ppm)	10	1
Polyaromatics (%)	4	0
Cetane number	53	90
GHG emissions	Baseline	-90%
PM emissions	Baseline	-46%
Nox Emissions	Baseline	-14%
Storage stability	Baseline	Good

Fig. 3. Comparison of HVO/HEFA and conventional low-sulfur diesel fuel [46].

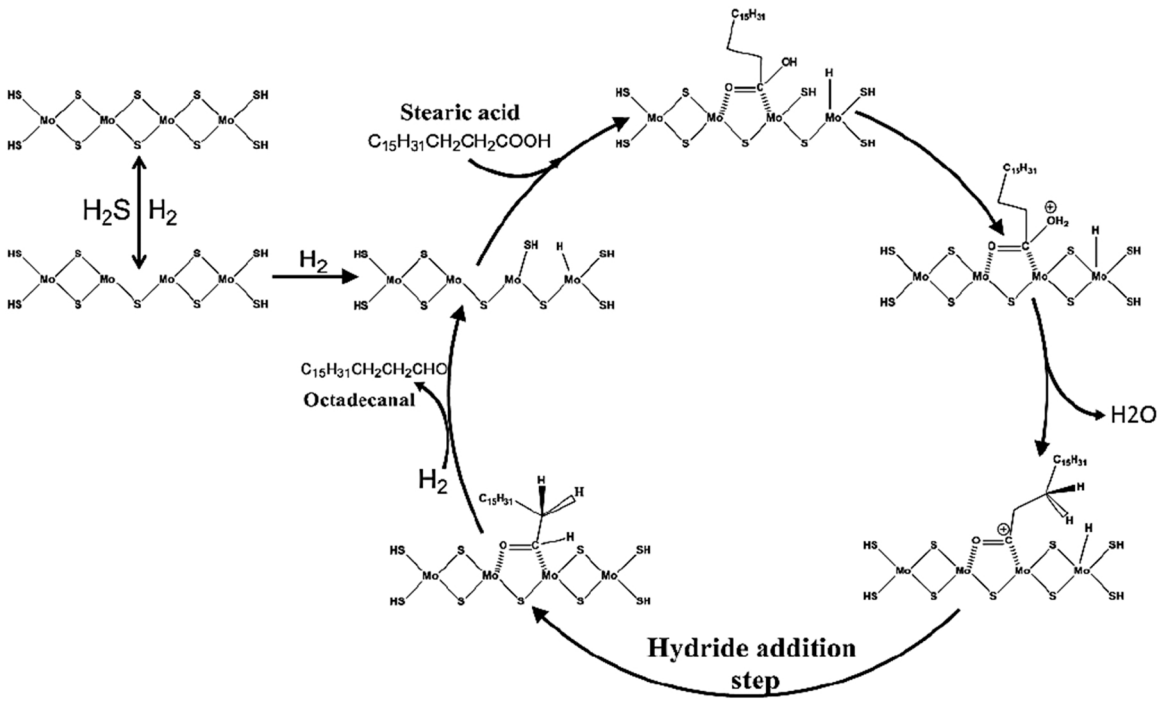

Fig. 4. Catalytic cycle for the first step of conversion of stearic acid (SA) to octadecanal (C18 =O) in the overall reaction scheme [53]. Brillouet, E. Baltag, S. Brunet, and F. Richard, Deoxygenation of decanoic acid and its main intermediates over unpromoted and promoted sulfided catalysts. Adapted from Appl. Catal. B: Environ., 148–149, (2014) 201–211, Copyright (2014), with permission from Elsevier.

yield and product distribution [62,63]. Hydrolysis requires the presence of moisture (H^+/H_2O) and the Lewis acid sites (e.g., alumina as support). HDO reactions produce water so hydrolysis of alkyl esters is quite possible in the catalyst bed. Another possible route can be the direct deoxygenation of such alkyl esters.

Laurent and Delmon tested sulfided CoMo and NiMo catalysts for hydrodeoxygenation of model compounds containing ester groups (Diethyl sebacate) [64]. During the reaction, a group of products has been identified demonstrating that the major pathways for deoxygenation are hydrogenation and decarboxylation. De-esterification to carboxylic acid occurs to a limited degree. The activation energy for the hydrogenation reaction was found lower for NiMo than CoMo catalysts while no appreciable differences in the decarboxylation activation energy were discerned although a higher decarboxylation degree was observed for NiMo catalysts.

Krause and coworkers [65,66] explored HDO activities of methyl esters (methyl heptanoate and methyl hexanoate) in flow and batch reactors over sulfided NiMo/γ-Al_2O_3 and CoMo/γ-Al_2O_3. Methyl ester conversion was found higher over NiMo/γ-Al_2O_3 and the formation of the corresponding deoxygenated products (n-heptane/heptenes and n-hexane/hexenes etc.) required more hydrogen than that with CoMo/γ-Al_2O_3. Analysis of the reaction products revealed that primary

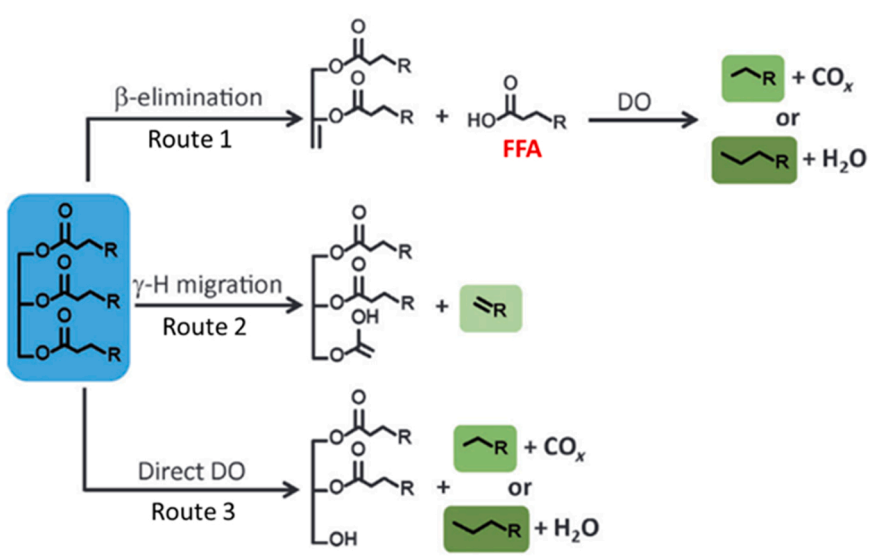

Fig. 5. β-elimination, γ-H migration, and direct HDO routes for alkyl esters [61]. Copyright (2013) Wiley, used with permission from R. W. Gosselink, S. A. W. Hollak, S. W. Chang, J. Haveren, K. P. de Jong, J. H. Bitter, and D. S. van Es, Reaction Pathways for the Deoxygenation of Vegetable Oils and Related Model Compounds, ChemSusChem, 2013, 6, 1576–1594, Wiley.

alcohols are produced from the methyl ester via hydrogenolysis of the C-O, σ-bond of the carboxyl group which upon dehydration yields alkenes, and further hydrogenation forms the n-alkanes. A second path proposed is the de-esterification to carboxylic acid and methanol which takes water from the alcohol dehydration reaction. The carboxylic acid can either further be reduced to alcohol under the reaction conditions or can be decarboxylated to alkenes. A third path can be direct decarboxylation of esters to one carbon atom with fewer product hexenes/-pentenes with additional methane/carbon dioxide as shown in Fig. 6.

Coumans et al. [52,67] investigated HDO of methyl oleate using sulfided NiMo over a few supports (γ-Al_2O_3, activated carbon, SiO_2, and SiO_2-Al_2O_3) in a fixed bed reactor under trickle flow conditions at 260 °C, 30 or 60 bar and WHSV of 6.5 h^{-1}. Hydrogenation of the double bond in methyl oleate produces predominantly methyl stearate during the early stage (~10 min) of the reaction. Besides, oleic acid and stearic acid are also observed in the reaction mixture. Initial hydrolysis of methyl oleate to oleic acid was found higher over NiMo/Al_2O_3, and NiMo/Al_2O_3-SiO_2 catalysts than others due to the presence of surface Al^{3+} which acts as Lewis sites as mentioned earlier. Blockage of such sites by carbonaceous deposits deactivates Al-containing catalysts while others show stable deoxygenation activity. High hydrolysis, high stability (168 h on stream), and selectivity to C18 hydrocarbons over NiMo/C were attributed to the activity of evolved metal sulfides and/or to surface acidic moieties.

2.3. Decomposition mechanisms of triglycerides

Triglycerides have the following three main decomposition pathways: Route 1: β-elimination; Route 2: γ-hydrogen migration; and Route 3: Direct deoxygenation (DO), as shown in Fig. 5. In Route 1, the removal of hydrogen at the β position and then hydrogenation occur alternatively in a stepwise manner from triglyceride to diglyceride to monoglyceride to glycerol, with the potential to release three free fatty acid molecules per triglyceride molecule. Also, most of the studies report the evolution of fatty acids during the deoxygenation of triglycerides [61]. However, the subsequent β-elimination of di-fatty acid ester is not possible without hydrogen and active sites. γ-hydrogen migration (Route 2) is reported to occur only at a higher temperature of 450 °C, so it is not likely at the typical HDO reaction conditions. Route 3 of direct deoxygenation (DO) occurs only in the presence of a highly active NiMo catalyst [61]. So it could be concluded that the triglycerides-based renewable feeds can yield fatty acids only through Route 1. Indeed, facile hydrolysis of a triglyceride molecule (triolein, glyceryl tioleate) to fatty acid intermediates has been demonstrated over sulfided NiMo/Al_2O_3 through route 1 [52].

2.4. HDO of commercial feedstocks (used cooking oil, tall oil, etc)

As mentioned earlier, oxygen from feedstocks like triglycerides, and fatty acids/alcohols are eliminated via water and carbon oxides as deoxygenation proceeds and yields hydrocarbons as mainly n-alkanes in the diesel range with high cetane values. Table 3 presents the state-of-the-art of sulfided catalysts for HDO of triglyceride-based feedstocks like waste vegetable/cooking oil and tall oil that have been studied exclusively via the catalytic HDO process. Kubička and co-workers investigated the deoxygenation of rapeseed oil over sulfided Ni, Mo, and NiMo over Al_2O_3 in a fixed bed flow reactor [68–71]. Bimetallic NiMo yields a higher amount of hydrocarbon than the monometallic catalysts for a given conversion. Ni and Mo-containing catalysts promote decarboxylation and direct-HDO respectively. Fatty acids are the only intermediates over Ni/Al_2O_3, thus no fatty esters form, while over Mo and NiMo containing catalysts fatty alcohol and fatty ester formation proceeds due to the rapid disappearance of fatty acids. Esterification of fatty alcohols and fatty acids was observed higher over Mo/Al_2O_3 [70]. The authors also detected that the hydrocarbon phase obtained (over 310 °C) was mostly composed of n-alkanes, n-C_{18}, n-C_{17}, and *i*-alkanes of varying amounts (based on the reaction conditions and catalyst). Such an organic liquid product is compatible with mineral diesel, thus meeting or exceeding the required quality. However, it suffered from poor low-temperature properties necessitating further processing. Furthermore, NiMo sulfides over SiO_2, TiO_2, and Al_2O_3 have been evaluated to elucidate the interaction of the active phase and support [71]. It was found that NiMoS over SiO_2 enhances hydrogenolysis of triglycerides to fatty acids at low deoxygenation degree while over TiO_2 fatty ester formation increases. As the deoxygenation progresses n-C_{17} yield increases over NiMo/SiO_2 demonstrating its preference for the decarbonation route, while the other two showed HDO preferences. Observed reactivity was thus ascribed to the differences in the support properties despite the active phase dispersion variation in the order of $SiO_2 > Al_2O_3 > TiO_2$.

M. Toba et al. [72] studied different grades of waste oils which can be converted to paraffinic hydrocarbons over NiMo/γ-Al_2O_3, CoMo/-γ-Al_2O_3, and NiW/γ-Al_2O_3. Modification of the alumina support by B_2O_3 promoted the formation of i-paraffins over the bimetallic catalysts. NiMo/B_2O_3–Al_2O_3 and NiW/Al_2O_3 showed high HDO and hydrogenation activity for a longer period (~80 h) while hydrogenation activity of CoMo/B_2O_3–Al_2O_3 decreases (approximately after 10 h on stream) resulting in high olefin formation. Compared to Mo-based catalysts, tungsten-based catalysts accelerated deoxygenation by decarboxylation/decarbonylation. H. Wang et al. [73] also investigated HDO of waste cooking oil over supported CoMoS, elucidating the deoxygenation activity, deactivation, and regeneration of the catalyst. Crude tall oil, distilled tall oil, and tall oil fatty acid (TOFA) were hydrotreated employing a commercial NiMo/γ-Al_2O_3 in a trickle-bed reactor at 5 MPa and 300–450 °C. Hydrocarbon fractions with 45 wt% paraffins were obtained at the most favorable tested conditions for crude tall oil. TOFA hydrotreating yielded more than 80% n-alkanes where the decarboxylation route was dominant over the direct-HDO route at high temperatures greater than 400 °C [74,75]. Soybean oil has been studied using sulfided NiMo/γ-Al_2O_3, and CoMo/γ-Al_2O_3 [76]. HDO yielded higher amounts of straight-chain alkanes (66%) over the NiMo catalyst than the CoMo (43%) catalyst due to isomerization and cracking enhancement in the latter. NiMoS over Mn-modified Al_2O_3 was reported to enhance triglyceride conversion and subsequent deoxygenation during the HDO of waste soybean oil [77]. Refined cottonseed oil has been hydrotreated with desulphurized petroleum diesel under refinery conditions and it

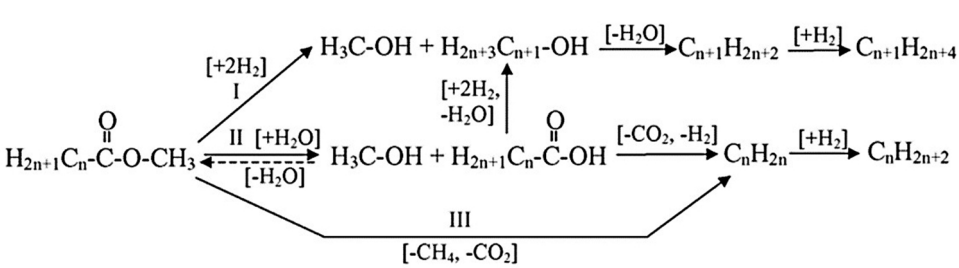

Fig. 6. HDO reaction pathways for aliphatic methyl esters [65]. Reprinted from Catal. Today, 100 (2005) 331–335, O. I. Şenol, T. R. Viljava, and A. O. I. Krause, Hydrodeoxygenation of methyl esters on sulphided NiMo/γ-Al_2O_3 and CoMo/γ-Al_2O_3 catalysts, Copyright (2005), with permission from Elsevier.

Table 3
State-of-the-art of sulfided catalysts for HDO of triglycerides-based feedstocks.

Sulfided catalyst	Feedstock	Solvent	Conversion (%)	Reaction conditions	Primary HDO product	Ref
Sulfided Ni, Mo and NiMo catalysts	Rapeseed oil	-	100% at 280 °C in 1 h	Fixed-bed reactor at 260–360 °C, 3.5–15 MPa, and 0.25–4 h	C17, C18 n-alkanes and i-alkanes	[68]
Commercial NiMo/ alumina		isooctane	See ref [69]	Flow reactor, 260–340 °C, 7 MPa, 70–90 h	C15-C18 alkanes and i-alkanes	[69]
Commercial NiMo/ γ-Al_2O_3		-	> 99	Flow reactor, 310 °C and 360 °C, 7 and 15 MPa	Organic liquid product ~83% (mainly hydrocarbon)	[70]
Sulfided NiMo over SiO_2, Al_2O_3 and TiO_2		-	See ref [71]	Fixed-bed reactor, 260–300 °C, WHSV: 2–8 h^{-1}	n-C17 over NiMo/SiO_2 and n-C18 over NiMo/TiO_2 and Al_2O_3	[71]
NiMo, CoMo, NiW supported over Al_2O_3 and B_2O_3–Al_2O_3	Waste cooking oil and trap greases	-	55–99.9	Batch reactor: 7 MPa, 250–350 °C, 3 h Flow reactor: 5 MPa, 350 °C WHSV: 2.8 h^{-1} and hydrogen-to-feed ratio:666 Nm^3/m^3	n-Paraffin (C17, C18), i-paraffin	[72]
Supported CoMoS	Waste cooking oil	Dodecane	-	Fixed bed microreactor, 275 °C, 7.58 MPa, 220 h, LHSV: 3 h^{-1}	n-alkanes (C15-C18) and alkenes	[73]
Commercial NiMo/ γ-Al_2O_3	Crude Tall oil (CTO), Distilled tall oil. Tall oil fatty acid (TOFA)	-	-	Trickle-bed reactor, WHSV:1–3 h^{-1} 5 MPa, 300–450 °C	45 wt% paraffin's (CTO), 80% of n-alkanes (TOFA)	[74, 75]
Sulfided NiMo/γ-Al_2O_3 CoMo/ γ-Al_2O_3	Soybean Oil	-	92.9% (NiMo), 78.9% (CoMo)	Batch reactor, 400 °C, 9.2 MPa, 2 h	n-alkane: 43 wt% (CoMo), 66 wt% (NiMo)	[76]
NiMo/Mn-Al_2O_3	Waste soybean oil	Heptane	Varying amount	Fixed bed continuous flow micro-reactor. 380–410 °C, 40 bar H_2	n-C15-C18 (dominant fraction of C17)	[77]
Commercial CoMo/Al_2O_3	Refined cottonseed oil (10 wt%)	Desulphurized diesel	~97	Trickle-bed reactor, 305–345 °C, 30 bar, WHSV of 5–25 h^{-1}, 43 days (10–12 per day)	Mixed diesel high cetane value	[78]
CoMo sulfides over MCM-41	Refined rapeseed oil	-	~100	Fixed bed reactor, 300–320 °C, 2–11 MPa, space velocities 1–4 h^{-1}	n-C17 and n-C18	[79]
NiMo/SAPO-11 and NiMo/Al_2O_3	Jatropha oil	Cyclohexane	~100	Fixed bed reactor, 380 °C, 3 MPa, 4 h, H_2 flow	High C17/C18 and isomerized paraffin over NiMo/SAPO-11	[80]

was found that such treatment increases the cetane number of the final product [78]. Kubička et al. also investigated CoMo sulfides over mesoporous MCM-41 for hydrotreatment of refined rapeseed oil and the observed deoxygenation activity is lower than that for CoMo/Al_2O_3 [79]. Al incorporated MCM-41 showed better deoxygenation activity towards hydrocarbon formation. Withdrawal of Al from the MCM-41 framework favored the formation of fatty esters instead of fatty acids with MCM-41. Jatropha oil has been hydrotreated using sulfided NiMo over acidic SAPO-11 and Al_2O_3 support. It was claimed that the higher amount of total and strong acidic sites in SAPO-11 affects the formation of different active phases of NiMo and in combination they promote decarbonation, hydrocracking and isomerization reactions [80]. Lower acid sites with alumina supported sulfided NiMo on the other hand shows high selectivity to diesel range ($C_{15–18}$) hydrocarbon fractions.

3. HDO of pyrolysis/lignin-derived bio-oil feedstocks

3.1. HDO of phenols/alkylphenols

Depolymerization and deconstruction of the complex structure of biomass can be performed via various processes for example enzymatically [81], thermally using fast pyrolysis [82], and catalytically. In all these processes, the operating conditions largely affect the composition and yield of final products. For example, hydrothermal liquefaction (HTL), is a technology where bio-oils are produced using water as a medium under supercritical or subcritical conditions [43]. Depolymerization and liquefaction of biomass can also be performed under oxidative or reductive conditions producing renewable-based oils [83]. For instance, the oxidative depolymerization reaction has the benefit to produce a pool of high-value and functionalized green chemicals. On the other hand, the reductive depolymerization gives a considerable yield of deoxygenated monomers, such as BTX (benzene, toluene, xylenes) products which are of interest as platform fuel precursors. The heterogenous structure of the biomass components like lignin impacts the selectivity for linkage cleavage and consequently on the selectivity for oligomeric, dimers, and monomeric products. One of the similarities of these processes is that the depolymerized lignin fragments contain different functional groups like methoxy (CH_3O-), hydroxyl (-OH), benzyl alcohol (C_7H_8O-), ketone (R-CO-R), and aldehyde (-CHO) groups which contribute to the high oxygen content of the bio-oils. Similar functionalities and product spectrum can be seen in bio-oils derived from the pyrolysis of biomass. The oxygen content in bio-oil contributes to negative properties like poor heating value, high viscosity, corrosiveness, thermal and chemical instability [84]. Due to such detrimental characteristics, an upgrading process like hydrotreatment which includes hydrodeoxygenation, hydrocracking, hydro-decarbonylation and decarboxylation, and hydrogenation is required before application as a biofuel. In a lab-scale experiment, the reaction atmosphere for hydrotreatment involves a temperature range of 300–450 °C and a hydrogen pressure of 50–200 bar mimicking the operating conditions of a refinery hydrotreating process. The hydrotreatment of the lignin feedstocks aims to first cleave the recalcitrant linkages such as the carbon-carbon (C-C) and ether (C-O-C) bonds present in the lignin chemical structure. Then the produced alkylphenols are further reacted to form deoxygenated aromatics and cycloalkanes. This section will present an overview of the use of sulfided catalysts in supported and unsupported form for the hydrotreatment of bio-oil model monomer compounds such as guaiacol, phenol, anisole, and cresol. More attention will be dedicated to the discussion on the reaction schemes of the hydrodeoxygenation of the oxygenates that are present in the bio-oils over sulfided catalysts. The catalytic mechanism such as the active sites of sulfided catalysts and reaction network when using different bio-oil model compounds will also be discussed.

Table 4 presents the state-of-the-art of metal sulfide catalysts for hydrotreating phenolic monomers. Various catalytic systems employing mixed oxide supported and sulfided catalysts have been reported for the HDO of phenolics. Garcia-Mendoza et al. have studied the activities of NiWS supported on TiO_2, ZrO_2, and the mixed oxide TiO_2-ZrO_2 for the

HDO of Guaiacol at 320 °C [85]. Their results show that the NiWS supported catalysts system shows remarkable influence in shifting the distribution of the product towards deoxygenated products with NiWS supported on TiO_2 showing an 80% HDO product selectivity at full guaiacol conversion [85]. The authors also speculated that the synergistic effect of NiWS and TiO_2, and also the NiWS phase were responsible for the high catalytic and deoxygenation ability [85]. In a similar catalyst system, Hong et al. have shown that a 2 wt% Ni loading and 12 wt% W loading on such mixed oxide sulfided catalysts can give full guaiacol conversion and a 16% cyclohexane yield under different reaction conditions [86]. The study also mentions that nickel (Ni) performs better than cobalt (Co) as a promoter in catalyzing the HDO of guaiacol [86]. Another study using CoMoS supported on the mixed oxide Al_2O_3-TiO_2 for the HDO of phenol has also shown that the mixed oxide improved the HDO activity with a better metal-support interaction than the conventional CoMoS supported on Al_2O_3 [87]. The use of activated carbon as catalyst support has also been reported in the literature [88–90]. Mukundan et al. have prepared an amorphous highly dispersed and disordered nanosized MoS_2 single-layer on activated carbon by a microemulsion technique for guaiacol HDO and found that the single-layer MoS_2/C promotes deoxygenation and hydrogenation better than a multi-layered MoS_2/C in the production of phenol [90]. The conclusion was made based on the ratio of phenol/catechol produced using single or multi-layered MoS_2/C, where the single-layered catalyst gave a higher ratio. This result inferred the importance of the morphology of the MoS_2 catalyst in affecting product selectivity. Moreover, Mukundan et al. proposed a reaction pathway for HDO of guaiacol based on the detected compounds over the course of 5 h as shown in Fig. 7 [90].

Templis et al. studied hydrotreatment of phenol over a NiMo/γ-Al_2O_3 catalyst in reduced and sulfided form [91]. Results demonstrated that the reaction routes for phenol hydrodeoxygenation occurred via two main parallel routes, the first one is direct deoxygenation (DDO) of phenol, and the second is the hydrogenation of the phenol ring forming cyclohexanol and followed by the hydrogenolysis removing the hydroxyl group producing cyclohexene and cyclohexane. The main difference between both catalysts was that the sulfided catalyst had a high cyclohexane selectivity of more than 90% while the reduced catalyst had higher activity for phenol conversion. Their results indicated that the sulfided catalyst favored the DDO route while giving high cyclohexane selectivity. Fig. 8a) shows the general reaction network for the HDO of phenol using a sulfided NiMo catalyst [91]. Adilina et al. also studied the classical NiMo catalysts supported on pillared clays (PILC) in reduced (NiMoPR) and sulfided (NiMoPS) forms for the HDO of guaiacol [104]. They have used techniques like quasielastic neutron scattering (QENS) and inelastic neutron scattering (INS) measurements to understand the interaction between guaiacol and the reduced and sulfided NiMo catalysts with the clay support [104]. Their results revealed that guaiacol adsorbed on these types of catalysts via two interaction modes, as illustrated in Fig. 8b): the first interaction is guaiacol adsorbed with the Ni-Mo-S site via an H-bonding interaction for sulfided catalysts and the second interaction is chemisorption of guaiacol on both the Ni-Mo site and also the clay support via phenate formation as can be observed in the reduced catalysts [104]. Their results with the sulfided catalysts also showed high activity and selectivity for guaiacol HDO.

The promoters play a role in conventional hydroprocessing catalysts. Badawi et al. have demonstrated that cobalt promotes both DDO (Direct cleavage of the hydroxyl group) and HYD pathways (Hydrogenation of the aromatic ring and followed by the cleavage of the hydroxyl group) in the HDO of phenol to different extents [92]. They have performed DFT calculations and have shown that both DDO and HYD pathways occur on sulfur vacancy sites (CUS) [92]. Romero et al. have also reported the same findings [95]. Using 2-ethylphenol as a model compound [95], they have found that both Ni and Co improve the deoxygenation rate, while Ni only facilitates the HYD pathway. The reaction mechanism for DDO and HYD is illustrated in Fig. 9, respectively [95]. The main difference between these two pathways is that HYD originated from flat adsorption by the aromatic ring while the DDO pathway adsorption occurred through the oxygen atom.

In addition to Ni and Co, a study conducted by Yang et al. has demonstrated that phosphorus (P) was able to promote the phenol HDO activity over a CoMoS-supported MgO catalyst, and they proved that DDO is the major pathway in phenol deoxygenation [96]. A non-conventional hydrotreating catalyst like supported ReS_2 has been reported in several studies [100,99,101,103,102]. For instance, ReS_2 supported on SiO_2 or γ-Al_2O_3 supports was applied in the processing of dimethyl dibenzothiophene and guaiacol [102]. Both Re-based catalysts showed high HDS and HDO activities; ReS_2 supported on SiO_2 showed high HDO rates giving 40% HDO products [102]. In addition to inexpensive transition metals used as promoters, research has examined the use of rare earth and noble metals as promoters for metal sulfide catalysts in phenolics HDO [98,99]. For instance, Ir and Pt have been incorporated into RuS_2/SBA-15 and used in the HDO of phenol [98]. The results have demonstrated a higher conversion rate of phenol (37–41%) and better cyclohexane selectivity (62–63%) than with the non-promoted RuS_2/SBA-15 [98]. It is important to note that the use of noble metals involves high costs for catalyst production, which limits their industrial application. The sulfur content in some bio-feedstocks, such as Kraft lignin, may act as a poison to such noble catalyst systems, nevertheless, studying such a system facilitates better insight into the reaction pathways of the HDO of phenolics.

Jongerius et al. studied a pool of lignin model compounds using CoMoS supported on Al_2O_3 under the same reaction parameters (300 °C, 50 bar H_2, 4 h, and batch system) for comparison [94]. Their main findings suggest that the mono-aromatic oxygenates underwent three distinct pathways that included HDO, demethylation, and methylation. This provided invaluable products like phenol, benzene, cresols, and toluene [94]. Less than 5% of hydrogenated products were detected in the reaction medium, indicating that hydrogenation is the least preferred reaction network for this catalyst system [94].

It is commonly found in the considerable number of studies on the HDO of phenolic compounds that sulfiding agents, such as dimethyl disulfide (DMDS) or carbon disulfide (CS_2), were co-fed during an experiment to create H_2S to maintain the sulfidation degree of the sulfided catalyst. Results show that adding a sulfiding agent during the HDO process had a negative effect on the HDO activity of phenolics but promoted the HDO of aliphatic oxygenates such as vegetable oils and animal fats [66]. As a result, one should note that the addition of a sulfiding agent also plays a role in affecting the effectiveness of the catalyst other than the type of reactant being used. Ferrari et al. have studied the effect of H_2S partial pressure and sulfidation temperature on the conversion and selectivities of phenolics [88]. It was found that the increase in H_2S partial pressure reduced the formation of deoxygenated products from the HDO of guaiacol over CoMoS supported on carbon [88].

Over recent decades, these traditional TMS catalysts have been tested by omitting the use of catalyst support, resulting in unsupported TMS. There are several methods to prepare unsupported TMS, that can be used in the hydrotreatment processes. One of these is a hydrothermal synthesis with synthesis parameters, such as moderate synthesis temperature (150–250 °C) and the absence of hydrogen pressure [112,123,122,124,105,125]. The synthesis method involved simple operation and also controllable catalyst morphology, allowing easy scale-up for industrial application. Wu et al. prepared a series of hydrophobic unsupported MoS_2, NiS_2-MoS_2, and CoS_2-MoS_2 using hydrothermal synthesis with the aid of silicomolybdic acid for the HDO of 4-ethylphenol [105]. The CoS_2-MoS_2 catalyst achieved a 99.9% 4-ethylphenol conversion with a 99.6% ethylbenzene selectivity after 3 h. The catalyst showed good recyclability after 3 runs at 225 °C [105]. Cao et al. also presented results for highly efficient unsupported Co/MoS_2-x (x is the molar ratio of Co/(Co + Mo)) catalysts with high dispersion, rich in defects, and curvy slabs in deoxygenation of p-cresol under mild HDO condition

Table 4
State-of-the-art sulfided catalysts for HDO of phenolic oxygenates.

Sulfided catalyst	Model compound (s)	Solvent	Conversion (%)	Reaction conditions	HDO product selectivity (%)	Ref.
NiWS supported on TiO_2, ZrO_2, and TiO_2-ZrO_2	Guaiacol	Hexadecane	100	Batch, 320 °C, 55 bar H_2, and 1000 rpm	80% cycloalkanes (NiWS-TiO_2)	[85]
CoMoS supported on Al_2O_3-TiO_2	Phenol	Dodecane	93	Batch, 300 °C, 54 bar H_2, and 1000 rpm	Benzene (65%), Cyclohexane (25%) and Cyclohexene (3%)	[87]
NiWS supported on TiO_2	Guaiacol	n-decane	100	Batch, 2.5 h, 300 °C and, 70 bar	Phenol (37%), Cyclohexane (16%), Benzene (1%), Creasol (3%) and others (43%)	[86]
NiMoS supported on γ-Al_2O_3	Phenol	Dodecane	-	Continuous, WHSV = 29/ 36 h^{-1}, 200/ 220/ 250 °C and 30 bar	Cyclohexene (traces), Cyclohexane (93.4%) and benzene (6.5%) for 200 °C and 29 h^{-1}	[91]
CoMoS supported on Al_2O_3	Phenol/2-ethylphenol	Toluene	-	Continuous, 400 °C, 70 bar	HDO activity (29.1 mmol.$h^{-1}g^{-1}$) for phenol and (22 mmol.$h^{-1}g^{-1}$) for 2-ethylphenol	[92]
NiMoS/CoMoS supported on γ-Al_2O_3	Guaiacol/Phenol	m-xylene /n-hexadecane	30–100	Continuous/batch, 200–350 °C, 75–80 bar	Cycloalkanes (55% for NiMo and 45% for CoMo) at 300 °C	[93]
CoMoS supported on Al_2O_3	Phenol, o-cresol, anisole, 4-methylanisole, catechol, guaiacol, 4-methylguaiacol,1,3-dimethoxybenzene, syringol, and vanillin.	Dodecane	25–90	Batch, 4 h, 300 °C and, 50 bar	See ref [94]	[94]
NiMoS supported on γ-Al_2O_3	Phenol and methyl heptanoate	Dodecane	100	Batch, 200/250 °C, and 75 bar	Cyclohexane (85%), cyclohexyl cyclohexane (14%), and others (1%)	[63]
MoS_2/NiMoS/CoMoS supported on Al_2O_3	2-ethylphenol	Toluene	22–24	Continuous, 340 °C, and 70 bar	Oxygenated compounds (19.1%) and deoxygenated compounds (80.9%) for NiMoS	[95]
CoMoP/MgO	Phenol	Supercritical hexane	17–90	Batch, 350–450 °C, 1 h and 50 bar	Benzene (65%) and other (26%) at 450 °C	[96]
NiMoS/CoMoS supported on γ-Al_2O_3	Phenol and methyl heptanoate	m-xylene	5–28	Batch/continuous, 250 °C, 1 h and 15 bar	See ref [66]	[66]
CoMoS supported on Al_2O_3	Methyl-substituted phenols	n-heptane/n-decane	10–50	Continuous, 300 °C and 28.5 bar	See ref [97]	[97]
CoMoS on activated carbon	Guaiacol, ethyldecanoate, and 4-methylacetophenone	-	17–19	Continuous, 270 °C and 75 bar	See ref [88]	[88]
MoS_2 on activated carbon	Guaiacol	Decalin	10–30	Batch, 300 °C, 50 bar, and 1000 rpm	See ref [89]	[89]
MoS_2 on activated carbon	Guaiacol	Dodecane	55	Batch, 300 °C, 50 bar, 5 h, and 1000 rpm	Phenol (52%), Cycloalkanes (12.2%), cyclohexanol (5%), anisole (0.3%), benzene (0.4%), catechol (1.8%), veratrole (0.8%), methanol (0.04%) and gases.	[90]
(Ir or Pt) RuS_2/SBA-15	Phenol	Decalin	37–41	Continuous, WHSV = 1.28 h^{-1}, 310 °C, 30 bar, and TOS = 4 h	For Ir-RuS_2/SBA-15, cyclohexane (63%), cyclohexene (11%), benzene (7%), and cyclohexanol (19%)	[98]
ReS_2/SiO_2	Guaiacol and phenol	Hexadecane and dodecane	15–20	Batch, 250 °C, 50 bar, and 4 h	For guaiacol, phenol (13%), catechol (1%), and cyclohexanol (0.5%)	[99]
ReS_2/SiO_2	Guaiacol	Dodecane	80	Batch, 300 °C, 50 bar, and 4 h	For ReS_2/SiO_2, phenol (60%), cyclohexane (20%) and others.	[100]
ReS_2/activated carbon	Guaiacol	Dodecane	40–80	Batch, 300 °C, 50 bar, and 4 h	See ref [101]	[101]
ReS_2/SiO_2(Al_2O_3)	Guaiacol and 4,6-dimethyldibenzothiophene	Dodecane	80	Batch, 300 °C, 50 bar, and 4 h	See ref [102]	[102]
Re/ZrO_2 and Re/ZrO_2-sulphated	Guaiacol	Decalin	10–70	Batch, 300 °C, 50 bar, and 4 h	See ref [103]	[103]
NiMo/pillared clay (Sulfided and reduced)	Guaiacol	-	1–100	Batch, 250–350 °C, 2.5–20 bar, and 6 h	For sulfided NiMo/pillared clay, at 350 °C and 20 bar, phenol (77%), o-cresol (20%), and p-cresol (3%).	[104]
MoS_2, NiS_2-MoS_2, and CoS_2-MoS_2[a]	4-ethylphenol and 4-propylguaiacol	Dodecane	44–81.5	Batch, 300 °C, 40 bar, 5 h and 900 rpm	See ref [105]	[105]
CoMoS nanosulfide[a]	p-cresol, anisole, and diphenyl ether	Decalin	100 after 3 h (p-cresol)	Batch, 300 °C, 40 bar, and 4 h	Arene yield (98%)	[106]
CoS_2/MoS_2[a]	Creosol and phenol derivatives	Dodecane	18–98	Batch, 250 °C, 40 bar, and 1 h	For CoMo-0.3, toluene (99%)	[107]
MoS_2 and $CoMoS_2$[a]	Phenol	n-decane	30–98	Batch, 350 °C, 28 bar, 150 rpm, and 1 h	See ref [108]	[108]
Amorphous NiMoS[a]	Phenol	n-decane	34.5–96.2			[109]

(*continued on next page*)

Table 4 (*continued*)

Sulfided catalyst	Model compound (s)	Solvent	Conversion (%)	Reaction conditions	HDO product selectivity (%)	Ref.
				Batch, 350 °C, 28 bar, 150 rpm, and 1 h	For NiMoS-0.3, benzene (30.4%), cyclohexane (52.4%), cyclohexene (9.8%), cyclohexanone (7.4%)	
MoS_2[a]	Phenol, 4-methylphenol, and 4-methoxyphenol	Hexadecane	34–52	Batch, 350 °C, 28 bar, 1000 rpm, and 7 h	For phenol, benzene (36%), methylcylohexane (6%) and cyclohexylbenzene (43%)	[110]
NiMoW[a]	Guaiacol	-	99	Continuous, 400 °C, 28 bar, and WHSV = 2.7 h^{-1}	Phenol (45%), creosol (15%), catechol (10%), and hydrocarbon (30%)	[111]
CoMoS[a]	p-cresol	Dodecane	78.8–98.7	Batch, 350 °C, 28 bar, 900 rpm, and 7 h	For CoMo-0.5–200, methylcyclohexane (6.3%), methylcyclohexene (1.5%) and toluene (92.2%)	[112]
Ni-WMoS[a]	p-cresol	Dodecane	85–97.9	Batch, 300 °C, 40 bar, 700 rpm, and 6 h	For W-Mo-0.5, methylcyclohexane (66.7%), methylcyclohexene (3.2%) and toluene (30.3%)	[113]
NiMo(W)S[a]	4-methylphenol	Decalin	93.9–97.8	Batch, 300 °C, 30 bar, 800 rpm, and 5 h	Toluene (87.2%), methylcyclohexane (11.3%), and 4-methylcyclohexene (1.5%)	[114]
NiMoWS[a]	4-methylphenol	Decalin	87–100	Batch, 300 °C, 30 bar, 800 rpm, and 5 h	Toluene (95.6%), methylcyclohexane (2.9%), and 4-methylcyclohexene (1.5%)	[115]
MoP, MoS_2, and MoO_x[a]	4-methylphenol	Decalin	30–100	Batch, 300 °C, 30 bar, 800 rpm, and 5 h	See ref [116]	[116]
MoS_2 (effect of adding CTAB)[a]	p-cresol	Dodecane	42–100	Batch, 275 or 300 °C, 40 bar, 900 rpm, and 5 h	See ref [117]	[117]
NiMoS[a]	p-cresol	Dodecane	67–100	Batch, 300 °C, 40 bar, 900 rpm, and 5 h	For NiMo-0.3, methylcyclohexane (67.1%), 3-methylcyclohexene (4.12%), and toluene (28.8%)	[118]
Fe-MoS_2[a]	p-cresol	Dodecane	63.3–98.3	Batch, 250 °C, 40 bar, 900 rpm, and 5 h	For FeMo-0.3, methylcyclohexane (3.7%), methylcyclohexene (1.6%), and toluene (94.7%)	[119]
CoMoS, zeolitic imidazolate framework-67 (ZIF-67) as Co precursor and template[a]	p-cresol	Decalin	24.7–99.1	Batch, 250 °C, 30 bar, and 2–6 h	For reduced CoMoS-0.18 at 250 °C, toluene (95,5%)	[120]
Co-doped nano-MoS_2[a]	p-cresol	Dodecane	3.8–98.7	Continuous fixed-bed, 180–220 °C, 30 bar, and LHSV of 10 h^{-1}	For Co/MoS_2-0.5 at 220 °C, toluene (95.3%)	[121]
Co-MoS_{2-x}[a]	4-methylphenol, 4-ethylphenol, guaiacol, and lignin oil	Dodecane	2–100	Batch, 120–200 °C, 30–40 bar, and 1.5–10 h	See ref [122]	[122]

[a] Unsupported metal sulfide catalysts.

[121]. During the hydrothermal synthesis of catalysts, the accommodation of Co atoms in the coordinative unsaturated sites (CUS) of MoS_2 and also edge sites resulted in the formation of a Co-Mo-S active phase that enhanced the HDO activity [121]. Their results further demonstrated that the Co/(Co + Mo) molar ratio of 0.3 provided the highest HDO activity and toluene selectivity, on the other hand, excessive Co introduction, causing the formation of large Co_9S_8 particles that hinder the HDO active sites with decreased HDO activity [121].

A two-step strategy for the synthesis of Co-MoS_{2-x} catalysts involved first the hydrothermal and then subsequently the solvothermal method as explored by Wu et al. [122]. They concluded that the reducing ability of MoS_{2-x} induced by the sulfur vacancy was able to reduce the Co precursor to Co metallic while decorating the edges of MoS_{2-x}, leading to the formation of the metal-vacancy interfaces that catalyze the HDO reaction [122]. They further performed Gibbs free-energy calculations (Fig. 10) and clarified that DDO of 4-methylphenol underwent a two-step, hydrogenation and dehydration with $CH_3C_6H_4OH^+$ and $CH_3C_6H_4$ being the transition states [122]. As can be seen in Fig. 10, the Gibbs free energies for the formation of the transition state species were decreased for Co-MoS_{2-x} in comparison to MoS_{2-x} indicating that the metal-vacancy interface favored the adsorption of 4-methylphenol and lowered the reaction energy barriers, hence enhancing the HDO activity [122]. Another study by Wang et al. has proposed a reaction network for p-cresol HDO using a hydrothermally prepared CoMoS catalyst, as shown in Fig. 11a) [112]. Two different deoxygenation routes for p-cresol have been proposed: the first is the DDO route, where the partially hydrogenated dihydrocresol is attacked and the dissociated H^+ and the OH_2^+ species are cleaved in the form of H_2O producing toluene [112]. The second route involves HYD where the partially hydrogenated p-cresol is fully hydrogenated to 4-methylcyclohexanol and then dehydrated to 3-methycyclohexene. The product, 3-methylcyclohexene then undergoes hydrogenation and forms methylcyclohexane [112]. The study also described a p-cresol adsorption scheme on an unsupported CoMoS catalyst [112], as shown in Fig. 11a). p-cresol could adsorb via its vertical orientation and coplanar position in relation to the DDO and HYD routes, respectively [112]. It can also be considered that there is a difference in the CoMoS properties which determine the adsorption orientation and thus the reaction route [112]. For instance, it was mentioned in their study that an increase in the number of MoS_2 layers and also reduced slab length can enhance the toluene selectivity and p-cresol conversion [112].

The use of a template like zeolitic imidazolate framework-67 (ZIF-67) was used to prepare a self-supported defect-rich CoMoS-*x* catalyst for HDO of p-cresol [120]. The main finding in this work highlighted the

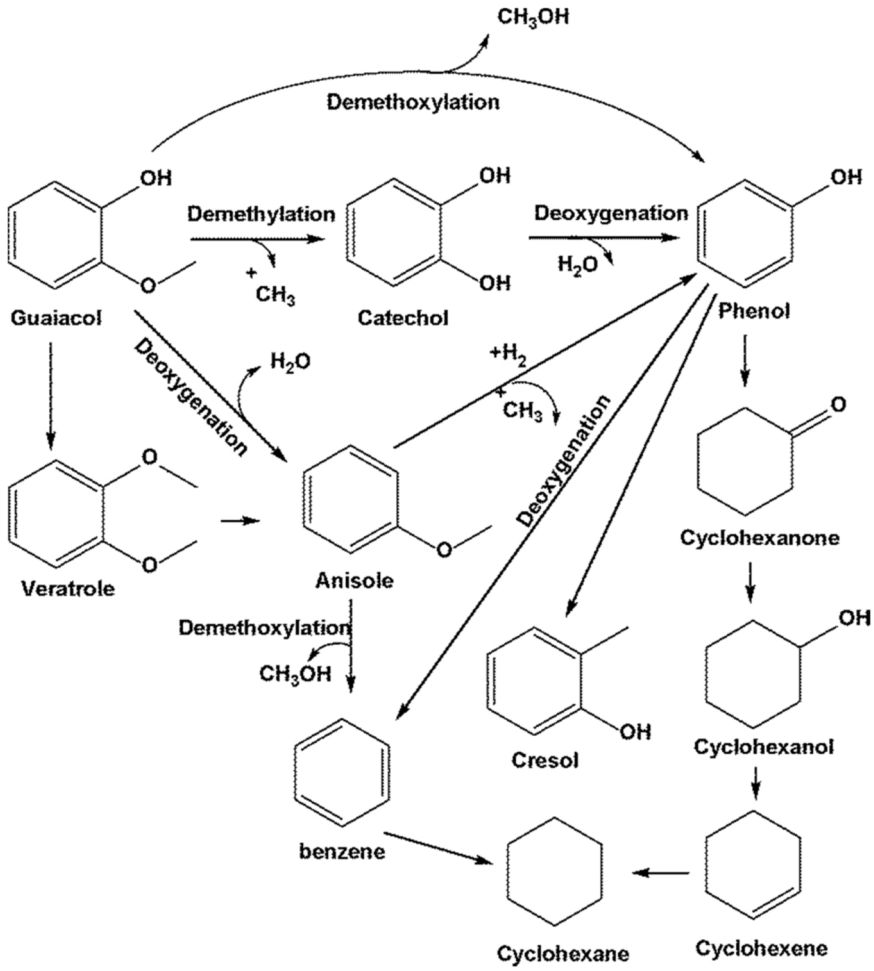

Fig. 7. Reaction pathway for guaiacol HDO over MoS_2/C by a microemulsion preparation method [90]. S. Mukundan, M. Konarova, L. Atanda, Q. Ma and J. Beltramini, *Catal. Sci. Technol.*, 2015, **5**, 4422–4432, reproduced by permission of The Royal Society of Chemistry.

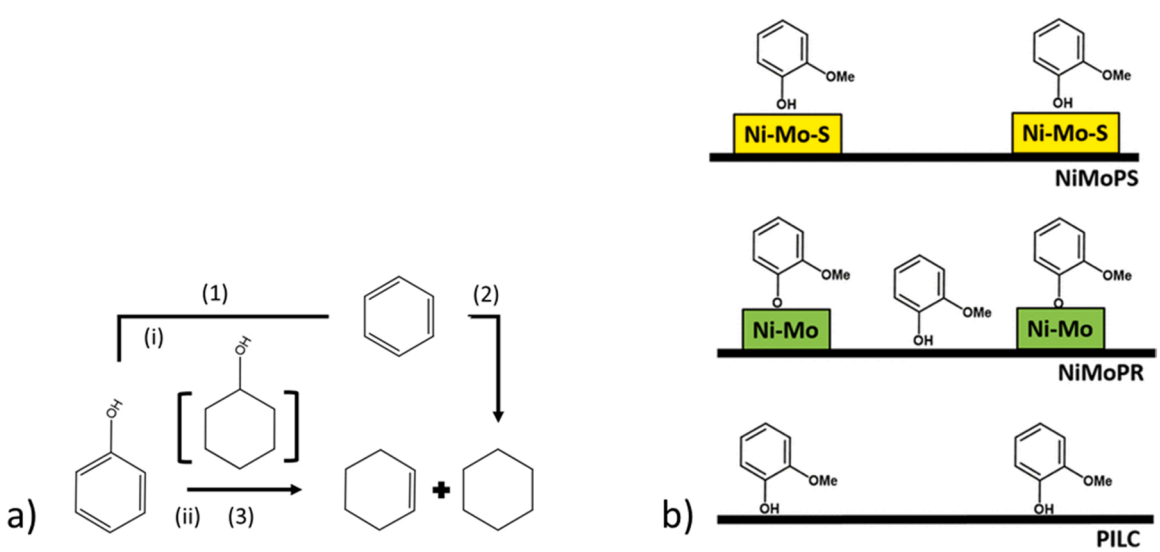

Fig. 8. a) Reaction scheme for phenol HDO over sulfide-supported NiMo catalyst [91]. Reprinted (adapted) with permission from Templis, C. C, Revelas, C. J, Papastylianou, A. A, Papayannakos, N. G., *Ind. Eng. Chem. Res.*, 2019, 58 (16), 6278–6287. Copyright (2019) American Chemical Society. b) Interaction between guaiacol and NiMo supported on pillared clay (PILC) in reduced (NiMoPR) and sulfided (NiMoPS) forms [104]. Reprinted (adapted) with permission from I. B. Adilina, N. Rinaldi, S. P. Simanungkalit, F. Aulia, F. Oemry, G. B. G. Stenning, I. P. Silverwood, and S. F. Parker, *J. Phys. Chem. C*, 2019, 123, 21429–21439. Copyright (2019) American Chemical Society.

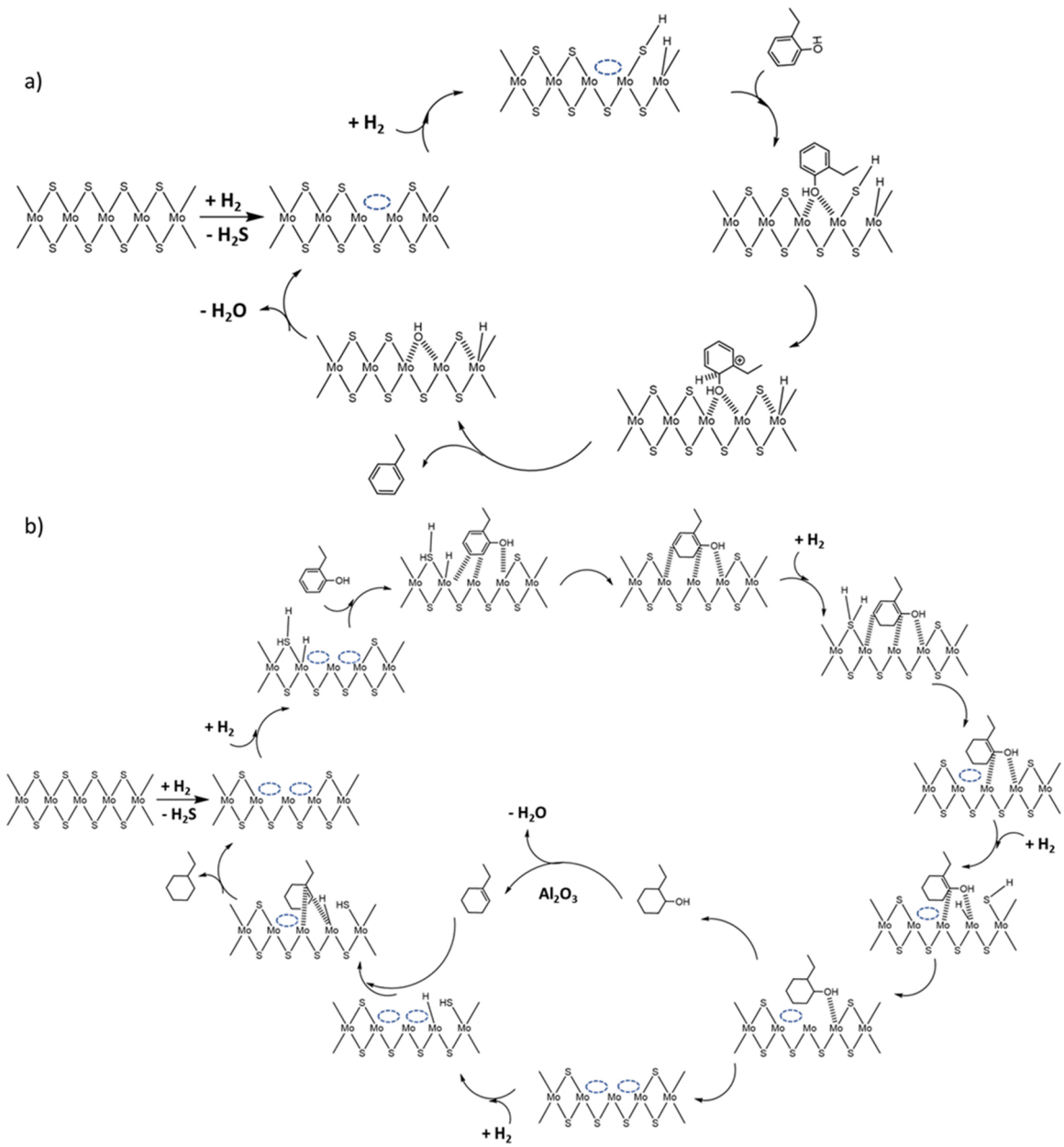

Fig. 9. a) DDO reaction pathway for HDO of 2-ethylphenol over supported MoS_2 catalysts [95] b) HYD reaction pathway for HDO of 2-ethylphenol over supported MoS_2 catalysts [95]. This figure was adapted from one in *Applied Catalysis B: Environmental*, Y. Romero, F. Richard, and S. Brunet, Hydrodeoxygenation of 2-Ethylphenol as a Model Compound of Bio-Crude over Sulfided Mo-Based Catalysts: Promoting Effect and Reaction Mechanism, *Appl. Catal. B Environ.*, 2010, 98 (3–4), 213–223, Copyright Elsevier (2010).

importance of a pre-reduction of the catalysts in decalin (300 °C, 30 bar H_2, and 6 h), and such pre-treatment promoted the formation of sulfur vacancies on the MoS_2 surface and facilitated the surface restructuring of Co-Mo interfaces resulting in the *in-situ* generation of an abundance CoMoS active sites favoring the DDO route, as shown in Fig. 12 [120]. A hard template like mesoporous silica SBA-16 has also been used to synthesize an unsupported NiMoW sulfide catalyst for the HDO of guaiacol in a fixed-bed reactor [111]. The NiMoW sulfide unsupported catalyst gave a 99.6% guaiacol conversion with minimal coke formation at 400 °C [111]. Adapted from the reference, shown in Fig. 12 b), guaiacol underwent HDO via demethylation (DME), demethoxylation (DMO), and transalkylation [111]. Phenol was formed by either the direct demethoxylation of guaiacol or the dehydroxylation of catechol; both reactions resulted in the production of benzene [111]. It is worth noting that phenol was first obtained from the HDO of guaiacol as a reaction intermediate caused by the higher bond dissociation energy for the hydroxy group on the aromatic ring than the methoxy group [84].

3.2. HDO of dimeric phenols

Furthermore, the cleaving and HDO of dimeric phenols are of interest because the depolymerized lignin streams and bio-oils can contain not only monoaromatic compounds but also various aromatic dimers and oligomer fragments. These intermediates are present in the reaction feed, and they should be cleaved during the deoxygenation process. Hence it is necessary to study the HDO of model fragments that can mimic specific structural linkages that can be found in lignin under HDO conditions. Metal sulfides have been explored for cleaving lignin model dimers having C-O-C ether and C-C linkages. The cleavage of lignin

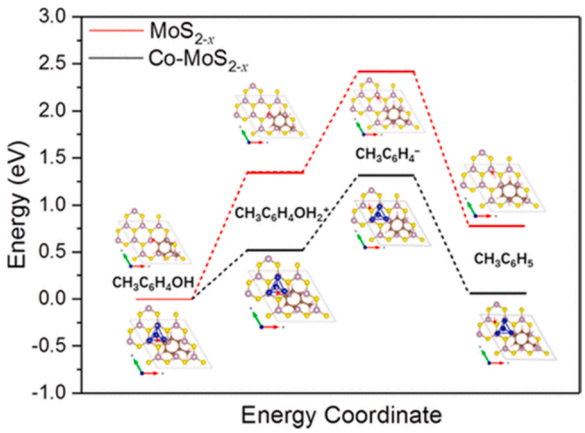

Fig. 10. Gibbs free-energy calculation for HDO of 4-methylphenol over MoS_{2-x} and Co-MoS_{2-x} catalysts [122]. Reprinted (adapted) with permission from K. Wu, W. Wang, H. Guo, Y. Yang, Y. Huang, W. Li, and C. Li, *ACS Energy Lett*, 2020, 5, 1330–1336. Copyright (2020) American Chemical Society.

dimers containing etheric linkages (α-O-4 or β-O-4, 4-O-5, etc) is faster due to their low bond dissociation energy while C-C linkages (5–5′, β-1, β-β, etc.) are quite recalcitrant. The bond dissociation energy of the etheric linkages is in the order of 4-O-5 (ca. 330 kJ/mol) > β-O-4 (ca. 289 kJ/mol) > α-O-4 (ca. 218 kJ/mol) while for the 5–5′ linkage it is ca. 490 kJ/mol [126–128]. The review for model lignin dimers (Table 5) is discussed in this section while Section 4 of this paper is focused on real lignin feed for hydrotreatment. These types of model dimer compound-related studies can provide a means of screening the effectiveness of catalysts and understanding reaction mechanism schemes that occur during lignin depolymerization. Various studies involving lignin dimers revealed that sulfided catalysts can effectively break down the dimers to monomers however to a different extent. Koyama et al. showed the hydrocracking of benzyl phenyl ether, diphenyl ether, benzyl phenols, diphenylmethane, and dibenzyl over sulfided NiMo/alumina, Fe_2O_3/alumina, and MoO_3/TiO_2 in the range of 340–450 °C [129]. Monomer yield increased with increasing temperature for model dimers having a phenolic hydroxyl group and C-O-C linkages while the C-C biphenyl bond was quite recalcitrant even up to 450 °C. Additional dimers were also found to be formed due to dehydroxylation and subsequent hydrogenation reactions.

As mentioned earlier, Jongerius et al. reported that with a commercial sulfided CoMo/Al_2O_3 the β-O-4 bonds of phenyl coumarin alkyl ether could be cleaved to monoaromatics while 5–5′ linkages could not be broken at 300 °C and 50 bar of H_2 pressure [94]. Shuai et al. reported a substantial yield of aromatic monomers from the selective cleavage of -CH_2- linked C-C phenolic dimers over a commercial CoS_2 catalyst at 250 °C and 50 bar of H_2 following 1.5 h of reaction [130]. However, β-1 and 5–5′ C-C linked dimers could not be cleaved but rather transformed into hydroxyl dimers via demethoxylation. Surface engineering of unsupported Co-promoted MoS_2 nanosulfides by Song et al. showed that diphenyl ether (4-O-5) could be cleaved efficiently to produce benzene selectively [106]. The same author also claimed that *in-situ* exsolution synthesized CoMoS on a sulfated zirconia support enhanced the 4–0–5 (diphenylether) C-O cleavage and the subsequent deoxygenation to benzene, toluene, and ethylbenzene [133]. Their work also compared the catalysts prepared by a conventional impregnation and physically mixed sulfated ZrO_2 supported CoMo sulfide catalysts, and showed that the exsolution method represented the best method based on the activity and characterization tests. The activity enhancement was mainly attributed to the better interaction between the CoMo sulfide phase and support, Lewis acid sites of sulfated ZrO_2, and highly-dispersed CoMo sulfide [133]. Ji et al. showed that nanocrystalline pyrite and marcasite (FeS_2), supported over activated carbon was highly active and selective for the hydrodeoxygenation of dibenzyl ether into toluene at 250 °C under an initial H_2 pressure of 100 bar for 2 h [134]. The high activity of such a catalyst was claimed to be due to the transformation of surface FeS_2 into $Fe_{(1-x)}S$ [134]. A proposed reaction pathway for the chemical transformation of dibenzyl ether to benzaldehyde and toluene is shown in Fig. 13a) [134]. The proposed chemical pathway involves the formation of phenylmethylium, and subsequent cleavage of the ether bond. Then hydride transfer takes place from phenylmethanolate to phenylmethylium, resulting in the formation of targeted products, benzaldehyde, and toluene. In another study, Zhang et al. proposed that the cleaving of lignin β-O-4 ether bonds can occur through a dehydroxylation-hydrogenation reaction over the acid-redox site of a NiMo sulfide catalyst which significantly lowers the bond dissociation energy and subsequently facilitates the formation of styrene, phenols, and ethers with H_2 and an alcohol solvent [135]. A potential main route for the conversion of 2-phenoxy-1-phenylethanol (β-O-4-A) over the NiMo sulfide catalyst was proposed in their work which involves the adsorbed β-O-4-A firstly losing a hydroxy group and generating carbocation intermediates ($PhCH^{\delta+}CH_2OPh$) at the weak and medium acid sites of the catalyst. The carbocation intermediates were then transformed into radical intermediates ($PhCH{\cdot}CH_2OPh$) by obtaining an electron from the catalyst redox cycle (Fig. 13b). Due to the lower bond dissociation energy (BDE) of the C_β-OPh ether bond in the radical intermediate (66.9 kJ/mol) than the one in β-O-4-A (274.0 kJ/mol), the C_β-OPh bond cleaves easily, and then the generated radical species react with activated H_2 or methanol to form various arene products like phenols and ethers [135].

A similar strategy of peroxidation via $O_2/NaNO_2$/2,3-Dichloro-5,6-dicyano-1,4-benzoquinone (DDQ)/N-Hydroxyphthalimide (NHPI) and subsequent hydrogenation over a NiMo sulfide catalyst was found beneficial for the overall cleavage of β-O-4 model compounds [136].

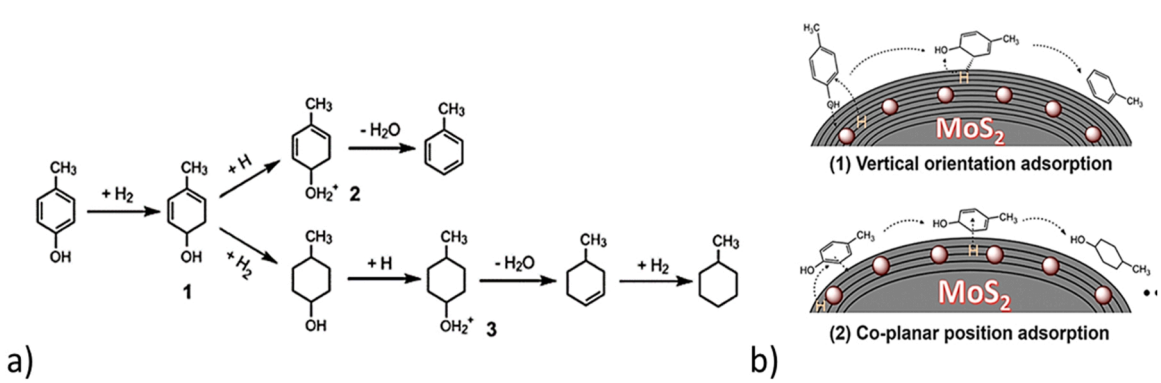

Fig. 11. a) A reaction network for p-cresol HDO over unsupported CoMoS catalyst [112] b) Adsorption scheme for HDO of p-cresol over unsupported CoMoS catalyst. Reprinted (adapted) with permission from Wang. W, Zhang. K, Li. L, Wu. K, Liu. P, Yang. Y., *Ind. Eng. Chem. Res.*, 2014, 53 (49), 19001–19009. Copyright (2014) American Chemical Society.

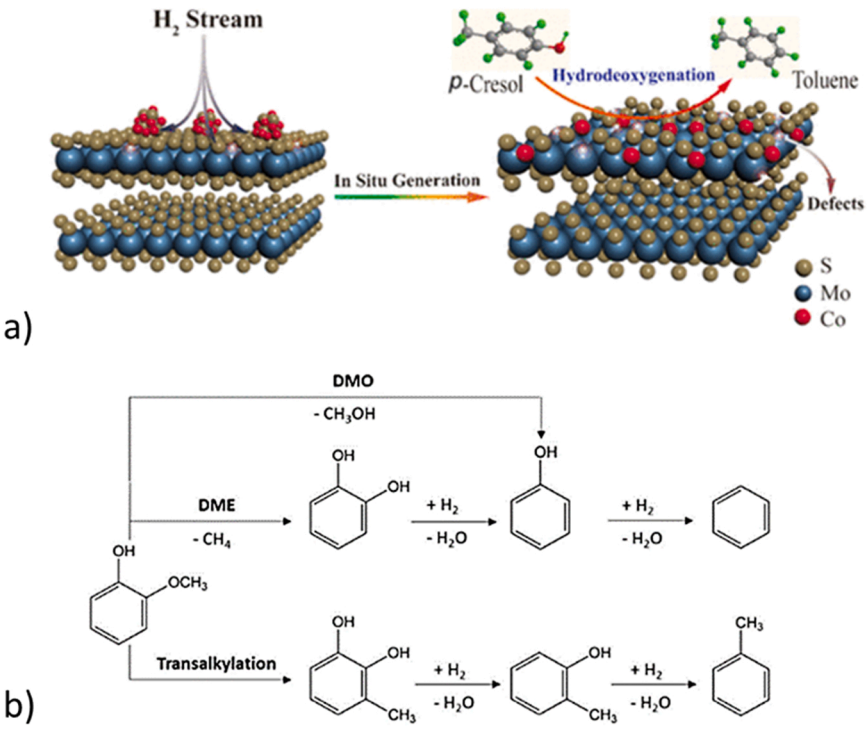

Fig. 12. a) *In situ* formation of CoMoS active phase for HDO of p-cresol. Reprinted (adapted) with permission from X. Liu, X. Hou, Y. Zhang, H. Yuan, X. Hong, G. Liu, *Ind. Eng. Chem. Res.*, 2020, 59, 15921–15928. Copyright (2020) American Chemical Society. [120]. b) A proposed reaction scheme for HDO of guaiacol over NiMoW catalyst [111]. This article was published in Catalysis Communications, Tran, C. C, Stankovikj, F, Kaliaguine, S, Unsupported Transition Metal-Catalyzed Hydrodeoxygenation of Guaiacol, Catal. Commun., 2017, 101, 71–76, Copyright Elsevier (2017).

Table 5
Cleaving of lignin dimers over sulfided catalysts.

Entry	Sulfided catalyst	Model compound	Reaction conditions	HDO product selectivity (%)	Ref.
1	$CoMoS/Al_2O_3$	1-hydroxy-1-(4-hydroxy-3-methoxyphenyl)− 2-(2,6-dimethoxyphenoxy)ethane (Synthesized) Phenylcoumaran 2,2′-biphenol	300 °C, 50 bar, batch	Monoaromatics	[94]
2	$NiMo/Al_2O_3$	Benzylphenylether (BPE), 4-hydroxydiphenylether (4HDPE), diphenylether (DPE), 4-hydroxydiphenylmethane (4HDPM), diphenylmethane (DPM), dibenzyl (DB), biphenyl (BP), and 2-hydroxybiphenyl (2HBP)	340–450 °C, 100 kg/cm^2 (98 bar), batch	Benzenes, monophenols, other dimers	[129]
3	Unsupported CoMoS	Phenol, p-cresol, Anisole, Diphenyl ether, Catecol, Guaicols	300 °C, 4 MPa of H_2, atuoclave (50 ml)	> 85% Yield of BTX	[106]
4	Commercial CoS_2, MoS_2 and FeS_2	Dimethylguaiacylmethane	250 °C, 50 bar H_2	88% monomer in 90 min reaction	[130]
5	NiMoS on alumina, USY, and mixed alumina-USY supports	Benzyl phenyl ether (BPE), 2-phenethylphenylether (PPE), and 2,2-biphenol (5–5′)	320 °C, 50 bar H_2, 6 h, and 1000 rpm	Monomers like cycloalkanes, deoxygenated aromatics and phenolics	[131]
6	NiMoS on USY with various silica-alumina ratios (SAR) (12, 30 or 80)	2-phenethylphenylether (PPE), 2,2-biphenol (5–5′), and 4–4′dihydroxydiphenylmethane (DHDPM)	345 °C, 50 bar H_2, 6 h, and 1000 rpm	Mostly cycloalkanes, BTX, ethylbenzenes	[132]

Recently our group studied lignin dimer hydrotreatment involving sulfided NiMo over Al_2O_3 and ultra-stable Y zeolite (USY). It has been found that the NiMoS-USY combination can give a high yield of mono-aromatics including deoxygenated aromatics, mono/alkyl phenols, and cycloalkanes via hydrogenolysis of etheric C-O bonds and subsequent cleavage of C-C intermediates formed by transalkylation reactions [131]. Interestingly, with the NiMoS-USY combination, recalcitrant β-1, -CH_2 linked dimers and 5–5′ linkages could be significantly cleaved due to a suitable balance between Brønsted acidity and Ni-promoted MoS_2 redox sites. This study led to a further study investigating USY with different silica/alumina ratios (SAR) as catalyst supports for NiMoS in valorizing lignin dimers [132]. Among all the studied catalysts, NiMoS on USY with an intermediate SAR of 30 was found to be most effective in cleaving β-O-4 and C-C linkages with a high degree of hydrogenolysis, hydrocracking, and HDO reactions owing to an apparent optimal balance between acidic and deoxygenation sites. Moreover, it was found that a higher surface acidity promoted the initial conversion of 2-phenethylphenylether (PPE) and 2,2-biphenol (5–5′) via transalkylation and isomerization [132]. These results suggested that tuning the acidity and pore sizes of the USY-zeolite and further impregnating with NiMoS was an effective way to create a catalyst that is efficient in both breaking recalcitrant lignin linkages and achieving a high level of deoxygenation.

3.3. HDO of complex feedstocks like pyrolysis/lignin oil upgradation

Pyrolysis oil produced from the fast pyrolysis of solid biomass contains a variety of compound groups like sugars, alcohols, phenols, ketones, aldehydes, furans, and acids. These compounds contribute to various detrimental properties of pyrolysis oil which need to be addressed before the full utilization of pyrolysis oil as a fuel or other applications by hydrotreatment in petroleum refineries. Shumeiko et al. performed a series of screening tests of lab-synthesized and commercial sulfided NiMo catalysts for long-term hydrotreatment of wheat/barley

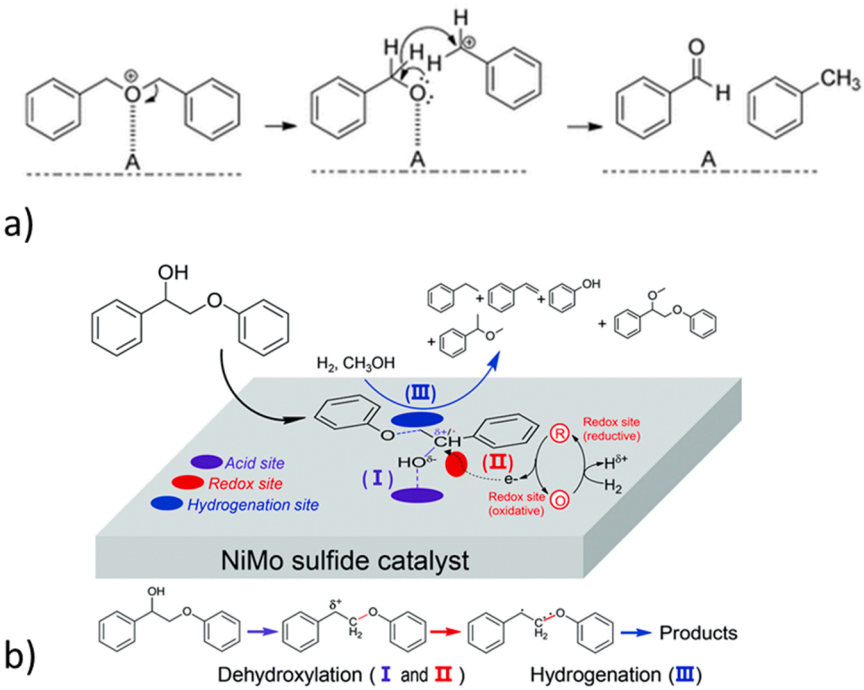

Fig. 13. a) Proposed reaction pathway for the formation of benzaldehyde and toluene from dibenzyl ether. "A" stands for a Brønsted or Lewis acid site [134]. Copyright (2015) Wiley, used with permission from N. Ji, X. Wang, C. Weidenthaler, B. Spliethoff, and R. Rinaldi, Iron(II) Disulfides as Precursors of Highly Selective Catalysts for Hydrodeoxygenation of Dibenzyl Ether into Toluene, ChemCatChem, 2015, 7, 960–966. b) The potential route for 2-phenoxy-1-phenylethanol (β-O-4-A) conversion over the NiMo sulfide catalyst [135]. C. Zhang, J. Lu, X. Zhang, K. MacArthur, M. Heggen, H. Li, and F. Wang, *Green Chem.*, 2016, **5**, 6545–6555, reproduced by permission of The Royal Society of Chemistry.

(50/50 wt%) straw-derived pyrolysis oil in a fixed-bed reactor aiming to produce a hydrotreated pyrolysis oil that is compatible with the petroleum refinery fraction for coprocessing [137]. The assessment of their results was based on the HDO and HDS activity. Their results showed that the catalysts synthesized by co-impregnation were better than the catalysts prepared by a two-step impregnation procedure despite having the same active NiMo phase loading and the same commercial alumina support. While the commercial catalysts performed worst among all the catalysts in terms of HDO activity, they showed the best HDS performance [137]. The difference in activity may be attributed to the different physicochemical properties of the catalysts and also preparation methods. These results suggest that the HDS activity of a sulfide catalyst is not suitable for indicating its HDO performance for pyrolysis oil. The long-term experiments (80 h) in their work were useful in understanding the deactivation of the sulfided catalysts [137]. Their experimental results showed that the product quality changes, which was indicated by a gradual loss of catalyst activity with increasing time-on-stream [137]. Thus, their work demonstrated the feasibility of using biomass-derived pyrolysis oil to obtain a compatible feedstock for co-processing in a refinery, however, the stability of the sulfided catalysts needs to be fully addressed before achieving a successful deployment of the technology. Another study conducted by Zhang et al., upgraded a pyrolysis oil produced by the fast pyrolysis of forest residues with light cycle oil (LCO) as a reaction medium using a dispersed unsupported MoS_2 catalyst [6]. The use of the dispersed unsupported catalysts was considered to allow better interaction between the active sites of the catalysts, hydrogen, and the heavy feedstock resulting in less solid yield. The low solid yield ranging from 0.8 to 1.8 g/100 g bio-oil at the end of their experiment showed that the use of dispersed unsupported materials can suppress the side reactions such as polymerization and re-polymerization of the large molecular weight compounds and reactive species that result in solid residues.

Priharto et al. studied the hydrotreatment of pyrolysis oil derived from lignin-rich digested stillage over commercial sulfided NiMo and CoMo catalysts [138]. They demonstrated the feasibility of utilizing solid waste residues from bioethanol processes for the production of pyrolysis oil. The further hydrotreatment of the pyrolysis oil also resulted in an appreciable oil yield of 60–64 wt% [138]. It should be noted that the nitrogen content in such feed should be refined employing hydrodenitrogenation (HDN), as, from their GCMS analysis, nitrogen-containing aromatic heterocyclic compounds present in the feed like indoles were converted to pyrroles. Hence, the removal of nitrogen content in pyrolysis oil by the means of hydrodenitrogenation (HDN) should be addressed in any future study with the aid of sulfided catalysts. For instance, Izhar et al. studied HDN of fast-pyrolysis oil derived from sewage sludge over a phosphorus-promoted sulfided $NiMo/Al_2O_3$ catalyst [139]. The main finding from their work showed that dissolving pyrolysis oil using a non-polar solvent like xylene improved nitrogen removal compared to using protic solvents due to the competition between denitrogenation and deoxygenation reactions [139].

4. Reductive liquefaction of lignin

Lignin (an amorphous solid) is a renewable and sustainable future source of aromatic compounds for the chemical industry [140]. Lignocellulosic biomass contains up to 33 wt% of lignin. Softwoods (coniferous woods, e.g. spruce), contains 27–33 wt% lignin. Hardwoods (deciduous species, e.g. birch) have 18–25 w% lignin and grasses constitute 17–24 wt% of lignin [141,142]. Chemically, lignin is a 3-dimensionally complex biopolymer composed of three basic structural units; sinapyl alcohol, coniferyl alcohol, and coumaryl alcohol. The composition of these structural units is different among the lignocellulosic biomasses. In softwoods, the coniferyl alcohol units form 90–95 wt % of the lignin with the remaining being only the sinapyl alcohols (10–5 wt%). In hardwood lignin, an equal amount of (50–50 wt%) coniferyl and sinapyl alcohols are observed. These woods are devoid of the coumaryl alcohol structural unit. Grasses contain 0–5 wt% of the coumaryl alcohol units, but the major contributions are from the coniferyl alcohol (75 wt%) and the sinapyl alcohol (20–25 wt%) units. The structural units in lignin are connected by various C-O-C ether linkages (α-O-4, β-O-4, 4-O-4) and C-C linkages (β-β, β-1, β-5, 5–5) (see Fig. 15) to generate the three-dimensional structure of lignin. Among these two kinds of linkages, the ether linkages (65%) dominate in lignin, of which the β-O-4 alone accounts for 50% of all ether linkages. The composition of the chemical linkages in softwood, hardwood, and grass lignin are

also dissimilar. For instance, softwood contains more C-C bonds than hardwood. Also, the C-O-C and C-C linkage patterns vary among the softwood/hardwood/grasses plants classes too. Lignin structure is very complex among and within the various lignocellulosic biomasses. This necessitates the exact structural determination of every isolated lignin which is very challenging to accomplish [143].

The natural sources of lignins are the many agricultural residues (grain dust, sunflower stalk, bagasse, etc.) and forest residues [3]. The lignins from these sources can be utilized only after their extraction. Otherwise, they need to be co-processed along with the cellulose and hemicellulose fractions of the biomass. On the other hand, commercial lignins (also known as the technical lignins: Kraft lignin, soda lignin, hydrolysis lignin, etc.) are already extracted lignins almost devoid of the cellulose and hemicellulose fractions. Commercial lignins are usually generated as the byproducts of various commercial pulping/hydrolysis processes. For instance, Kraft lignin is generated as the byproduct of the Kraft pulping process, likewise, the soda pulping process generates soda lignin as a byproduct, and hydrolysis lignin is produced during the enzymatic hydrolysis of cellulosic biomass to ethanol [3]. The severity of the pulping processes and the chemical reagents used in the processes (NaOH, Na_2S, H_2SO_4, etc.) [140] adversely affect the lignin structure. Bonds are broken and new ones are generated during the processes. Hence, the structures of commercial lignins are different from their natural counterparts. Currently, most of the commercial lignins produced are utilized as a combustion fuel in the pulping process to regenerate heat energy for the pulping process. This gives rise to a low value-addition of the lignin ($70–150 per ton). On the other hand, the conversion of commercial lignins to chemicals (e.g.: phenols, benzenes, toluene, xylenes, etc.), and fuels significantly improves its value-addition (approximately $1300 per ton) [7].

The sole way to obtain the different monomeric aromatic compounds from lignin is through its depolymerization. In general, lignin depolymerization can be achieved by techniques such as pyrolysis, gasification, hydrogenolysis (H_2), chemical oxidation (O_2), and hydrolysis (H_2O) [144]. Other methods include microwave-assisted lignin depolymerization, biological depolymerization, and a so called lignin-first approach, as summarized in Fig. 15. There are many excellent reviews available in the literature on various lignin depolymerization techniques and their different advantages [3,140,141,143,144–151]. Anyways, the produced bio-liquids needs further upgrading to produce bio-fuels. For instance, the liquid bio-oil obtained from the pyrolysis of lignin is corrosive and high in oxygen content. To produce value-added compounds from this bio-oil, an additional step involving catalytic hydrotreatment is necessary. On the contrary, chemical depolymerization especially using heterogeneous catalysts has the advantages of high product selectivity to either value-added oxygenates or deoxygenates in a single step, high efficiency of the reagents used, and moderate reaction conditions, and the ease of reaction control [140]. This part of the review focuses on the chemical reductive method (H_2) of lignin valorization using sulfided catalysts.

The first step in lignin depolymerization is its thermal degradation to oligomeric lignin fragments (Scheme 1) [152]. The macromolecular structure of lignin is a major hurdle for employing solid catalysts during this step, since, in most of the porous solid catalysts, their pore dimensions do not match with the dimensions of the lignin macromolecules. However, homogeneous catalysts may better facilitate the first step. In the second step, the formed smaller fragments undergo further degradation to form oxygenated monomeric molecules. Solid catalysts can perform this step. In the third step, deoxygenation (catalytic HDO) of these monomers to liquid aromatic products ensues. Further catalytic hydrogenation of aromatics to cyclic aliphatic compounds follows in the final step (Scheme 1). The gaseous products of lignin depolymerization are mainly, CO_2, CO, CH_4, and C_2-C_4 alkanes. At any stage of the lignin depolymerization, the repolymerization of the depolymerized lignin fragments, aromatic oxygenates, and aromatics may occur. This repolymerization occurs mainly through C-C bond formation (on the other hand, the C-O-C bonds may undergo further breakage) leading to the formation of a solid phase composed of polycondensed aromatic structure, usually called as lignin depolymerization char [152]. The main challenge in lignin depolymerization is to reduce the char formation and concurrently to increase the formation of the liquid products [153].

The conversion in lignin depolymerization in the literature is expressed in contrasting ways by different research groups. Some authors separate the unconverted lignin from the char through solvent extraction to calculate the actual lignin conversion to liquids and gases. While others consider only the total amount of solid products (also containing unconverted lignin) obtained after the depolymerization in their calculation. The liquid product yields are also represented in different ways in the literature. The weight of bio-oil produced after depolymerization (sometimes expressed as the wt% of a particular solvent-soluble fraction) is the common method found in the literature. In the very early reports on lignin depolymerization, both the conversion and the composition of bio-oils are rarely mentioned. Whenever the composition of the bio-oil was specified in the literature, it is briefly

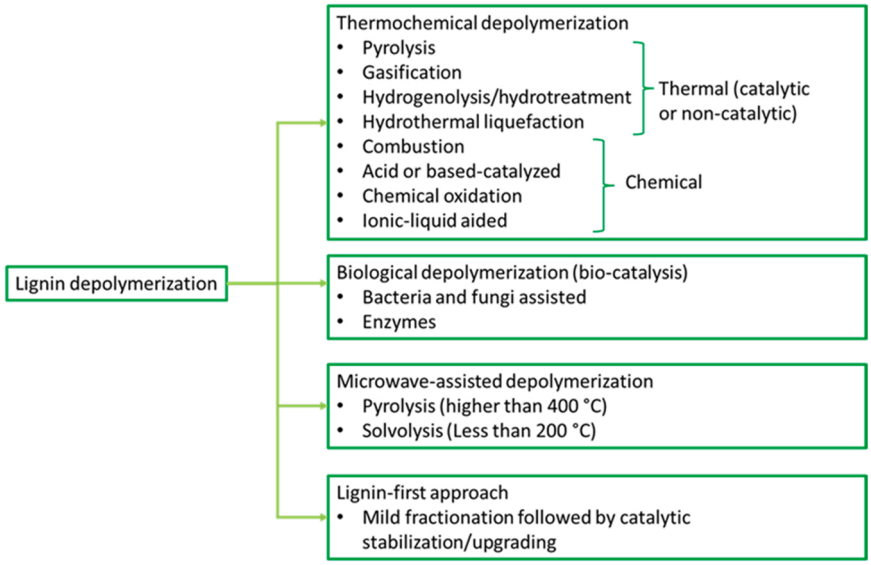

Fig. 14. Methods for lignin depolymerization.

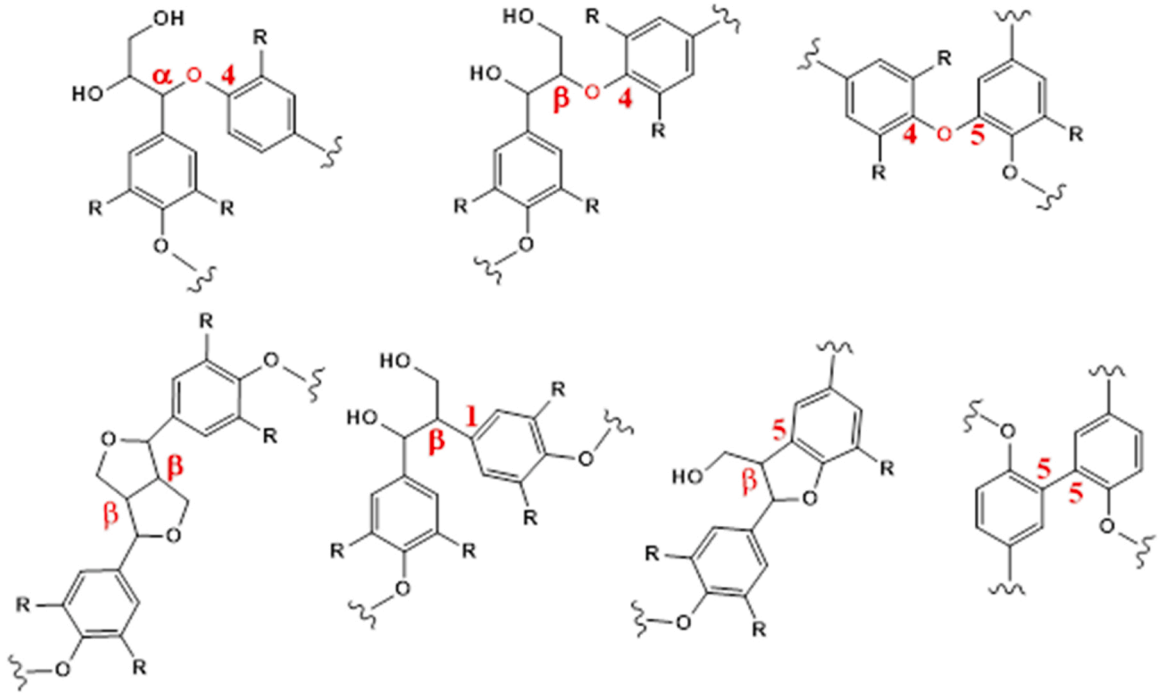

Fig. 15. Different linkages found in lignin.

stated in this section of the review. However, to obtain more detailed information about the full composition of the bio-oil and conversion, it is recommended to follow the corresponding cited references. Moreover, some literature represents the char yield as 'char', while others refer to it as 'solid residue' obtained after the reaction. These terms can be synonymous, but in some cases, the 'solid residue' could also include char as well as unconverted lignin.

4.1. Batch processes using commercial catalysts

Early reports on the use of sulfided catalysts in lignin conversion were mainly focused on examining to what extent lignin valorization could be achieved rather than the catalyst structure, and the activity correlations. The choice of the various sulfided catalysts for this was purely based on their reputation for sulfur tolerance and capability for desulfurization/hydrogenation/hydrogenolysis activity. One such early study was reported by Vuori et al. in 1988, where they compared the lignin liquefaction under mild thermolysis conditions (< 400 °C) and catalytic conditions [153]. A commercial sulfided $CoMo/Al_2O_3$ was employed as the hydrotreating catalyst. Kraft lignin was the feedstock and tetralin was chosen as a hydrogen donor solvent (tetralin can act both as a solvent and 4-hydrogen atom donor to the reaction medium). The liquid products of the reaction (345 °C, 20 bar of H_2, 5 h) mainly constituted phenols and acids (ether soluble fraction) amounting to 11.5 wt% in yield. This yield was not very much higher than the thermolytic reaction where the liquid product yield was 8.1 wt%. In the gaseous products, CH_4 (from lignin) contributed around 2.7 wt% yields from the catalytic reaction as compared to 1.1 wt% from the thermolytic conditions, suggesting an enhancement in reaction rate under catalytic conditions. Surprisingly, the authors found more char formation with the catalytic process (33 wt%) than the thermolytic process (21 wt%), leading to a conclusion that the catalyst could improve the reaction rate, however, was incapable of preventing the condensation reactions leading to char. Even the presence of both the hydrogen donor solvent (tetralin) and H_2 pressure (20 bar) was unable to prevent condensation reactions from lignin fragments [153].

In general, solvents in lignin depolymerizations can stabilize the reactive intermediates, enhance the catalyst-lignin interactions, and promote the solubility of lignin. The role of solvents in lignin depolymerization was reviewed in detail by Raikwar et al. [154]. To understand the effect of hydrogen-donor and non-donor solvents on the lignin liquefaction process, Schuchardt et al., employed a set of different solvents such as xylene, pyridine, cyclohexanol, isopropanol, and tetralin; the latter three being hydrogen-donor solvents [155]. The catalyst of choice was ferrocene *in situ* sulfided with CS_2 or S. Among these solvents, tetralin gave the maximum heavy-oil yield of 44 wt% at 65 wt% of lignin conversion (400 °C, 270 bar at 400 °C, 0.5 h). This was attributed not only to the high hydrogen-donor ability of tetralin but also to its heavy-oil extraction ability.

The C-C bonds in lignin are more difficult to cleave than the C-O bonds (vide supra). Therefore, catalysts for lignin depolymerization also need to be efficient for the C-C bond cleavage since a large amount of char (repolymerized lignin-containing a large amount of C-C bonds) formed during the depolymerization needs to be broken down as well for higher monomer yield. A comparative study using unsupported MoS_2 and CoS_2 on the model compound dimethylguaiacylmethane containing a methylene bridge and Kraft lignin showed the CoS_2 catalyst to be superior in C-C bond cracking (11.7 wt% yields to the aromatic monomer from Kraft lignin at 250 °C, 50 bar H_2, 15 h) than MoS_2 [130]. However, the catalyst has a limitation, not all C-C bonds could be cleaved by CoS_2. It is efficient only if there are hydroxy groups on any of the benzene rings related to the *ortho* position of the methylene/C-C bond. In the absence of these -OH groups, no C-C bonds were cleaved. The influence of the -OH group was more effective than the -OMe group in the C-C bond cleavage. Further studies showed that the active phase of the catalyst for C-C bond breakage is not CoS_2 but CoS generated by the reduction of CoS_2 in the H_2 atmosphere. Complementary to this, the surface composition of the catalyst after the reaction showed a larger contribution of CoS (Fig. 16a). The recycling studies showed a decrease in catalytic activity. The Co:S atomic ratio was reduced from 1:1.7–1:1 in the third run and the presence of the CoO phase was noticed. Conditional experiments with CoO showed less activity, indicating that the most active phase of the reaction was its sulfided form. The decrease in activity during the recycle runs can thus be attributed to its oxidation to the oxide phase. Both the supported catalysts sulfided $CoMo/Al_2O_3$ and unsupported CoS/S_2 are effective for the breakage of the C-C bonds in

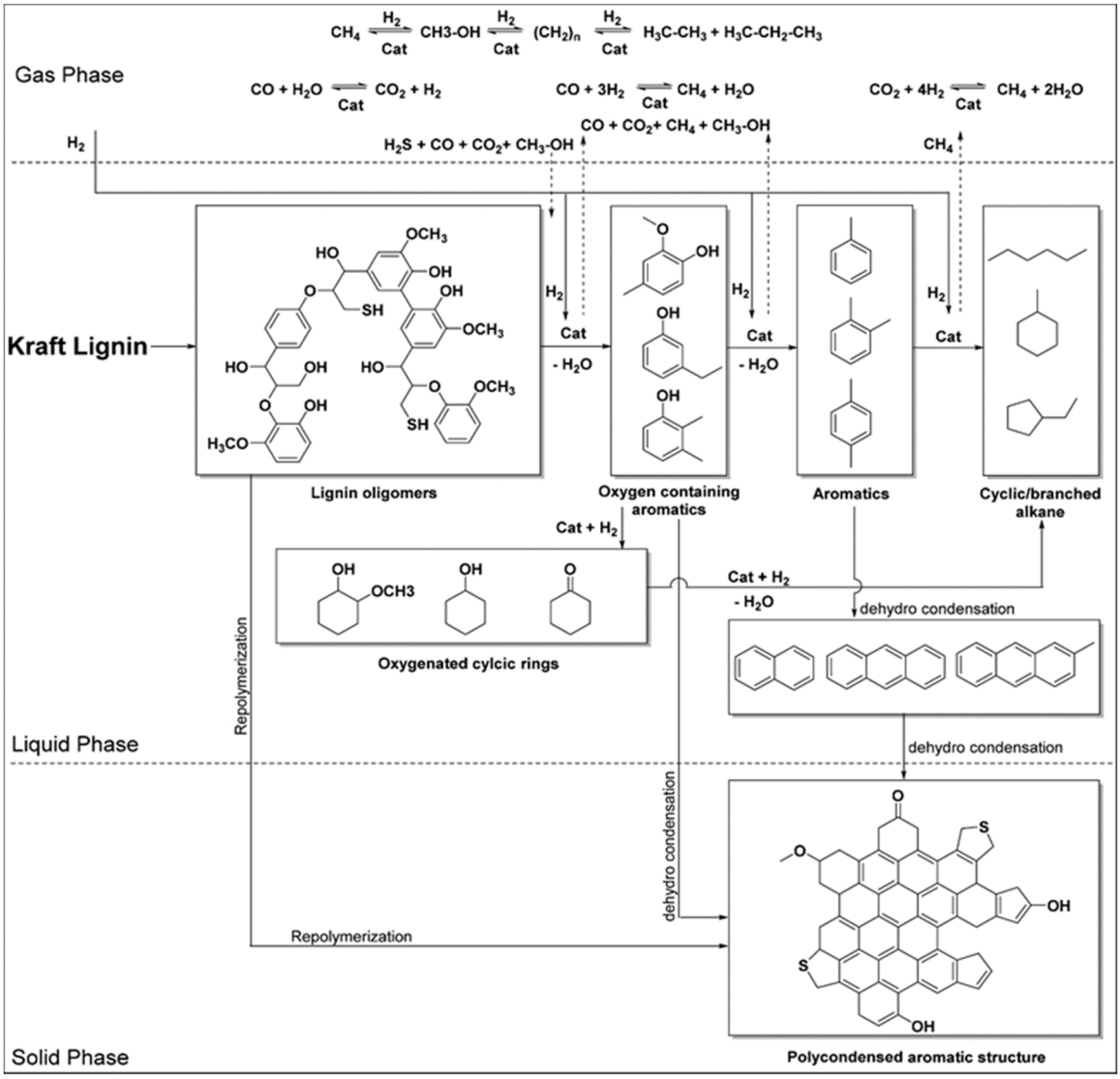

Scheme 1. Kraft lignin depolymerization network [152]. Reprinted (adapted) with permission from R. Chowdari, S. Agarwal, and H. Heeres, *ACS Sustainable Chem. Eng.*, 2019, 7, 2044–2055. Copyright (2019) American Chemical Society.

lignins.

Lignin depolymerization behavior in the presence of a sulfided catalyst during the heating period of the batch reactor is often overlooked. This information gives an idea about the lignin fragmentations happening in the presence of the sulfided catalysts in the early hours of the reactions where there is a large temperature variation. This was investigated by Joffers et al., using Protobind 1000 lignin and a commercial sulfided NiMo/Al_2O_3 catalyst [157]. The time taken for the reactor to reach the desired temperature of 350 °C was only 14 min. Immediately following the 14 min, the lignin conversion was 27 wt%. This lignin conversion resulted in 24 wt% yields of liquids (mainly monomeric phenols), and 3 wt% of gases (CH_4, CO, CO_2, and C_2-C_5 hydrocarbons). The remaining was the lignin residue (solid). Gel permeation chromatographic (GPC) analysis of the tetrahydrofuran soluble fraction of this lignin residue (oligomers) showed a molecular weight of 3575 g/mol, corresponding to 20 phenylpropane units (parent lignin had 26 units). These monomer units were further reduced to 6 after 28 h of reaction [156]. The THF-soluble lignin residue still contained stronger C-C linkages between monomer units, which were difficult to break. This could be due to the reaction conditions or perhaps due to the choice of a NiMo/Al_2O_3 catalyst than a CoMo/Al_2O_3 catalyst. Characterization of the catalyst after the reaction confirmed coke formation. Moreover, the sulfur content in the catalyst was decreased to 7 wt% as compared to the 9 wt% in the freshly sulfided catalyst (Protobind 1000 had only 0.1 wt% of sulfur in it). Fig. 16b) shows the changes in the BET surface area, pore volume, and pore diameter of the catalyst as a function of reaction time. All these textural properties decreased in the first hour of the reaction and became almost constant after 28 h of the reaction. The sulfided catalyst showed good stability for longer reaction runs. The main cause of its deactivation is due to the loss of sulfur. Therefore, an additional sulfidation step is necessary to regenerate most of the initial activity.

4.2. Semi-continuous processes

To increase the monomer yield during lignin depolymerization, i.e., effectively removing the products from the catalyst preventing their further transformation, and competition for active sites, the lignin depolymerization process was attempted in a semi-continuous mode using sulfide catalysts. In the case of both a batch reactor and a fixed-bed reactor, the semi-continuous mode involves the continuous withdrawal of the reaction products under the flow of the H_2. The lignin and the solvent (if any) are already placed in the reactors; they are not in a continuous feeding mode. In one such study, a NiMo/Al_2O_3 catalyst was

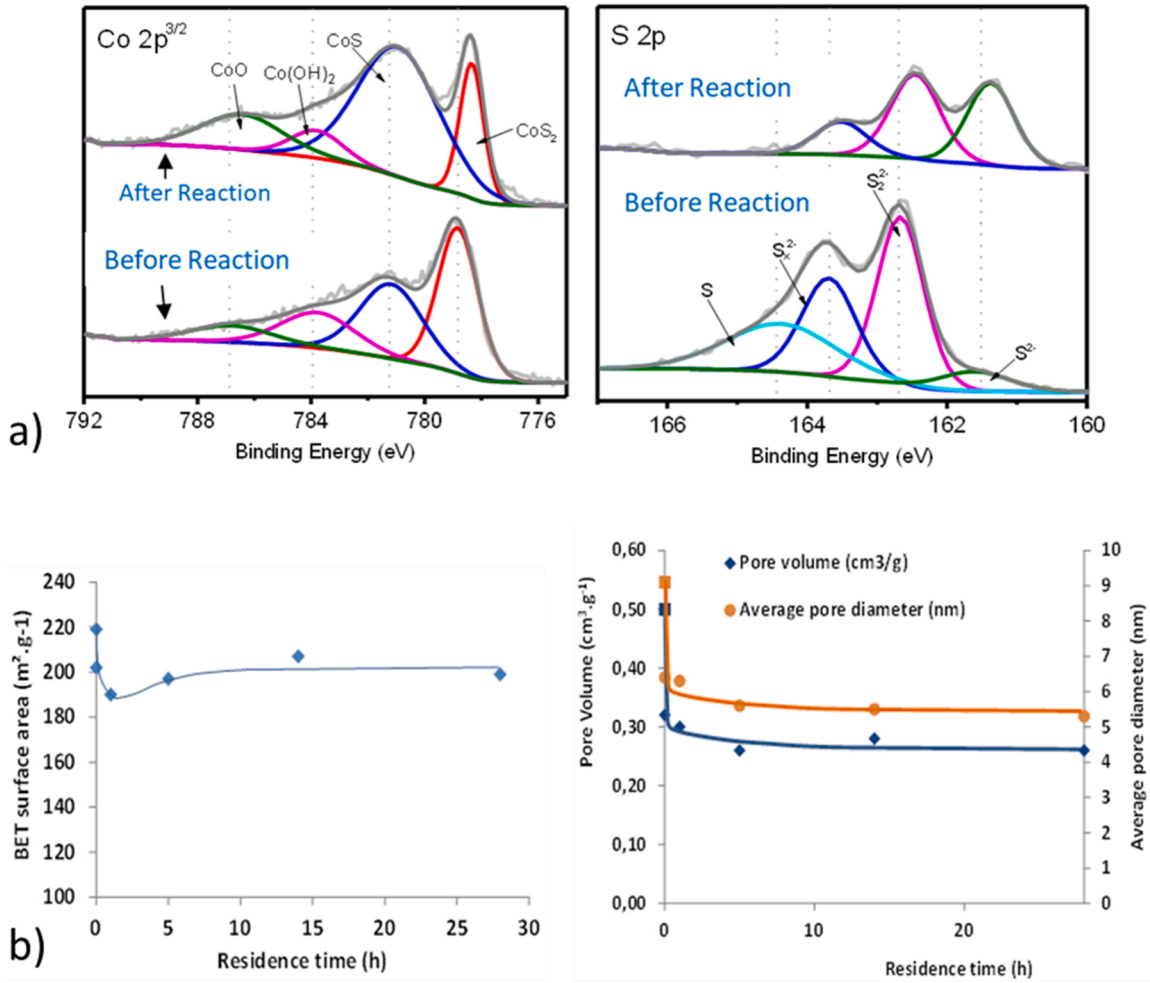

Fig. 16. a) Surface composition of CoS_2 catalyst before and after the reaction [130]. Reprinted (adapted) with permission from L. Shuai, J. Sitison, S. Sadula, J. Ding, M. C. Thies, and B. Saha, *ACS Catal.*, 2018, 8, 6507–6512. Copyright (2018) American Chemical Society. b) Changes in surface area (left panel), pore-volume, and pore diameter (right panel) of sulfided $NiMo/Al_2O_3$ catalyst as a function of lignin hydrotreatment time [156]. This article was published in Applied Catalysis B: Environmental, B. Joffres, M. T. Nguyen, D. Laurenti, C. Lorentz, V. Souchon, N. Charon, A. Daudin, A. Quignard, and C. Geantet, Lignin hydroconversion on MoS_2-based supported catalyst: Comprehensive analysis of products and reaction scheme, Appl. Catal. B Environ., 2016, 184, 153–162, Copyright Elsevier (2016).

mixed with lignin (hydrolysis lignin) and packed into a tubular reactor [158]. No solvents were used in the depolymerization. At the reaction temperature (380 °C, 40 bar of H_2, 4 h), the lignin underwent thermal degradation to smaller fragments, which were then subsequently transformed at the catalyst active site. The H_2 gas which was continuously flowing through the reactor enabled the mass transfer. The liquid products were collected in a gas-liquid separator during the depolymerization, and it consisted of an aqueous phase and an organic phase. The liquid products were composed of hydrocarbons, oxygenates, and phenols. The gaseous products were CO, CO_2, CH_4, etc. The solid product was mainly the lignin condensation product, char, which was separated from the catalyst by sieving. The catalyst was sulfided either *in situ* in the presence of the lignin in the reactor using dimethylsulfide at a temperature range of 200–220 °C (this temperature range is lower than the decomposition temperature of the lignin), or *ex-situ* (a pre-sulfided catalyst mixed with lignin and loaded into the reactor). The elemental analysis of the *in situ* and *ex situ* sulfided catalysts showed a Mo/S ratio of 1.86 and 1.49 (w/w) respectively, indicating a lower degree of sulfidation in the *in situ* sulfided catalyst. The pre-sulfided catalyst was more efficient (higher amount of liquid and gaseous products, and a lower amount of char) than the *in situ* sulfided catalysts. The sulfidation state of the catalyst is the crucial factor for its activity. Increasing the catalyst-to-lignin ratio increased the liquid and gaseous product yield, and consequently decreased the solid residue. This behavior was attributed to the proximity effect between the catalyst active sites and the reactants, which increased with an increase in catalyst amount. Similarly, an increase in H_2 pressure favored a higher rate of hydrogenation and deoxygenation during the hydrocracking process. The study showed the adaptability of commercial sulfided catalysts for process modifications.

A slightly modified semi-continuous batch process with a sulfided $CoMo/Al_2O_3$ catalyst was reported by Pu et al. [159]. A constant flow of H_2 to maintain the reactor pressure and a reflux system to extract continuously the light aromatic products and H_2O from the reactor were the main features of the semi-continuous setup. The semi-continuous approach helped to remove the gases formed during the reaction so that their contribution to catalyst properties/deactivation could be avoided. However, the contribution of H_2O which was not completely removed until the reaction temperature was reached, to catalyst deactivation, could not be avoided. When the catalyst was characterized after the reaction (350 °C, 80 bar H_2, 13 h), significant changes in its composition and textural properties were observed (Fig. 17). Coking had started at the early hours of the reaction. The carbon content in the catalyst after the first hour of the reaction was 12 wt% and remained the same until the end of 13 h (Fig. 17a). The sulfur content was also reduced from 7.5 to 6 wt% after 13 h of reaction (Fig. 17b). However, based on XPS analysis, the S/Mo atom ratio had decreased significantly when comparing the freshly sulfided catalyst to that after 13 h reaction

(2.2 and 1.7 respectively, Fig. 17b). Sulfur loss during the reaction appears to be inevitable for the sulfided catalysts. Other notable changes were observed in the textural properties of the catalyst. The surface area and pore diameter decreased from 193 to 185 m^2/g, and from 0.47 to 0.29 cm^3/g respectively in the first hour and remained the same (Fig. 17a), while the average pore diameter decreased from 7.9 to 6.2 during the first hour and remained almost the same until 13 h. The changes in both the composition and textural properties of the catalyst occurred during the heating period where lignin started to undergo depolymerization (the 0th hour is immediately following the heating period in Fig. 17). Nevertheless, with all these changes in its properties, the catalyst was active for oligomer cracking and deoxygenation reactions during the 13 h (the liquid fraction increased from 44 to 82 wt %). Perhaps, the most important aspect influencing the activity of the catalyst is its sulfur content. If there was a continuous source of sulfur, it can be presumed that the catalyst could have maintained its activity for longer reaction times.

Instead of the ordinary organic solvents used for lignin depolymerization, the use of slurry-oils with sulfided catalysts was also reported. Meier et al. studied the performance of a sulfided $NiMo/Al_2O_3$ catalyst in 5 different slurry-oils [160]. They were, (1) light fraction oil from bitumen and lignin coprocessing (S = 2 wt%), (2) heavy fraction oil of the same bitumen and lignin coprocessing (S = 4 wt%), (3) a recycled residual oil from (2), (4) standard vacuum gas oil, and (5) lignin-derived slurry oil. The performance of the catalyst in different slurry oils is compared in Table 6. Since the lignin-derived slurry oil already contained phenols, the calculation of phenolic yields solely from the lignin feedstock resulted in negative values because the amount of the initial phenol in the lignin slurry oil was subtracted from the total phenols produced after the reaction. The highest yield for solid residue (coke, 10.7 wt%) was obtained when the heavy fraction oil was used as the slurry oil. This amount was about 1.5 times lower than without the catalyst. The minimum yield to the solid residue (0.3 wt%) was obtained with lignin oil. Although the total amount of oil obtained from lignin with different slurry oils was in the high range of 68–83 wt%, the highest being in lignin slurry oil, the amount of phenol obtained ranged only between − 1.4–4.1 wt%. The phenolics yield without the catalyst was only 2.9 wt%. Hence, the catalyst had only a small effect in improving the phenolic yield during the hydrocracking process. When the heavy fraction slurry oil was used in its 3rd recycle run, a higher yield to total lignin oil (79 wt%), with a low yield to the solid residue (4.9 wt %) was obtained. The results of using slurry-oils containing sulfur in combination with a commercial sulfided $NiMo/Al_2O_3$ catalyst appeared highly promising for maintaining the sulfidation state of the catalyst and the commercialization of the process as other noble metal catalysts would normally undergo sulfur poisoning during the reaction.

Table 6
Influence of various slurry oils in organocell lignin hydrocracking [160].

Slurry oil	T (°C)[a]	Solid residue (wt%)	Middle oil (wt %)	Light oil (wt %)	Total oil (wt %)	Phenolics (wt%)
Light fraction[b]	400	16.4	46.0	20.4	66.4	2.9
Light fraction	375	2.7	61.6	15.6	72.2	1.3
Heavy fraction	375	10.7	61.2	7.2	68.4	4.1
Heavy fraction (3rd recycle)	375	4.9	66.9	12.2	79.1	-
Vacuum gas oil	400	3.5	75.2	6.7	81.9	-
Lignin oil	375	0.3	77.6	5.5	83.1	-1.4

[a] 180 bar H_2, 2 h.
[b] without the $NiMo/Al_2O_3$ catalyst.

4.3. Solvent-free processes

Sulfided catalysts were also used for solvent-free hydrotreatment of lignin. The solvent-free attempt was aimed at alleviating the techno-economic issues resulting from solvent recovery and recycling that would arise for large-scale production. Meanwhile, solvents have the advantages that they can impart good heat and mass transfer properties which are poorer in a solvent-free reaction [161]. The earliest study on a solvent-free depolymerization process using sulfided catalysts was reported by Oasmaa et al., who mainly focused on the process and influence of lignin types rather than the catalysts [162]. Five technical lignins; 3 pine Krafts, 1 birch Kraft, and 1 organocell, over a combination of two commercial catalysts; a sulfided NiMo/aluminosilicate catalyst and 20 wt%Cr_2O_3/Al_2O_3 catalyst (1:1) was used for the process. In general, the product oil yields (395–400 °C, 100 bar of H_2, 0.5 h) followed the trend as organocell (71 wt%) > pine Kraft (63 wt%) > birch Kraft (49 wt%)). Out of the produced bio-oil, the detectable aromatic yield was in the range of 19 wt% for organocell, 21 wt% for pine, 14 wt

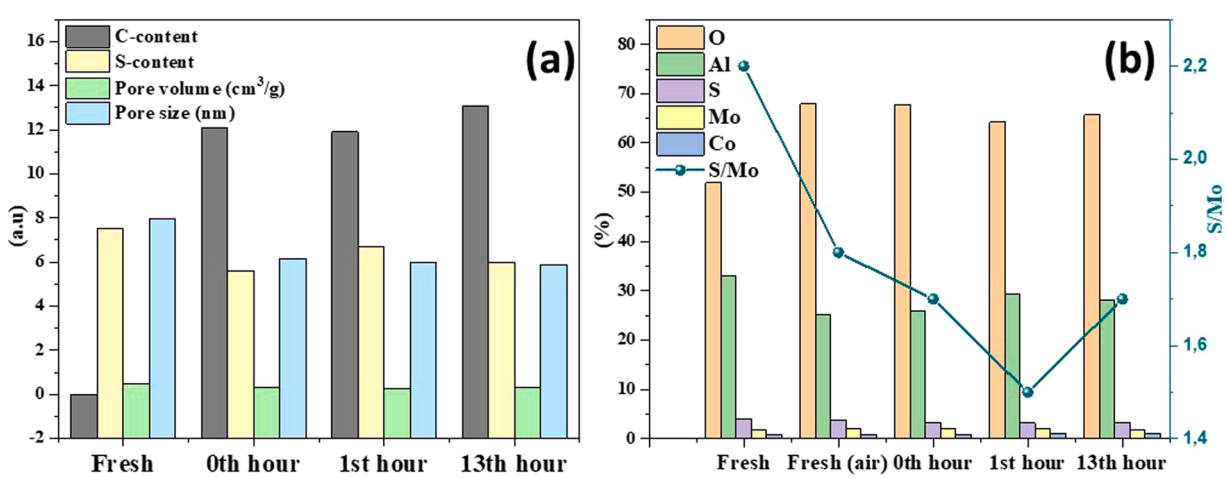

Fig. 17. (a) Variation of C-content (grey bar), S-content (yellow bar), pore-volume (green bar), and pore size (blue bar) of sulfided $CoMo/Al_2O_3$ during lignin depolymerization (350 °C and 80 bar of H_2), and (b) variation of surface composition (O, Al, S, Mo, and Co) from XPS analysis with respect to reaction time. Fresh (air) corresponds to freshly sulfided catalyst exposed to air [159]. The 0th hour immediately follows the heating period. This article was published in Applied Catalysis B: Environmental, J. Pu, T. Nguyen, E. Leclerc, C. Lorentz, D. Laurenti, I. Pitault, M. Tayakout-Fayolle, and C. Geantet, Lignin catalytic hydroconversion in a semi-continuous reactor: An experimental study, Appl. Catal. B Environ., 2019, 256, 117769, Copyright Elsevier (2019).

% for birch Kraft lignins. The amount of solid residue produced after the reaction was however lower for pine Kraft lignin (4 wt%) than organocell and birch Kraft lignins (7 wt%). The study demonstrated that the sulfided catalyst could efficiently depolymerize the lignins to monomers under solvent free conditions at least in laboratory scale (70 g of lignin).

Later, a comparative study of sulfided NiMo on two different supports including activated carbon (AC), and MgO-La_2O_3 oxide was attempted under solvent-free conditions [161]. The sulfided NiMo/AC gave 55 wt% yields (350 °C, 100 bar of H_2, 4 h) to the dichloromethane soluble fraction (average molecular weight being 700 g/mol) with only 9 wt% yields to the solid residue. The monomers in this fraction were largely composed of alkyl phenolics and aromatics. The NiMo/MgO--La_2O_3 gave 48 wt% yields of the dichloromethane soluble fraction having an average molecular weight of 660 g/mol, however with 12.7 wt% of the solid residue. The NiMo/AC catalyst was slightly more effective in producing low molecular weight fragments from the lignin during the depolymerization. The XRD of NiMo/MgO-La_2O_3 after the reaction showed NiS, Ni_3S_4, and MoS phases on the catalyst, indicating its sulfidation state after the reaction (Fig. 18). Only a negligible decrease in the surface area (from 29 to 23 m^2/g) and pore volume (from 0.16 to 0.14 cm^3/g) was observed between the fresh and used catalysts. However, an increase in particle size from 4.3 to 15.7 nm of the supported NiMo occurred after the reaction (Fig. 18), probably due to the severity of the experimental conditions and due to the low heat dispersion effect under solvent-free conditions.

4.4. Other sulfided catalysts

4.4.1. Unsupported catalysts

The main active component of the supported sulfided Ni(Co)Mo/Al_2O_3 catalyst is the MoS_2 phase wherein Ni and Co act mainly as promoters and Al_2O_3 acts as a dispersing medium. The unsupported form of sulfided catalysts has the advantage that they could be synthesized in different morphologies and compositions. Moreover, the unsupported MoS_2 can offer more sulfur vacancies at the edge of its slabs. Unsupported sulfided catalysts were also studied in lignin depolymerization. Li et al., synthesized MoS_2, and MoS_2-based composite catalysts (MS_x/MoS_2, M = Ni, Co, Ag) with a flower morphology (Fig. 19a-d) for lignin (corn stover) depolymerization [163]. A bio-oil yield of > 78 wt% (310 °C, 25 bar H_2, 1 h) was obtained over MoS_2. The performance of other sulfided catalysts (NiS_2, CoS_2, and Ag_2S) was inferior (< 65 wt% yields) to that of MoS_2. A significant improvement in bio-oil yield (>85 wt%) was obtained when the composite catalysts NiS_2/MoS_2, and CoS_2/MoS_2 were used (5 wt% of MS_2). The enhancement in the catalytic activity of MoS_2 when other metal sulfide components were present was explained by the Edge Decoration (ED) model. Characterization studies showed that the parent MoS_2 had the typical layer structure where the edges of the layers are wedge-shaped providing the hydrogenation sites. When NiS_2 and CoS_2 were present, the layer structure of MoS_2 became more curved and less stacked, increasing the amount of potential surface-active sites. This was in conjunction with the enhancement in the surface area of MoS_2 (5 m^2/g) when NiS_2 and CoS_2 were present (6 and 15 m^2/g for NiS_2/MoS_2 and CoS_2/MoS_2 catalysts, respectively). According to the ED model, the NiS_2 weakened the Mo-S bond, thereby promoting the breakage of the Mo-S bond for the generation of S vacancies (active site for hydrogenation). Further comparison of MoS_2 with FeS_2 and CuS showed the activity trend for bio-oil production as (250 °C, 1 h, no H_2 pressure) MoS_2 (82 wt%) > CuS (65 wt%) > no catalyst (53 wt%) > FeS_2 (37 wt%) [164].

Another unsupported sulfided catalyst reported for lignin depolymerization is VS_2 where different morphologies of catalyst (sheets and nanoflowers) were compared (Fig. 19 e-h) [165]. When VS_2 sheets were used, the lignin conversion was at about 77 wt% with 59 wt% yields to the bio-oil (250 °C, 20 bar of H_2, 1.5 h). The solid residue amount accounted for nearly 22 wt% yields. The use of VS_2 nanoflowers decreased the conversion (65 wt%) and bio-oil yield (50 wt%) and increased the solid residue amount (35 wt%). The flower morphology imparted steric hindrance to the reactant and eventually decreased its catalytic performance. According to the proposed mechanism, the H atoms from thermally broken H_2 molecules adsorbed on the VS_2, leading

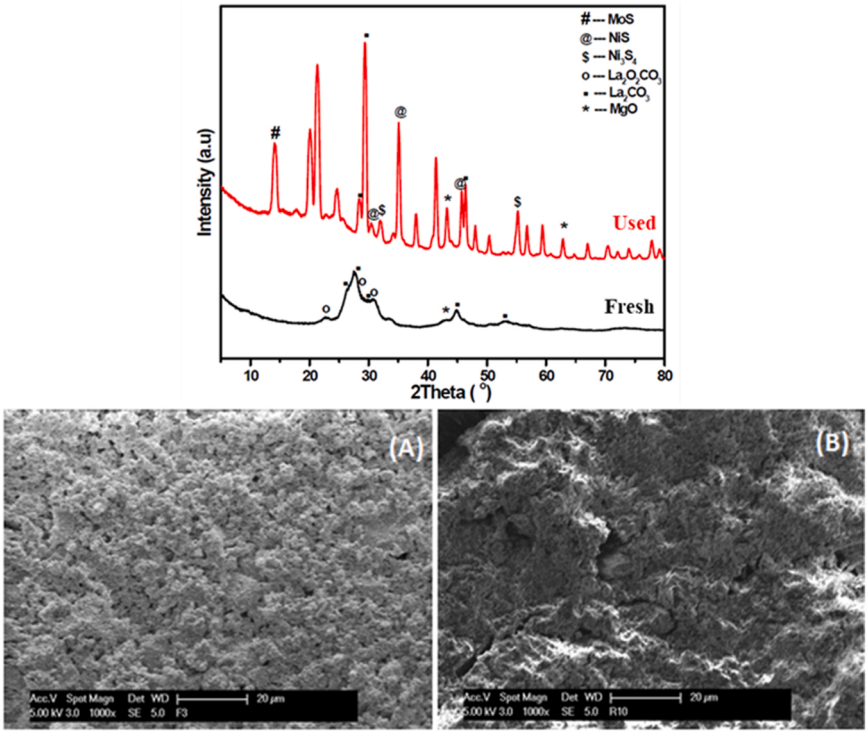

Fig. 18. XRD (top panel) of fresh oxide NiMo/MgO-La_2O_3 and after the reaction showing sulfide phases. SEM images (bottom panel) of oxide NiMo/MgO-La_2O_3, (A) before and (B) after reaction showing particle agglomeration [161]. C. R. Kumar, N. Anand, A. Kloekhorst, C. Cannilla, G. Bonura, F. Frusteri, K. Barta, and H. J. Heeres, *Green Chem.*, 2015, **17**, 4921–4930, reproduced by permission of The Royal Society of Chemistry.

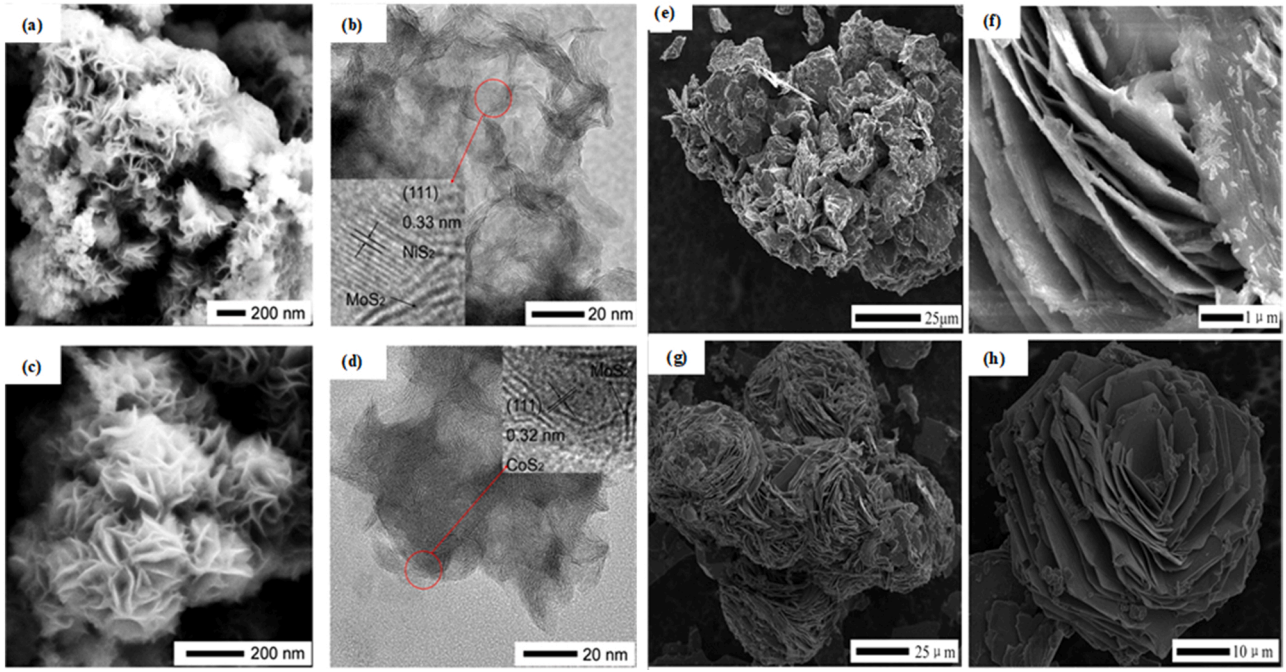

Fig. 19. (a) & (b) SEM and TEM images of NiS_2/MoS_2, (c) & (d) SEM and TEM images of CoS_2/MoS_2 [164], (e) & (f) SEM images of VS_2 nanosheets, and (g) & (h) SEM images of VS_2 nano flowers [165]. Reprinted (adapted) with permission from Q. Tian, N. Li, J. Liu, M. Wang, J. Deng, J. Zhou, and Q. Ma, *Energy Fuels*, 2015, 29, 255–261. Copyright (2015) American Chemical Society.

to the formation of -VH and -SH bonds. These bonds were unstable and could undergo breakage to form the VS_2 catalyst, meanwhile transferring the hydrogen to the unsaturated reactant molecule.

4.4.2. *Supported catalysts*

Narani et al. [166] found better results with sulfided a NiW/AC catalyst than NiMo/AC catalyst for the hydrotreatment of Kraft lignin in supercritical methanol (320 °C, 35 bar of H_2, 8 h). Two fractions (methanol and dichloromethane soluble fractions) of liquid products were identified. The methanol soluble oil was composed of aromatic monomers and low molecular weight (500 g/mol) oligomers, and the dichloromethane soluble fraction was composed of solely high molecular weight (2725 g/mol) oligomers. When sulfided NiMo/AC was used, a 57 wt% yield to the methanol soluble oil was obtained. Only a trace amount of char was formed over the catalyst. The performance of sulfided CoMo/AC was inferior to that of the NiMo/catalyst (41 wt% yield to methanol soluble oil with 9 wt% yield to char), possibly due to the increase in acidity of the catalyst when Ni was replaced with Co. Sulfided NiW/AC increased the methanol soluble oil yield to 82 wt% with no concurrent char formation. The acidity of the sulfided NiW/AC catalyst was even lower than NiMo/AC and was ascribed to the reason for the increase in the product yield (18.4 *versus* 44.5 $\mu mol g^{-1}$ of NH_3 adsorption). Over the non-sulfided NiW/AC catalyst, substituted guaiacols were the predominant product. Sulfidation improved the activity towards deoxygenation (involving removal of $-OCH_3$) leading to more phenols. By prolonging the reaction time from 8 to 24 h up to 35 wt% yield to monomers was obtainable. Nonetheless, this longer reaction time did not lead to over-hydrogenated compounds, highlighting the selectivity of the catalyst for phenols. The effect of different supports such as acidic ZSM-5, and basic $MgO–La_2O_3$, $MgO–CeO_2$, and $MgO–ZrO_2$ were also investigated for the depolymerization. Their performance was inferior to that of AC. The $MgO–La_2O_3$ (291 $\mu mol g^{-1}$ of CO_2 adsorption, the highest of all basic supports) gave similar results like NiW/AC. Different characterization techniques were used to analyze the structure and composition of the used catalysts. XRD of the spent NiW/AC catalyst showed peaks corresponding to WS_2 and Ni_3S_2 phases, indicating its sulfided state. In support of this, the EDX analysis of the spent catalyst showed 2 wt% of sulfur on it, which was homogeneously distributed. Morphological analysis of the spent catalyst by TEM confirmed the preservation of its spherical morphology (Fig. 20a), however, particle agglomeration was observed. The catalyst was in its active state even after a long reaction time of 24 h, indicating its high stability for longer reaction runs.

Another important factor that affects the activity and stability of a sulfided catalyst during lignin hydrotreatment is the impurities in the lignin. Recently, our group has reported the role of inorganic impurities of a commercial Kraft lignin (Na, K, Ca, Fe, etc.,) on the activity of sulfided $NiMo/Al_2O_3$ catalyst [7]. These impurities in the lignin come from the Kraft pulping process which uses reagents NaOH and Na_2S, and from the source wood. These inorganic impurities were deposited on the catalyst during the depolymerization, of which the major impurity element was the Na because of its higher amount in the lignin. Conditional studies using poisoned catalyst showed that at lower loadings of individual inorganic impurities, their promotor effect was prominent (the monomer yields were higher than in their absence on the catalyst, Fig. 20b). However, at their higher loadings, their poison effects were dominant. When all these elements were present together on the catalyst, their poisoning effect was much stronger. The number of moles of impurities, their strength, and their synergism were the main factors responsible for the catalyst deactivation.

In summary, both supported and unsupported sulfided catalysts have been used for the hydrotreatment of various lignins. Supporting the metal sulfide active phase on various metal oxides (Al_2O_3, $MgO–La_2O_3$, etc.) is helpful for its high dispersion. On the other hand, the unsupported catalysts have the advantages that they can be synthesized in different morphologies and compositions to tune the activity. But, the unsupported catalysts are prone to particle agglomeration (increase in their crystallite sizes) under long heat treatments. Supported sulfided catalysts were employed to study process modifications in lignin hydrotreatments. The catalysts showed good adaptability in batch, semi-continuous, and solvent-free lignin hydrotreatments. The deactivation of the sulfided catalyst occurs mainly through the removal of lattice sulfur atoms, and through the deposition of impurities from the feedstock. The latter is a common mode of deactivation in most catalytic

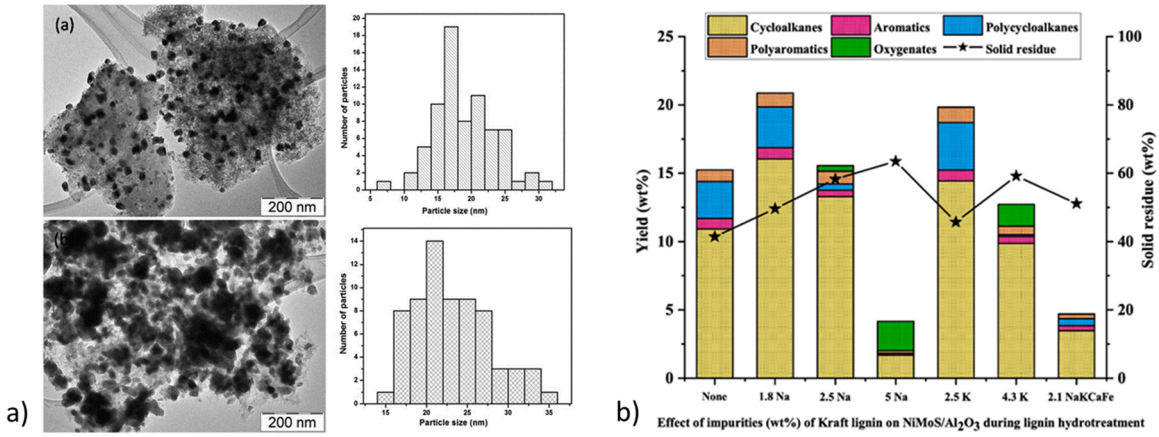

Fig. 20. a) TEM images of NiW/AC catalyst (a) before, and (b) after the reaction at 320 °C, 35 bar of H_2, 8 h [166]. A. Narani, R. K. Chowdari, C. Cannilla, G. Bonura, F. Frusteri, H. J. Heeres, and K. Barta, *Green Chem.*, 2015, **17**, 5046–5057, reproduced by permission of The Royal Society of Chemistry. b) The role of impurities of Kraft lignin on the activity of sulfided $NiMo/Al_2O_3$ catalyst during depolymerization (345 °C, 45 bar H_2, and 8 h) [7]. J. Sebastian, Y.W. Cheah, D. Bernin, D. Creaser, L. Olsson, *Catalysts,* **11**, 2021, 874, reproduced by permission of MDPI.

processes and can be solved by using impurity-free feedstocks. A crucial factor governing the stability of sulfided catalysts is the sulfidation state of the catalyst. During deoxygenation reactions, there is a high risk that the removed oxygen atoms could substitute the lattice sulfur atoms, decreasing the sulfur vacancies and sulfidation state of the catalyst. The H_2 gas used in the hydrotreatment could also remove some fraction of S as H_2S. In these circumstances, a simple re-sulfidation of the catalyst can regenerate its sulfidation state and restore the activity. Another method to maintain the sulfidation state of the catalyst is to provide a continuous supply of sulfur sources during the hydrotreatment. The use of lignins containing a significant amount of sulfur (e.g, Kraft lignin) has the advantage of maintaining the sulfidation state of the catalyst longer than the use of sulfur-free lignins (e.g, hydrolysis lignin).

5. Kinetic modeling studies based on metal sulfide catalysts

The kinetics for deoxygenation of oxygenates presented in biomass-derived oils have been studied using model compounds and real feedstocks in the currently reported literature. The subject remains important as it allows a better understanding of the reaction mechanisms, and the function of catalysts and it facilitates the upscaling of the reaction process. The approach for kinetic modeling studies, for lab-scale level research, involves the construction of mathematical expressions for the mass and heat transfer phenomena, in some cases phase equilibrium, and further develops the kinetic model based on a lumped or molecular-based approach depending on the complexity of the feedstocks. The following section discusses the kinetics of HDO reactions for triglycerides, phenolics, lignin, and biomass-derived oils over metal sulfides.

5.1. Kinetics for the HDO of triglycerides

A kinetic study based on a sulfided $CoMo/Al_2O_3$ catalyst for the hydrotreatment of a mixture of 10 wt% cottonseed oil with desulphurized diesel to produce renewable diesel has been reported by Sebos et al. [78] A plug flow approximation for the reactor was considered to study the kinetics of the HDO of the triglycerides of the feedstock. Overall kinetics were presented including the influence of internal mass transfer resistance. The first-order reaction kinetics was presented with the reaction rate constant (k_{HDO})calculated as:

$$k_{HDO} = -\ln(1-x) \bullet \dot{m}/m_{cat}$$

where x is the conversion, $\dot{m}$ is the mass feed (a mixture of 10 wt% of refined cottonseed oil in desulfurized diesel (S < 50 ppm)) and m_{cat} is the mass of the catalyst. The experimental conversion values were plotted with the one proposed by the model to estimate the goodness of the model as shown in Fig. 21A).

A pseudo-first-order lump-type kinetic model was developed by Sharma et al. to study the deoxygenation of triglycerides (jatropha oil) over mesoporous titanosilicate (MTS) supported sulfided CoMo catalyst to determine the triglyceride conversion pathway at 300 °C and 320 °C [167]. The best-fitted model showed that the triglycerides were converted not only to deoxygenated (C15 – C18) and oligomerized (> C18) products but also were directly cracked to lighter (< C9) and middle (C9 – C14) range hydrocarbons (as shown in Fig. 21B). Among all, the oligomerized product formation rate is the highest at these temperatures from the triglycerides (Table 7).

A recent study on the reaction kinetics based on the hydrodeoxygenation of stearic acid (SA) was reported by Arora et al. over a sulfided $NiMo/\gamma\text{-}Al_2O_3$ catalyst [59]. A Langmuir-Hinshelwood (LH) type kinetic model was developed that showed good agreement with the experimental variation of selectivities with different reaction conditions. In their work, a simplified pathway for HDO of SA is shown (Scheme 2) and the LH type rate expressions used are presented in Table 8. The reaction scheme includes intermediates like octadecanal (C18 =O) and octadecanol (C18-OH) and explains the selectivity for the three major reaction routes (decarboxylation, decarbonylation, and direct-HDO). A single catalytic reaction site was considered here and hence an SA inhibition term is included in all the rate expressions. The presented results show that the model can predict well the increase in the conversion rate of stearic acid with the increase in temperature. The key in their work was that a phase equilibrium model was used to predict the saturation concentration of H_2 in the liquid phase which depends on the reaction temperature. It was assumed in their study that the gas-liquid transport was fast compared to the rate of reaction and hence allowed the activation energies for the reactions to be predicted. The model could also predict well the conversion and selectivity with variations in residence time, pressure, and feed concentration [59].

Hočevar et al. explored the kinetics of HDO using model compounds involving primary/secondary alcohol (1-hexanol), aldehyde (hexanal), methyl ester (methyl hexanoate), ether (dihexyl ether), carboxylic acid (hexanoic acid) [168]. Based on the kinetics constants and activation energies obtained from mathematical modeling and DFT calculation, it was observed that the primary alcohol is more resistant to HDO which undergoes a dehydration reaction to form ethers at the studied conditions. The secondary alcohol follows the typical path like that one highlighted in Scheme 2. Interestingly, experiments with a high initial concentration of aldehyde (hexanal) led to a parallel aldol condensation

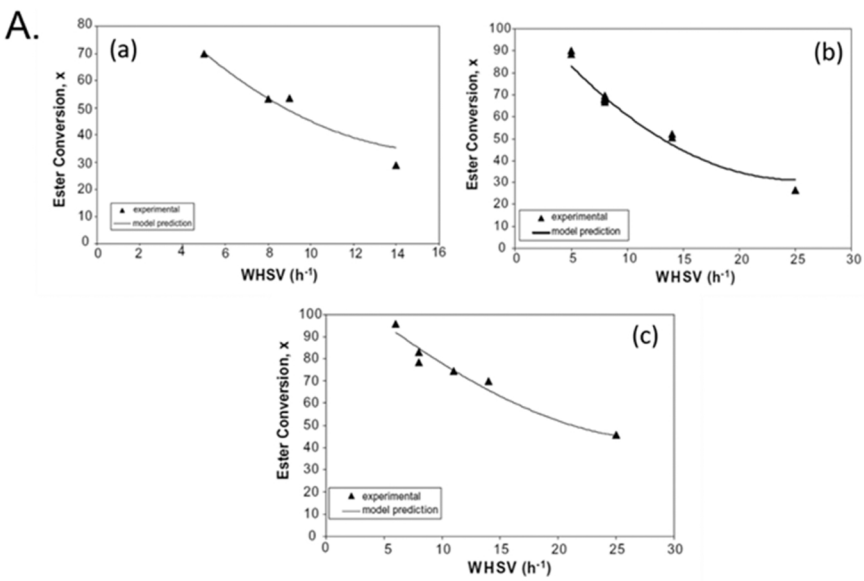

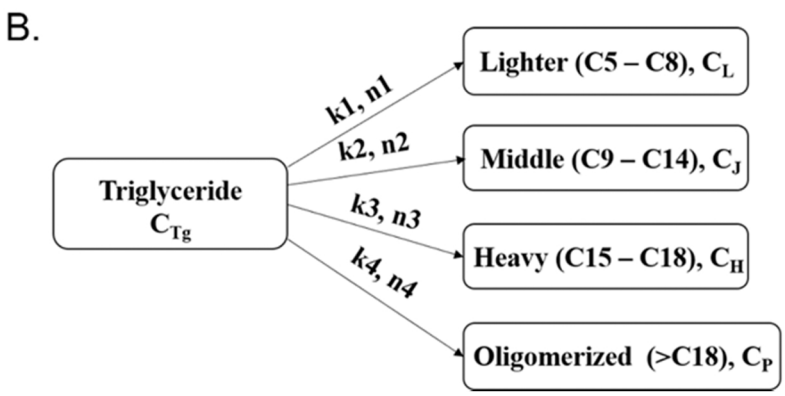

Fig. 21. A) Conversion of ester w.r.t. WHSV for 10 wt% cottonseed oil in desulphurized diesel at P = 30 bar, P_{H2S} = 1 vol%, catalyst mass = 5 g for (a) T = 305, (b) T = 320 and (c) T = 335 ℃ respectively [78]. This article was published in Fuel, I. Sebos, A. Matsoukas, V. Apostolopoulos, and N. Papayannakos, Catalytic hydroprocessing of cottonseed oil in petroleum diesel mixtures for production of renewable diesel, Fuel, 2009, 145–149, Copyright Elsevier (2009). B) Triglyceride conversion pathway over CoMo/MTS catalyst [167]. This article was published in Catal. Today, R. K. Sharma, M. Anand, B. S. Rana, R. Kumar, S. A. Farooqui, M. G. Sibi, and A. K. Sinha, Jatropha-oil conversion to liquid hydrocarbon fuels using mesoporous titanosilicate supported sulfide catalysts, Catal. Today, 2012, 314–320, Copyright Elsevier (2012).

Table 7
Kinetic rate constants for possible reaction network in the conversion of triglycerides over CoMo/MTS catalysts [167].

Parameter	300 ℃			Parameter	320 ℃		
	Value	Error (%)	R^2		Value	Error (%)	R^2
k'	7.39	0.47	0.97	k'	14.35	1.63	0.99
k_1	0.03	0.25	-	k_1	0.04	0.47	-
k_2	0.02	0.25	-	k_2	0.11	0.47	-
k_3	0.07	0.25	-	k_3	1.24	0.48	-
k_4	7.27	0.34	-	k_4	13.25	1.17	-

reaction (C-C coupling to C12 hydrocarbon) in addition to the deoxygenation reaction (C6). However, the products of the aldol condensation reaction were not noticed for HDO of any other model compounds owing to its very low concentration and high reactivity for hydrogenation [168].

5.2. Kinetics for the HDO of phenolics

The kinetic analysis of the HDO of phenolic compounds dates back to 1987 when Gevert et al. [169] studied the reaction kinetics of 4-methylphenol HDO over a sulfided $CoMo/Al_2O_3$ catalyst and concluded that the HDO reaction of methyl-substituted phenols can occur through two independent pathways, one forming aromatic products (by direct

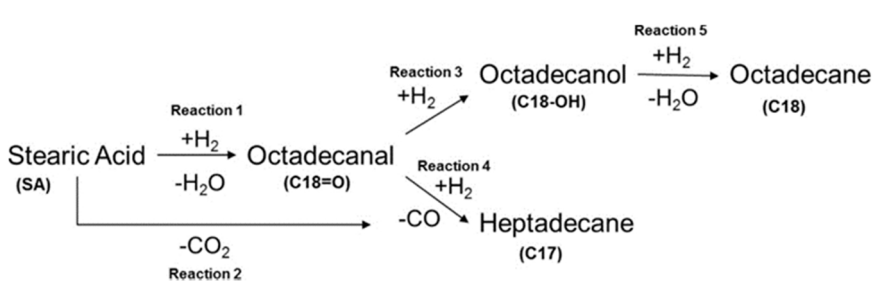

Scheme 2. Simplified reaction scheme (HDO of stearic acid) for a kinetic model [59]. This article was published in Chemical Engineering Journal, P. Arora, E. L. Grennfelt, L. Olsson, and D. Creaser, Kinetic study of hydrodeoxygenation of stearic acid as a model compound for renewable oils, Chem. Eng. J., 2019, 376–389, Copyright Elsevier (2019).

Table 8
Reactions and rate expressions for the HDO of SA [59].

	Reaction	Rate expression
r1	$C_{18}H_{36}O_2 + H_2 \rightarrow C_{18}H_{36}O + H_2O$	$r_1 = \frac{k_1 C_{SA} C_{H2}}{(1 + K_{SA} C_{SA})}$
r2	Decarboxylation $C_{18}H_{36}O_2 \rightarrow C_{17}H_{36} + CO_2$	$r_2 = \frac{k_2 C_{SA}}{(1 + K_{SA} C_{SA})}$
r3	Direct-HDO $C_{18}H_{36}O + H_2 \rightarrow C_{18}H_{37}OH$	$r_3 = \frac{k_3 C_{C18=O} C_{H2}}{(1 + K_{SA} C_{SA})}\left(1 - \frac{a_{C18OH}}{a_{C18=O} a_{H2} K_{eq}}\right)$
r4	Decarbonylation $C_{18}H_{36}O \rightarrow C_{17}H_{36} + CO$	$r_4 = \frac{k_4 C_{C18=O}}{(1 + K_{SA} C_{SA})}$
r5	$C_{18}H_{37}OH + H_2 \rightarrow C_{18}H_{38} + H_2O$	$r_5 = \frac{k_5 C_{C18OH}}{(1 + K_{SA} C_{SA})}$

deoxygenation of phenol, DDO) and the other naphthenic products (ring hydrogenation followed by deoxygenation of saturated or partially saturated phenols to cycloalkanes, HYD). No oxygen-containing products were detected. The rate-limiting step in path 1 has been considered as the C-O bond cleavage and that in path 2 as the hydrogenation of phenol's aromatic ring [169].

The reaction network is shown in Scheme 3 A) where (a) represents 4-methylphenol, (b) is toluene, and (c) represents methylcyclohexane plus methylcyclohexene. The authors also calculated that the adsorption constant for path 1 is twice as large as that of path 2. This indicated that the two reaction paths proceed on two different types of active sites. The poisoning effect of H_2S on such HDO reactions was also studied which showed that H_2S strongly suppresses toluene formation from path 1 whereas it hardly affects path 2, which supports their hypothesis that the two paths occur on two different catalytic active sites [169]. However, it was worth highlighting that authors tend to explain the deoxygenation pathways in different ways. For instance, in the study conducted by Wang et al. [112], they considered that the adsorption scheme of p-cresol on the sulfided catalyst surface differed between the deoxygenation paths.

Later the effects of methyl substituents of methyl-substituted phenols on the HDO reaction over a sulfided $CoMo/Al_2O_3$ catalyst were studied by Simons and co-workers [97]. They also investigated the relationship between the relative reactivities of the methyl-substituted phenol species and the intrinsic properties of the reactant determined from electronic structure calculations. These properties include the electrostatic potential in the reactant molecules and also the electron-binding energies of various molecular orbitals. The reaction data were analyzed using Langmuir-Hinshelwood (LH) kinetics to determine the adsorption and rate constants leading to the two independent aromatic and cyclohexane paths.

The following LH equations were considered here:

$$\frac{\partial A}{\partial \tau} = -\frac{k_1 K_A A + k_2 K_A A}{(1 + C_0 K_A A)^n} \quad (1)$$

$$\frac{\partial B}{\partial \tau} = \frac{k_1 K_A A}{(1 + C_0 K_A A)^n} \quad (2)$$

$$\frac{\partial C}{\partial \tau} = \frac{k_2 K_A A}{(1 + C_0 K_A A)^n} \quad (3)$$

where the mole fractions of the methyl-substituted phenolic feed (A), the aromatic benzene (B), and the cyclohexane and cyclohexene (C) formed from two different pathways as discussed above [169].

K_A= equilibrium constant when A is adsorbed on the catalyst surface.

k_1= rate constant for the formation of the aromatic product (DDO pathway).

k_2= rate constant for the formation of hydrocarbon products (HYD pathway).

C_0= feed concentration of A.

τ= space-time variable and n = order of inhibition.

The kinetic analysis of their work showed that the optimal n parameter in Eqs. (1), (2), and (3) was $n = 2$, which resulted in the best fit of the data. This result has been interpreted as the reactions for both pathways involving an adsorbed species and an active site. The assumption of having only one adsorption site, K_A was also examined by applying two separate adsorption constants, K_B and K_C, for each reaction with modified Eqs. (1), (2), and (3). Their results from the regression analysis demonstrated that both K_B and K_C constants were identical and within the experimental errors, which is the equivalent to a single value (K_A). Hence, a single catalytic site was considered to be present for both reaction pathways due to the same adsorption constant being calculated.

Fig. 22A (a) shows the variation of the adsorption constant depending on the location of the methyl groups. The k_1 rate constant leading to the aromatic products is the lowest for phenols and highest for 3,5-DMP (Fig. 22A (b)). The k_2 rate constant for the aromatic ring hydrogenation path shows a different trend from k_1. k_2 seems to drop significantly with the methyl group in position 2 (Fig. 22A (c)). Overall, from Fig. 22 the authors showed significant variations in the adsorption and rate constants as the location and number of the substituent methyl groups varied [97]. A correlation between the derived adsorption, rate constants, and molecular parameters is also studied in this work.

A kinetic study of guaiacol (GUA) conversion over a ReS_2/SiO_2 catalyst using an LH kinetic model was studied by Leiva et al. [170]. They observed two different kinds of active sites for the guaiacol conversion over ReS_2/SiO_2 and dissociative adsorption of hydrogen was considered. The two active sites are the metal ion vacancy (M) and the

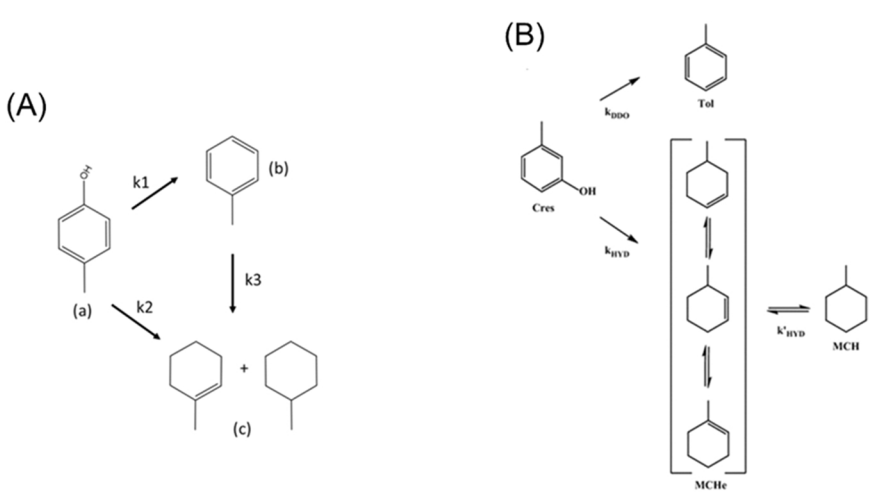

Scheme 3. A) Simplified reaction paths for HDO of 4-methylphenol [169]. This article was published in Applied Catalysis B: Environmental, S. Gevert, J. Otterstedt, and F. Massoth, Kinetics of the HDO of methyl-substituted phenols, Applied Catalysis, 1987, 119–131, Copyright Elsevier (1987). B) Reaction network of the deoxygenation of m-cresol isomers over sulfided catalysts [170]. This article was published in Applied Catalysis A: General, K. Leiva, C. Sepulveda, R. Garcia, D. Laurenti, M. Vrinat, C. Geantet, and N. Escalona, Kinetic study of the conversion of 2-methoxyphenol over supported Re catalysts: Sulfide and oxide state, Applied Catalysis A: General, 2015, 505, 302–308, Copyright Elsevier (2015).

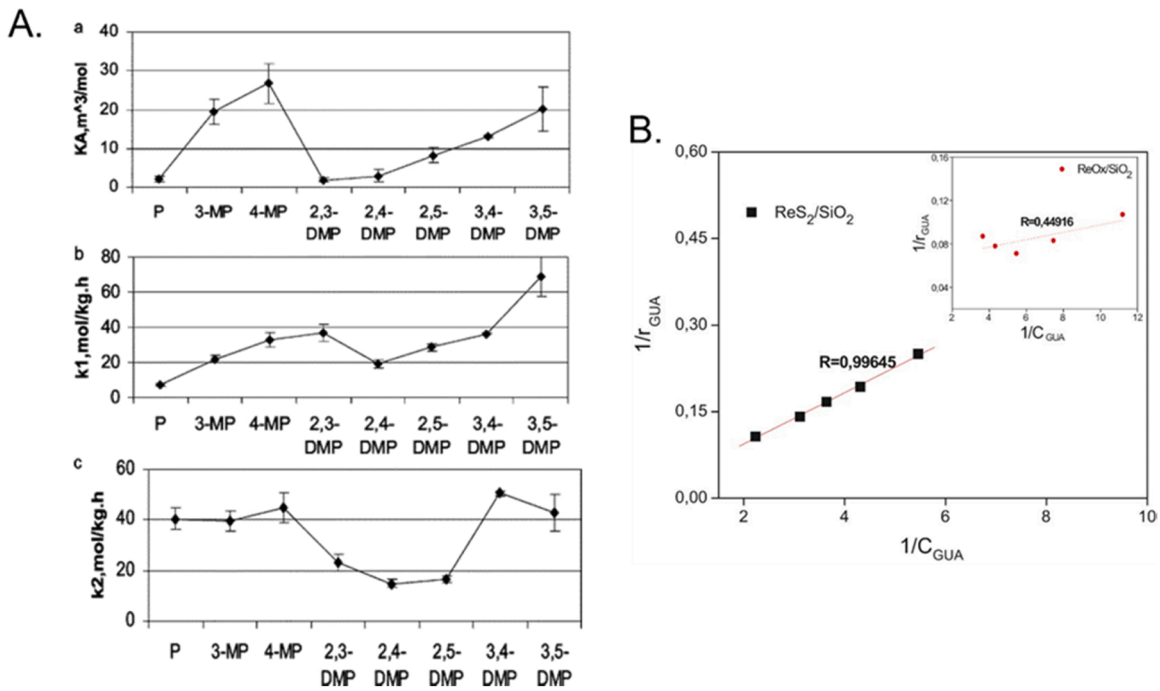

Fig. 22. A) Effect of methyl position on (a) adsorption constant, (b) rate constant, k_1 and (c) rate constant, k_2 for the HDO of methyl-substituted phenols [97]. Reprinted (adapted) with permission from F. E. Massoth, P. Politzer, M. C. Concha, J. S. Murray, J. Jakowski, and J. Simons, *J. Phys. Chem. B*, 2006, 110, 14283–14291. Copyright (2006) American Chemical Society. B) Linearization of the kinetic Model for ReS_2/SiO_2 catalyst. Inset: linearization of the kinetic model for ReO_x/SiO_2 catalyst [170]. This article was published in Applied Catalysis A: General, K. Leiva, C. Sepulveda, R. Garcia, D. Laurenti, M. Vrinat, C. Geantet, and N. Escalona, Kinetic study of the conversion of 2-methoxyphenol over supported Re catalysts: Sulfide and oxide state, Applied Catalysis A: General, 2015, 505, 302–308, Copyright Elsevier (2015).

sulfur stable ion (X^{2-}-M). The rate-determining step considered here was the H^+ attack on the oxygen of the methoxy group. The reactions considered for the model are as follows:

Adsorption of GUA:

$$GUA + M \leftrightarrow GUA - MEquilibriumK_{GUA} \tag{4}$$

Hydrogen dissociative adsorption:

$$H_2 + M + X^{2-} - M \leftrightarrow H^- - M + H^+ - X^{2-} MEquilibriumK_{H2} \tag{5}$$

Addition of H^-:

$$GUA - M + H^- - M \leftrightarrow GUAH^- - M + MEquilibriumK_3 \tag{6}$$

Addition of H^+:

$$GUAH^- - M + H^+ - X^{2-} - M \rightarrow Ph + MeOH + 2M \text{ Rate constant } K_4 \tag{7}$$

The rate expression used here is:

$$\frac{1}{r_{GUA}} = \frac{1}{k_{GUA} C_{H2}} + \frac{1}{k_{GUA} K_{GUA} C_{H2} C_{GUA}} \tag{8}$$

Fig. 22B clearly shows the goodness of fit of the model (Eq. (8)) which follows a linear behavior. This result indicates the presence of two different active sites on the sulfided catalyst. The authors also showed that this kinetic model did not fit well the catalytic activity of ReO_x/SiO_2 (shown in the inset in Fig. 22B) suggesting that ReO_x/SiO_2 followed a different pathway for the conversion of GUA [170].

The HDO of cresol isomers over sulfided Mo/Al_2O_3 and $CoMo/Al_2O_3$ was investigated by Gonçalves et al. [171]. They reported that over both catalysts the reactivity of cresols follows the order: m-cresol > p-cresol > o-cresol. The kinetic analysis of the HDO of m-cresol was studied in this work and the role of cobalt on the HDO of three cresols was investigated [171].

Scheme 3B shows that the HDO of cresols follows two independent pathways. The desired direct deoxygenation (DDO) pathway forms toluene (TOL) (strongly promoted by Co), whereas, the hydrogenation (HYD) route forms methylcyclohexene (MCHe) and methylcyclohexane (MCH) (not affected by Co). A pseudo-first-order reaction kinetic model was assumed to apply for the reactions. k_{DDO} and k_{HYD} are the kinetic rate constants for the DDO and the HYD pathways respectively, k'_{HYD} is the intrinsic rate constant for the hydrogenation of methylcyclohexene to methylcyclohexane, C_{TOL}, C_{MCHe} and C_{MCH} represent the molar concentrations of toluene, methylcyclohexenes, and methylcyclohexane [171].

$$C_{CRE} = C_{CRE,0}.e^{-k_{HDO}.\tau} \tag{9}$$

$$C_{TOL} = \frac{C_{CRE,0}.k_{DDO}}{k_{HDO}}\left(1 - e^{-k_{HDO}.\tau}\right) \tag{10}$$

$$C_{MCHe} = \frac{C_{CRE,0}.k_{HYD}}{k_{HDO} - k'_{HYD}}\left(e^{-k'_{HYD}.\tau} - e^{-k_{HDO}.\tau}\right) \tag{11}$$

$$C_{MCH} = C_{CRE,0}\left(1 - e^{-k_{HDO}.\tau}\right) - \frac{k_{DDO}}{k_{HDO}}\left(1 - e^{-k_{HDO}.\tau}\right) - \frac{k_{HYD}}{k_{HDO} - k'_{HYD}}\left(e^{-k'_{HYD}.\tau} - e^{-k_{HDO}.\tau}\right) \tag{12}$$

The selectivity of each product i (in mol%) can be calculated from Eqs. (10)–(12) as:

$$S_i = \frac{C_i}{C_{CRE,0} - C_{CRE}} \times 100 \tag{13}$$

Fig. 23 shows that the experimental data points and those predicted by the model fit well for the selectivity of products as a function of the conversion of m-cresol validating the model. It has been shown from the values of the rate constants that the hydrogenation of methylcyclohexene to methylcyclohexane was 2.9 times higher over $CoMo/Al_2O_3$ when compared to Mo/Al_2O_3, showing that Co acts as a promoting agent

improving the hydrogenating properties of molybdenum sulfide [171].

Further, the promotional effect of isolated Co atoms decorated on monolayer MoS_2 sheets ($^{S}MoS_2$) was studied by Liu et al. [172]. A kinetic study was developed for the conversion of 4-methylphenol to toluene and it was demonstrated that cobalt immobilization on the MoS_2 monolayer (Co- $^{S}MoS_2$) showed a 34 times higher rate (396.4 ml $s^{-1}mol_{Mo}^{-1}$) when compared to non-promoted $^{S}MoS_2$ (11.7 ml $s^{-1}mol_{Mo}^{-1}$) at 30 bar and 300 °C (Fig. 24a). The activity order shows: Co- $^{S}MoS_2$ > $^{S}MoS_2$ > $^{F}MoS_2$ > bulk MoS_2. $^{F}MoS_2$ stands for few-layer MoS_2. It was also shown that the incorporation of single Co atoms on the basal planes of $^{S}MoS_2$ facilitates the formation of more basal sulfur vacancy sites during hydrogen activation at 300 °C that enhances the activity of the Co-doped monolayer MoS_2 for the HDO of 4-methylphenol. The rate of the HDO reaction was calculated considering a pseudo-first-order reaction (Eq. (14)) [172]:

$$\ln(1-x) = -kC_{cat}t \tag{14}$$

k = pseudo first order reaction constant (ml s^{-1} mol^{-1}).
x = conversion of 4-methylphenol.
C_{cat} = concentration of catalyst under reaction system.
t = reaction time (s).

Recent work by Cheah et al. investigated the role of transition metals (Ni, Cu, Zn, Fe) on γ-Al_2O_3 supported MoS_2 for the HDO of propylguaiacol (PG) [173]. In this work, the authors developed a kinetic model considering the reaction network to elucidate the reaction pathway of demethoxylation and dihydroxylation of PG. The experimental results were nicely fitted to the model, thus validating the model. Initially, the authors developed a simplified pseudo-first-order kinetic model to fit the kinetic data for the HDO of PG considering the route: A = 4-propylguaiacol → B = 4-propylphenol → C = propylbenzene → D = propylcyclohexane as shown in Fig. 24b). However, this simple kinetic model could not fit the experimental results well as shown in Fig. 24b), because it did not take into consideration any of the side reactions. Thereafter, another model was proposed taking into consideration all the main side reactions, including intermediates and reactants. The fit for the reaction kinetics for all the catalysts improved with this modified model with over a 90% coefficient of determination [173]. More importantly, their work also provided a means of evaluating how the promoters (Ni, Fe, Zn, and Cu) for MoS_2/Al_2O_3 influenced the product selectivity for different pathways and eventually the products of the reaction with the aid of the kinetic model. Their results suggested that Ni is a promoter for the Mo catalyst while doping metals such as Fe, Zn, and Cu acted as inhibitors for the formation of deoxygenated cycloalkanes. On the other hand, both Zn and Fe had a negative impact on the HDO activity for PG but changed the selectivity towards aromatics like propylbenzene at full conversion.

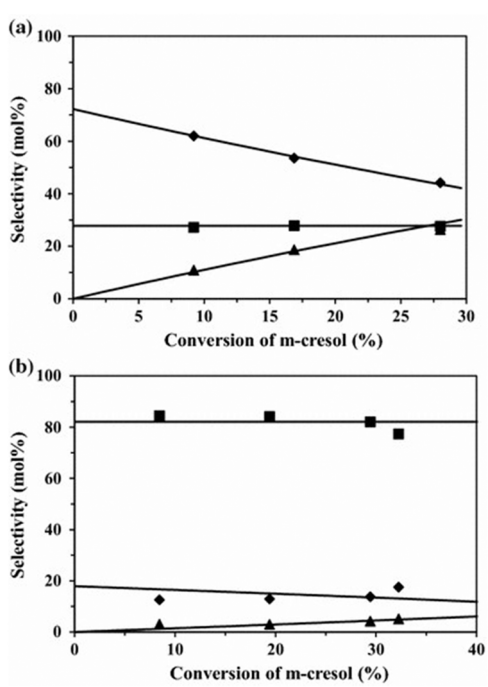

Fig. 23. Selectivity of (a) Mo/Al_2O_3 and (b) $CoMo/Al_2O_3$ during the transformation of m-cresol (340 °C, 40 bar). Experimental points: toluene (*filled square*), methycyclohexene (*filled diamond*), and methylcyclohexane (*filled triangle*); lines: calculated from the first-order kinetics model (Eqs. 9–13) [171]. Reprinted by permission from Springer, Catalysis Letters, Hydrodeoxygenation of Cresols Over Mo/Al_2O_3 Sulfided Catalysts, V. O. O. Gonçalves, S. Brunet, and F. Richard, 146, 1562–1573 (2016).

5.3. Kinetics for the HDO of lignin and biomass-derived oil

Due to the complex nature of lignin, a typical hydrotreatment experiment produces a broad spectrum of especially liquid phase products. The kinetic modeling for the hydrotreatment of a feedstock like lignin can be important to understand the complex series of reactions involved in the transformation of lignin, how they are influenced by operating conditions and catalyst properties, and eventually aid in an effective scale-up of a lignin hydrotreatment process. Pu et al. developed a kinetic model for lignin hydrotreatment over a CoMoS-supported catalyst in a semi-batch reactor using a lumped approach [174]. There were three main lumps divided further into product groups: lignin oligomeric residues (solid): (i) THF-insolubles, THF-solubles, and solubilized oligomers; (ii) liquid product lumps: dimethoxyhenols, methoxyphenols, alkylphenols, catechols, alkanes (< C_{13}), alkanes (≥ C_{13}), aromatics, naphthenes, and H_2O; (iii) gas products lumps: CO_2, CO, CH_4 and C_2-C_6 (light hydrocarbon) with v_i^j, the overall stoichiometric coefficient for component i in reaction j (Scheme 4). The model accounted for gas hydrodynamics which was characterized by Residence Time Distributions (RTD), liquid-gas mass transfer resistance, and vapor-liquid equilibrium effects with reactions (1) to (10) from Scheme 4. This resulted in a model that fitted well with the obtained experimental data [174]. The model results were able to well describe the main overall lignin depolymerization reactions and further deoxygenation reactions of phenolic monomers in the liquid phase [174].

Reaction (1): THF-insolubles $\overset{k_1}{\rightarrow}$ v_{TSB}^1·THF-solubles$_B$.

Reaction (2): THF-solubles$_A$ $+v_{H_2}^2$·H_2 $\overset{K_2}{\rightarrow}$ v_{TSB}^2·THF-solubles$_B$ $+ v_{CH_4}^2$·CH_4 $+ v_{H_2O}^2$·H_2O $+ v_{C_2C_6}^2$·C_2 – C_6.

Reaction (3): THF solubles$_B$ $+ v_{H_2}^3$·H_2 $\overset{K_3}{\rightarrow}$ v_{SO}^3·Solubilized oligomers $+ v_{CH_4}^3$·CH_4 $+ v_{H_2O}^3$·H_2O $+ v_{C_2C_6}^3$·C_2 – C_6 $+ v_{AP}^3$·Alkylphenols $+ v_{AK1}^3$·Alkanes (< C_{13}) $+ v_{AK2}^3$·Alkanes (≥ C_{13}).

Reaction (4): Solubilized oligomers $\overset{K_4}{\rightarrow}$ v_{AP}^4·Alkylphenols.

Reaction (5): Dimethoxyphenols $+ v_{H_2}^5$·H_2 $\overset{K_5}{\rightarrow}$ Alkylphenols + 2·H_2O + 2·CH_4.

Reaction (6): Methoxyphenols $+ v_{H_2}^6$·H_2 $\overset{K_6}{\rightarrow}$ Alkylphenols + H_2O + CH_4.

Reaction (7): Methoxyphenols $+ v_{H_2}^7$·H_2 $\overset{K_7}{\rightarrow}$ Catechols + CH_4.

Reaction (8): Catechols $+ v_{H_2}^8$·H_2 $\overset{K_8}{\rightarrow}$ Alkylphenols + H_2O.

Reaction (9): Alkylphenols $+ v_{H_2}^9$·H_2 $\overset{K_9}{\rightarrow}$ Aromatics + H_2O.

Reaction (10): Alkylphenols $+ v_{H_2}^{10}$·H_2 $\overset{K_{10}}{\rightarrow}$ Naphthenes + H_2O.

Grilc et al. screened a series of catalysts covering the commercial NiMo catalysts in sulfided, oxide, and reduced form and other catalysts in the hydrotreatment of a solvolyzed biomass-derived oil [175]. A complex reaction pathway was proposed and followed by constructing a lumped kinetic model based on the quantified functional groups by Fourier transform infrared spectroscopy (FTIR) [175]. Among all the

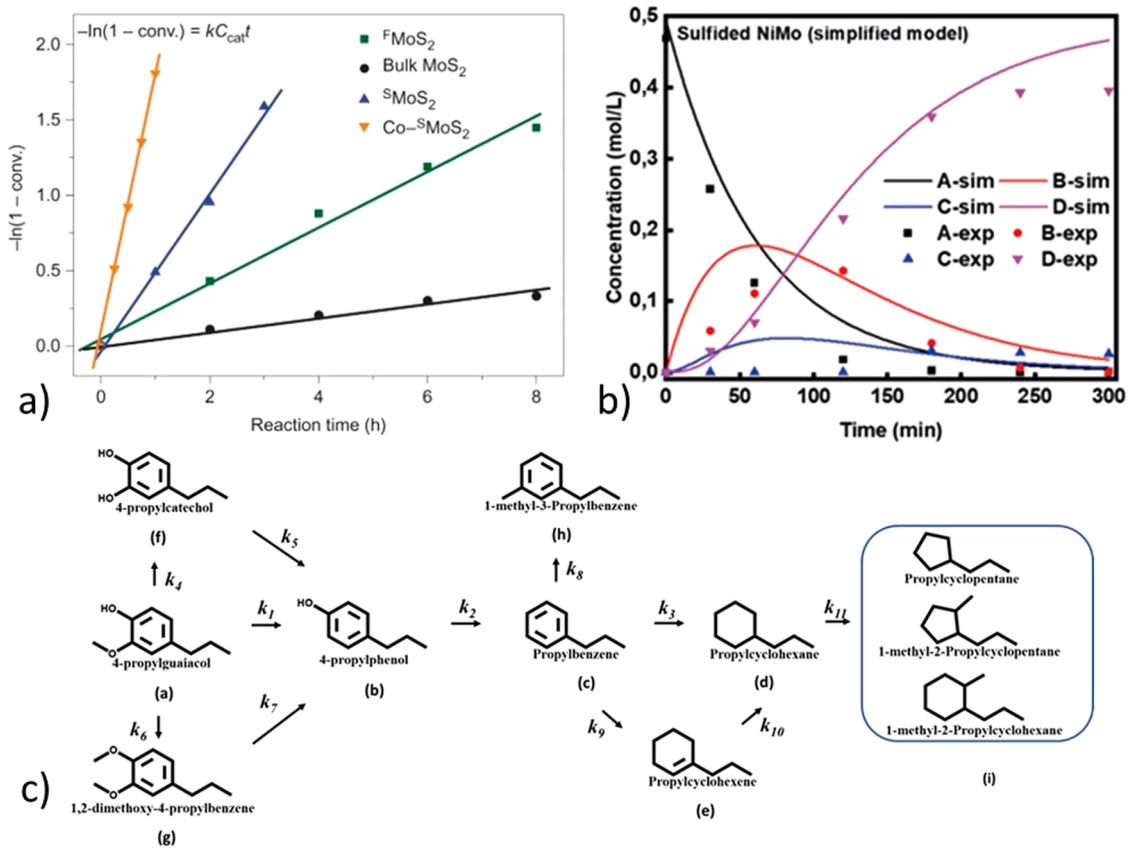

Fig. 24. a) A kinetic study of the HDO of 4-methylphenol to toluene [172]. b) Concentration profiles for HDO of PG over NiMo catalyst at a total pressure of 50 bar and 300 °C. The solid line denotes the modeling results (simplified model) and the symbols correspond to the experimental values. c) Proposed reaction routes of the HDO of PG over sulfided catalysts [173]. Y. W. Cheah, M. A. Salam, P. Arora, O. Öhrman, D. Creaser, and L. Olsson, *Sustainable Energy Fuels.*, 2021, **5**, 2097–2113, reproduced by permission of The Royal Society of Chemistry.

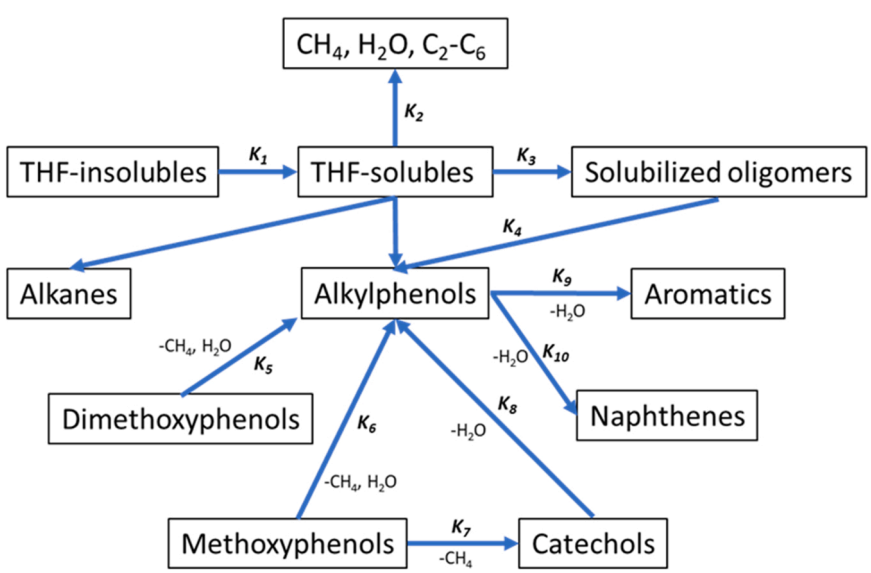

Scheme 4. Catalytic hydrotreatment of straw soda lignin over CoMoS supported catalysts [174].

tested catalysts, the commercial sulfided NiMo catalyst was found to be suitable for yielding bio-oils with high gross calorific value. The authors also discovered that the unsupported bulk MoS_2 resulted in high HDO activity and selectivity which is worth further investigation [175]. The same authors then extended their work by comparing the selectivity and activity of several synthesized and commercial unsupported Mo catalysts in oxide, carbide, and sulfide form, and also unsupported WS_2 nanotubes [176]. A similar lumped kinetic model was developed giving apparent kinetic constants that correspond to main reactions like hydrodeoxygenation (k_1), decarboxylation (k_4), decarbonylation (k_3), dehydrogenation (k_2), and hydrocracking of a solvolytic oil as shown in Scheme 5a) [176]. One of the observations was that the urchin-like

MoS_2 possessed the highest k_1 value among all other unsupported sulfided catalysts which corresponds to the removal of the hydroxyl group in the form of water. While the decarbonylation, decarboxylation, and hydrocracking reactions occurred to a lesser extent using the unsupported materials which could be explained by the absence of the use of an acidic catalyst support that can cleave the C-C linkages [176].

Grilc et al. also studied the simultaneous liquefaction and hydrotreatment of biomass (Sawdust samples like beech, fir, and oak) over a sulfided catalyst (NiMo on alumina), a reduced Pd on alumina catalyst, and zeolite Y. Emphasis was placed on studying the effect of different process parameters like time, pressure, temperature, wood, and solvent type. The yield and product composition from the simultaneous reactions were identified and correlated to a lumped kinetic model accounting for liquefaction, decarboxylation, decarbonylation, HDO, and char formation reactions as shown in Scheme 5a). Their modeling results showed that reaction temperature played an important role in the liquefaction and HDO of biomass. The increase in reaction temperature from 300° to 350°C resulted in a 2.5-fold higher yield for HDO products, while the solid residue yield decreased by 39%. However, when the reaction temperature is increased over 350 °C, a lower oil yield was achieved which was mainly attributed to an increased formation of char [177]. Also, in their work, sulfided NiMo on alumina was found to achieve higher oil yield as compared to the noble metal Pd on alumina.

6. Deactivation of metal sulfide catalysts

Common pathways for catalyst deactivation include poisoning, coking, sintering, fouling/physical blockage, leaching or vapor formation, and solid-state transformations [178]. Based on the literature, it can be deduced that metal sulfide catalysts used for upgrading renewable feedstocks can lose activity due to loss of sulfur, impurities present in renewables, evolved products, coking, and sintering of the active phase [48,179–182].

Since bio-based renewables have high oxygen contents, often sulfides catalyst loses sulfur through a sulfur-oxygen exchange during HDO. Such an exchange more easily takes place on sulfur edges over unpromoted MoS_2 than the promoted sites (in the case of CoMoS) in the presence of a high H_2O partial pressure as observed via combined CO adsorption and IR studies during HDO of 2-ethyl phenol [179]. The authors also demonstrated via DFT that in the presence of a large amount of water the exchange is stronger and irreversible over MoS_2 while Co promotion makes the catalyst more water tolerant and enables the poisoning to become more reversible. Hence, a continuous supply of sulfiding agents (e.g., H_2S) in the feed at a sufficiently low concentration can restore the catalytic activity, while an inhibition can occur at a higher H_2S concentration [183]. Resulfidation of the catalyst can also restore its initial activity as has been demonstrated for a sulfided $CoMo/Al_2O_3$ catalyst while hydroprocessing 2-hydroxydiphenylmethane (250 °C, 155 bar, WHSV = 0.49 h^{-1}) [184]. It is often criticized that the addition of such agents will however contaminate the product oils. Since TMS catalysts, e.g. Ni/Co-promoted Mo/W sulfides are also highly active in hydrodesulfurization, the final product typically contains only traces of sulfur.

Bio-oil impurities depend on their source of production and prior pretreatment processes. Typical impurities include alkali, alkaline-earth metals (Na, K, Ca, Mg, etc.), phosphorus, sulfur, and nitrogen.

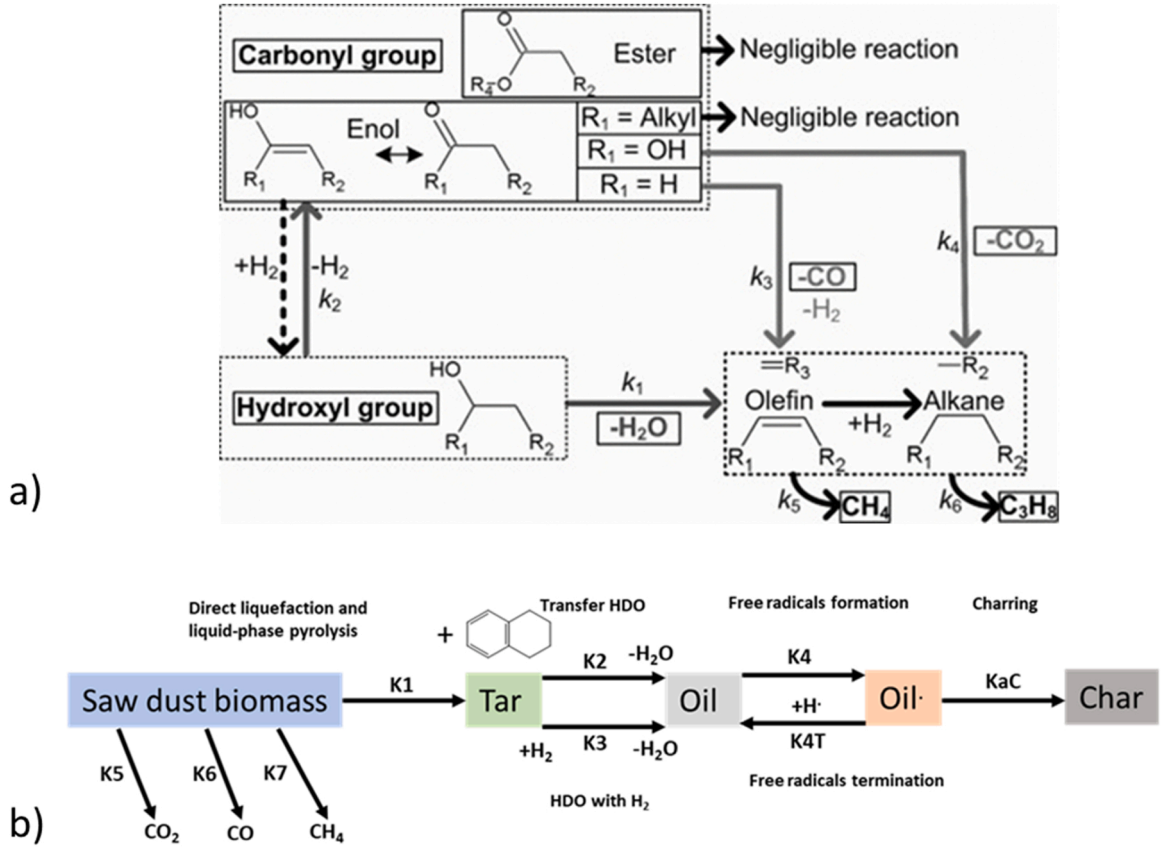

Scheme 5. a) Reaction scheme for the upgrading of solvolytic oil over unsupported sulfide catalysts [176]. This article was published in Applied Catalysis B: Environmental, M. Grilc, G. Veryasov, B. Likozar, A. Jesih, and J. Levec, Hydrodeoxygenation of solvolysed lignocellulosic biomass by unsupported MoS_2, MoO_2, Mo_2C, and WS_2 catalysts, Appl. Catal. B Environ., 2015, 163, 467–477, Copyright Elsevier (2019). b) Proposed reaction mechanism for simultaneous liquefaction and hydrotreatment of biomass [177]. Copyright (2015) Wiley, used with permission from M. Grilc, B. Likozar, and J. Levec, Simultaneous Liquefaction and Hydrodeoxygenation of Lignocellulosic Biomass over $NiMo/Al_2O_3$, Pd/Al_2O_3, and Zeolite Y Catalysts in Hydrogen Donor Solvents, ChemCatChem, 2015, 7, 960–966, Wiley.

Irreversible K deactivation of $NiMoS_2/ZrO_2$ (K impregnated as KNO_3 to the catalyst at a K/(Ni+Mo) molar ratio of 1) was attributed to the preferential occupation of edge vacant sites of the promoted MoS_2 during HDO of phenol and octanol [180]. Trap grease phospholipids also containing alkali metals were shown to cause severe deactivation of a commercial CoMoS/γ-Al_2O_3 catalyst via coking and severe pore plugging while upgrading rapeseed oil [185]. Fe was found to preferentially block the Ni-promoted sites in NiMoS/γ-Al_2O_3 while upgrading fatty acids [48]. Bio-oil phospholipids having phosphate and choline moieties have also been shown to lower the activity of NiMoS/γ-Al_2O_3 during HDO of oleic acid [49]. Nitrogen-bearing compounds (e.g. amines, pyridines, quinolines, etc.) have been shown to cause the deactivation of TMS catalysts [186–188].

The presence of water in bio-oil or produced during HDO may influence the activity of TMS-based catalysts via oxidation of the sulfide phase or deterioration of the structure of the active phase [65]. Couman and Hensen et al. [52] reported that water had little influence on sulfided NiMo/ γ-Al_2O_3 below a concentration of 5000 ppm during HDO of fatty esters. Krause and co-workers reported that the inhibition effect of water can be compensated for by H_2S during HDO of an aliphatic ester (methyl heptanoate) [65]. The decarboxylation route has been reported to be affected by H_2O perhaps via keto-enol isomerization during HDO of fatty esters [52]. Support material used can also be affected by the water e.g. γ-Al_2O_3 reportedly transforms to its boehmite phases or poisons the acidic sites [179]. The interaction of water with active sites may also lead to the formation of an inactive sulfate layer [179]. However, water may affect the HDO of phenolic compounds over metal sulfides to a varying extent [64,179]. The presence of a small amount of water (water/p-cresol molar ratio < 1) was found to increase the direct-HDO route of p-cresol to toluene while a high amount of water (water/-p-cresol molar ratio > 1) significantly reduces the deoxygenation rate and toluene selectivity due to preferential occupancy of active sites [124]. Additionally, CO formed during HDO under reduction conditions can strongly inhibit the direct-HDO pathways owing to the lower adsorption energy of CO over metal sulfides (e.g., MoS_2, CoMoS) [183, 189].

Coking is one of the leading challenges to deal with for hydrotreating catalysis. TMS-based HDO catalysts may deactivate via carbonaceous deposits (reactive/soft or refractory/hard) formed either by physical or chemisorbed processes [190]. Such deposits arise from the undesired side reactions (e.g. cracking, aromatization, dehydrogenation, cyclization, condensation, etc.) involving adsorbed species/precursor molecules (alkenes, aromatics, oxygenates, etc.). Condensation and rearrangement reactions typically play a major role in low-temperature coke deposition (<200 °C) while dehydrogenation and hydrogen transfer reactions lead to the formation of polyaromatic hydrocarbons (>350 °C) [191]. On the other hand, carbon species can be bonded to the active site via weak interaction [192] or can partially replace sulfur atoms at the edge sites of MoS_2 in the form of a Mo-S-C bond in a $MoS_{2-x}C_x$ phase [193]. The latter can be synthesized via the thermal treatment of MoS_2 with a mixture of dimethyldisulfide in N_2/H_2 which is reported to stabilize the MoS_2 crystallites with a smaller size (i.e., carbon species restricts the crystal growth) with lower stacking, thus enhancing the activity instead [194]. In addition, metal carbides (Co-C and Mo-C bonds) may form which may be observed by EXAFS analysis [192].

Catalyst/support combination is another critical parameter in determining the activity, selectivity, and coke formation. Unsupported TMS like MoS_2 may undergo agglomeration [181,182] under reaction conditions which can be prevented in the presence of hydrogen and hydrocarbon feed [193]. It is important to note that sintering or agglomeration may occur through Ostwald ripening or coalescence to obtain higher thermodynamic stability which lowers the surface area and catalytic activity [195]. Segregation of the promoter (e.g. Ni/Co) [196,197] as sulfides (Co_9S_8/Ni_3S_2) may influence the catalyst deactivation [182]. Acidity/basicity of the active phase or support materials can also play an important role [198] in aiding coke-forming reactions. Both Lewis acid sites (LAS) have a high affinity for basic precursors and Brønsted acid sites (BAS) via proton donation and carbonium cation formation may contribute to coke formation. BAS, in addition, promotes coupling/isomerization reactions [199]. The deactivation of MoS_2 by phenolic compounds is indirect. The basicity of the phenolic compounds and their substituent nature gives different adsorption mechanisms as in Scheme 6a). Due to their basicity, they adsorb as phenolates on the acidic alumina support. If they are adsorbed closely to the MoS_2, they could block the accessibility of other reactants for deoxygenation to the MoS_2 active site, resulting in the deactivation of the whole catalyst for deoxygenation reactions [200]. In addition, the oxygenates that adsorbed on the sulfide phase reduce the active phases and cause catalyst poisoning [201]. Thermal instability and repolymerization reactions of phenolic compounds in bio-oil derived from fast pyrolysis and lignin lead to premature deactivation of the catalyst [202]. Recently, Kraft lignin impurities (Na, K, etc.) have been demonstrated to deactivate a sulfided NiMoS/Al_2O_3 catalyst especially at high loading as discussed above in Section 4.4.2 [7].

With a representative model compound, 2-hydroxydiphenylmethane, and using a sulfided CoMo/Al_2O_3 catalyst, a decline in the catalytic activity was noticed after 20 h of reaction (250 °C, 155 bar, WHSV $= 0.49\ h^{-1}$). But, a simple re-sulfidation of the catalyst restored its initial activity. The mode of deactivation of the CoMo/Al_2O_3 catalyst could be ascribed due to the loss of sulfur. Another interesting aspect of the CoMo/Al_2O_3 catalyst was revealed when 4-methyl guaiacol was used as the model compound. The char formation from this experiment was around 40 wt%, far less than the non-catalytic thermal reaction indicating that the CoMo/Al_2O_3 catalyst had generated products with less char forming tendency. This observation is somewhat contrary to the previous reports where more char was formed in the presence of the catalyst [153]. However, the role of temperature/pressure in char formation could not be neglected (vide supra). The deactivation of TMS catalysts while upgrading lignin/lignin-derived phenolic compounds has been discussed in Section 4.

7. Theoretical studies and computational approaches to understand the application of TMS in deoxygenation

Apart from the experimental approaches described in the previous section, computational approaches based on density functional theory (DFT) calculation, can also provide a better insight into the physiochemical properties of the sulfided-based catalytic materials and their relationship with their observed reactivity in deoxygenation. The deactivation mode of the metal sulfides can also be understood through DFT calculation. For instance, recent work by Liu et al. investigated the detailed mechanism of the *in situ* and *ex situ* substitution of sulfur atoms in the active phase (Co(Ni)MoS edge) by oxygen atoms under the presence of water via the DFT [203]. The calculation was also performed for the energy change, Gibbs free energy evolution, and reaction coordination to gain an understanding of the water deactivation of Co(Ni)MoS under HDO conditions [203]. It was outlined in their work that, for *in situ* oxygen substitution, the oxygen atoms from water molecule occupied the positions of the edge sulfur atoms; while for the *ex situ* substitution, the water molecules occupied directly the unsaturated sites after the desorption of edge sulfur as hydrogen sulfide [203]. It was found that the substitution of sulfur atoms depends on the ratio of partial pressure between hydrogen and water, and also between hydrogen and hydrogen sulfide. Moreover, it was found that the CoMoS is more prone to water deactivation than NiMoS, and when compared to MoS_2, both promoted Co(Ni)MoS showed better water resistance. Another recent study by Diao et al. used DFT calculations to demonstrate and validate that the Co-doped MoS_2 and Mo-doped Co_9S_8 enhanced the vertical adsorption of oxygenates which further undergoes C-O cleavage of diphenyl ether (DPE) and were also able to avoid benzene ring hydrogenation [204]. It was further shown that the Mo-doped Co_9S_8 surface promoted the adsorption and C-O bond activation in DPE. Besides, there

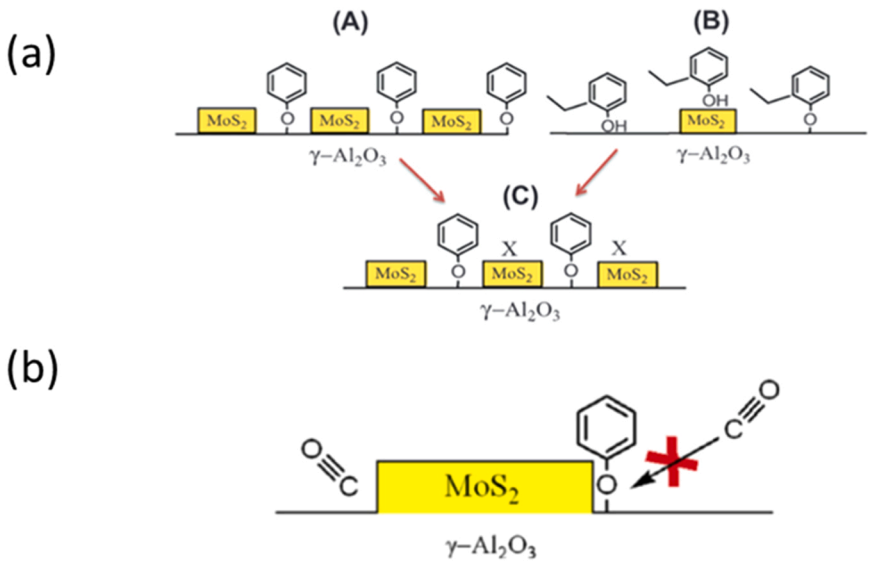

Scheme 6. a) The interaction mechanism of phenolic compound with sulfided (Co)Mo/Al_2O_3 catalyst: (A) Phenol at room temperature, (B) 2-ethylphenol at room temperature, (C) ethylphenol at 623 K, b) Indirect poisoning mechanism of the sulfide sites by phenol adsorption on the Al_2O_3 support [200]. This article was published in Journal of Catalysis, A. Popov, E. Kondratieva, L. Mariey, J. M. Goupil, J. E. Fallah, J. Gilson, A. Travert, and F. Maugé , Bio-oil hydrodeoxygenation: Adsorption of phenolic compounds on sulfided (Co)Mo catalysts, Journal of Catalysis, 2013, 297, 176–186, Copyright Elsevier (2013).

are also excellent reviews on the summary and studies of the application of the computational approach to study other catalyst systems such as transition metal phosphides (TMP) [205], transition metal catalysts [206,207], and transition metal sulfides (TMS) [208]. With this in mind, there is still a need to engage in theoretical studies that can disclose the reaction mechanisms in the complex catalytic reaction and strive to improve the existing catalyst systems, eventually aiding the selection and implementation of these catalysts into the complex refinery.

8. Summary, challenges, and outlook

Recently, the European Commission (EC) has published its ambitious legislative package 'Fit for 55 targeting a 55% reduction in GHG emissions by 2030 compared to the 1990 level [209]. The presented package provides tools to tackle the climate crisis, and different solutions taking sustainability into account must be endorsed and applied. Advanced biofuels play a key role in decarbonizing the transport sector. Therefore, many research efforts have been dedicated to the development of heterogeneous catalysts for application in advanced biofuel production in the past few decades. Metal sulfides remain the core catalysts in hydroprocessing industries as they are effective in the removal of heteroatoms such as sulfur, nitrogen, oxygen, halides, and metals. This review has emphasized the use of hydrotreating catalysts, metal sulfides in the valorization of triglyceride feeds, oxygenates in monomer and dimeric form, biomass-derived pyrolysis oil, and lignin feed. Besides the type of catalysts, the catalytic performance and progression of reactions during hydroprocessing also depend largely on the reaction parameters like reactor type, reaction temperature, pressure, residence time, and solvent system. These aspects have been discussed in this work.

The major challenges associated with the hydroprocessing of various renewable feedstocks and the possible future research and development in respective areas are listed in Table 9. Numerous research papers report the use of alumina as a catalyst support for hydroprocessing catalysts due to its good textural and mechanical properties, and low relative cost [210,211]. The acidic nature of alumina is found to be beneficial in breaking the C-O bond in anisole which is also found in the lignin structure [210]. The sulfur vacancies located at the edges of the metal sulfides act as unsaturated sites and Lewis acids sites and are found to be active in cleaving C-O linkages [44]. Other supports like silica and activated carbon were also used as supports for NiMo hydrotreating catalysts and studied in vacuum residue hydrotreating reactions [211]. Carbon as catalyst support has also gained attention owing to its high surface area, inert nature, high thermal stability, and low cost [212]. An important conclusion made is that the effectiveness of the hydrotreating catalysts depends on the pore size diameter, pore-volume, and metal dispersion that ultimately improves the efficiency of hydroconversion. As discussed in this work, the unsupported or self-supported metal sulfides have also gained interest because of their higher activity per catalyst mass as compared to the supported sulfide catalysts [208]. In addition, the direct use of the active metal sulfides phase allows the elimination of the transport resistance

Table 9
Major challenges involved in improving efficiency and scaling up of bio-feedstock hydrotreatment processes.

Feedstocks	Major challenges involved for the use in industry	Potential areas of development and research
Triglycerides	• Pressure drop build-up • Cloud point and isomerization • Decrease in HDN activity of catalysts • Metal/inorganic compounds like alkali, Fe, P, etc.	• Catalysts poisoning study for better understanding • Designing sulfided catalysts and prediction of deactivation with the aid of DFT tools
Pyrolysis oil	• Alkali metals present in pyrolysis oil • Feeding issues and catalyst deactivation issues • Catalyst bed plugging due to coking • Pressure build-up in the reactor	• Study of a mixture of model compounds of pyrolysis oil to understand the effect of the individual components • Pretreatment of pyrolysis oil for the removal of inorganic elements or using a multistage HDO reactor • Co-refining with fossil feed for renewable material integration in existing refineries • Stabilization of pyrolysis oil
Lignin	• The condensation reaction of lignin fragments leading to char formation • Cleavage of the recalcitrant C-C linkages present in the lignin molecules • Low liquid yield • Sulfur leaching and replenishment	• Catalysts poisoning/deactivation • Co-processing of lignin oils and petroleum feedstocks • Understanding the origin of char formation and char formation routes • Deactivation mechanism
Solid biomass	• Inorganic compounds present in the feedstocks cause catalyst deactivation	• Hydrodenitrogenation of solid biomass • Carbon balance calculations • Product separation and isolation

interference due to the support during the reaction. With this, ExxonMobil and Albemarle Catalysts developed an unsupported catalyst by so-called NEBULA technology that claims to show superior activity as compared to the conventional hydrotreating catalysts [213,214]. Another great example is the Eni Slurry Technology (EST) process which uses highly dispersed MoS_2 nanoparticles and has proven the feasibility of using unsupported catalyst materials in hydrotreating [215]. Apart from developing stable, active, and cost-effective metal sulfide catalysts, the issue related to sulfur leaching and replenishment when using sulfided catalysts remains a central research topic. Some studies have been communicated in this regard exploring the benefits of applying sulfiding agents to compensate for sulfur loss during the process [14,62,66]. There is also a need and an interest in the research community in designing metal sulfide catalysts and also understanding the mode of sulfide deactivation aided by DFT tools. A better understanding of the physicochemical properties of metal sulfides aided by the *first principles approaches* can eventually benefit the tailored synthesis of metal sulfides and improve desired product selectivity. A review by Raybaud in 2007 and extended by others provided insights into the understanding of the sulfide active phases, the localization and role of promoters, electronic properties, and morphological changes influenced by the operating parameters, synthesis methods, or addition of promoter [10,12,216–220].

In addition, when dealing with hydrotreating of complex feedstocks like lignin, the diffusion of depolymerized lignin oligomeric fragments into the catalyst pores to access active sites is likely to be limited by pore transport resistance, and therefore, the self-supported sulfide catalysts may be seen as beneficial to gain better active site accessibility. Depolymerized lignin fragments that do not undergo deoxygenation reactions due to the inaccessibility of active sites, may instead repolymerize to form solid residues like char, which is usually undesirable. Studies related to process improvement could also be another way to ensure an efficient hydroconversion of solid lignin. A recent example shows that a modification to a semi-batch reactor operating mode by injecting a lignin slurry into a reactor that has reached the desired reaction temperature can effectively avoid the repolymerization and recondensation reactions resulting in better lignin conversion [221]. Supported and unsupported versions of NiMoS catalysts was also reported effective in this regard [222,223].

The hydroprocessing of various renewable feedstocks such as triglycerides, model compounds for bio-oil, and lignin-derived oils are discussed in this work. There are different challenges involved while using these different feedstocks for the scale-up of a hydrotreatment process. One of the common challenges when dealing with bio-feedstocks is the deactivation of the catalyst caused by the presence of inorganic impurities in the feedstocks. These inorganic elements can act as poisons to the catalytic sites, causing a decrease in the catalyst lifetime during the time-on-stream. Future research should focus on understanding the role of these impurities on the catalytic activity of a typical hydrotreating catalyst and also the in-depth deactivation mechanism. For instance, one recent study revealed that low concentrations of impurity elements like Na, K, Ca, and Fe promotes the deoxygenation ability of a $NiMoS/Al_2O_3$ catalyst. However, when they are present in higher concentrations, these impurities are deposited on the catalyst, ultimately leading to the poisoning of the catalyst [7]. More of these types of studies should be pursued using different bio-feedstocks as they can be seen as highly relevant for operation in refineries in terms of the stability of the catalysts and also it could possibly provide a way to regenerate, recycle and reuse the catalyst. Issues like catalyst pore plugging due to coking and inorganic impurities present in bio-feed should also be addressed and investigated in the future by studying different guard bed materials like catalysts or adsorbents to improve the catalyst lifetime. Research related to catalytic material development that is more resistant to deactivation and can be easily restored following deactivation is of high interest. In addition to these, the pretreatment of these bio-feedstocks for the removal of inorganic elements that are responsible for the catalyst deactivation is required to better improve the properties of the feedstock. The pretreatments and enhancement methods to improve the quality of the feedstocks is desirable to achieve efficient refining of bio-feedstocks. The removal of nitrogen content in bio-feedstocks also remains an area that is less explored and requires more attention. For instance, pyrolysis oil derived from sewage sludge contains high nitrogen and sulfur-bound polyaromatics compounds which reduces the quality of the product fuels and also generates toxic emissions upon combustion.

To sum up, we have comprehensively reviewed the use of industrially-relevant metal sulfide catalysts for the upgrading of biomass feedstocks like triglycerides, monomeric and dimeric phenolic compounds, pyrolysis oil, and waste lignin. Various aspects such as sulfide deactivation, reaction kinetics, and mechanisms have been discussed. The challenges and future research opportunities concerning the efficient upgrading of bio-feedstocks to liquid fuel were explored. Metal sulfides will remain as a core in the processing of renewable feedstocks in existing refinery infrastructures and both the research community and industries play a significant role in realizing future biorefineries.

Declaration of Competing Interest

The authors declare that they have no known competing financial interests or personal relationships that could have appeared to influence the work reported in this paper.

Data availability

Data will be made available on request.

Acknowledgments

This research is a collaboration work between Chemical Engineering, Competence Centre for Catalysis (KCK) at Chalmers, Preem AB, and RISE Research Institutes of Sweden Energy Technology Center (ETC). The authors would like to acknowledge the Swedish Energy Agency (2017-010890 and 2018-012459) and Preem AB for financial support.

References

[1] D. Mohan, C.U. Pittman, P.H. Steele, Pyrolysis of Wood/Biomass for Bio-oil, A Critical Review, Energy & Fuels 20 (2006) 848–889.
[2] L. Zhang, C. (Charles) Xu, P. Champagne, Overview of recent advances in thermo-chemical conversion of biomass, Energy Conversion and Management, 51 (2010) 969–982.
[3] J. Zakzeski, P.C.A. Bruijnincx, A.L. Jongerius, B.M. Weckhuysen, The Catalytic Valorization of Lignin for the Production of Renewable Chemicals, Chem. Rev. 110 (2010) 3552–3599.
[4] P.M. Mortensen, J.D. Grunwaldt, P.A. Jensen, K.G. Knudsen, A.D. Jensen, A review of catalytic upgrading of bio-oil to engine fuels, Appl. Catal. A Gen. 407 (2011) 1–19.
[5] A. Ben Hassen Trabelsi, K. Zaafouri, W. Baghdadi, S. Naoui, A. Ouerghi, Second generation biofuels production from waste cooking oil via pyrolysis process, Renew. Energy 126 (2018) 888–896.
[6] Y. Zhang, J. Monnier, M. Ikura, Bio-oil upgrading using dispersed unsupported MoS_2 catalyst, Fuel Process. Technol. 206 (2020) 106403.
[7] J. Sebastian, Y.W. Cheah, D. Bernin, D. Creaser, L. Olsson, The Promotor and Poison Effects of the Inorganic Elements of Kraft Lignin during Hydrotreatment over NiMoS Catalyst, Catalysts 11 (2021) 874.
[8] V.C. Krauch, M. Pier, Kohleveredelung und katalytische Druckhydrierung, Angewandte Chemie 44 (1931) 953–958.
[9] J.R. Anderson, M. Boudart, Catalysis Science and Technology 11 (1984).
[10] C. Dupont, R. Lemeur, A. Daudin, P. Raybaud, Hydrodeoxygenation pathways catalyzed by MoS_2 and NiMoS active phases: A DFT study, J. Catal. 279 (2011) 276–286.
[11] S. Rangarajan, M. Mavrikakis, On the Preferred Active Sites of Promoted MoS_2 for Hydrodesulfurization with Minimal Organonitrogen Inhibition, ACS Catal 7 (2017) 501–509.
[12] M. Sun, A.E. Nelson, J. Adjaye, Ab initio DFT study of hydrogen dissociation on MoS_2, NiMoS, and CoMoS: mechanism, kinetics, and vibrational frequencies, J. Catal. 233 (2005) 411–421.
[13] Y.W. Cheah, M.A. Salam, J. Sebastian, S. Ghosh, O. Öhrman, D. Creaser, L. Olsson, Thermal annealing effects on hydrothermally synthesized unsupported MoS_2 for enhanced deoxygenation of propylguaiacol and kraft lignin, Sustain. Energy Fuels 5 (2021) 5270.

[14] H. Ojagh, D. Creaser, S. Tamm, P. Arora, S. Nyström, E. Lind Grennfelt, L. Olsson, Effect of Dimethyl Disulfide on Activity of NiMo Based Catalysts Used in Hydrodeoxygenation of Oleic Acid, Ind. Eng. Chem. Res. 56 (2017) 5547–5557.
[15] H. Wang, J. Male, Y. Wang, Recent Advances in Hydrotreating of Pyrolysis Bio-Oil and Its Oxygen-Containing Model Compounds, ACS Catal 3 (2013) 1047–1070.
[16] R.R. Chianelli, G. Berhault, B. Torres, Unsupported transition metal sulfide catalysts: 100 years of science and application, Catal. Today 147 (2009) 275–286.
[17] M. Wang, L. Zhang, Y. He, H. Zhu, Recent advances in transition-metal-sulfide-based bifunctional electrocatalysts for overall water splitting, J. Mater. Chem. A 9 (2021) 5320–5363.
[18] S. Chandrasekaran, L. Yao, L. Deng, C. Bowen, Y. Zhang, S. Chen, Z. Lin, F. Peng, P. Zhang, Recent advances in metal sulfides: from controlled fabrication to electrocatalytic, photocatalytic and photoelectrochemical watersplitting and beyond,Chem, Soc. Rev. 48 (2019) 4178–4280.
[19] R. Barik, P.P. Ingole, Challenges and prospects of metal sulfide materials for supercapacitors, Curr. Opin. Electrochem. 21 (2020) 327–334.
[20] C.H. Ko, S.H. Park, J.K. Jeon, D.J. Suh, K.E. Jeong, Y.K. Park, Upgrading of biofuel by the catalytic deoxygenation of biomass, Korean J. Chem. Eng. 29 (2012) 1657–1665.
[21] Z. He, X. Wang, Hydrodeoxygenation of model compounds and catalytic systems for pyrolysis bio-oils upgrading, Catal. Sustain. Energy 1 (2013) 28–52.
[22] S. Tan, Z. Zhang, J. Sun, Q. Wang, Recent progress of catalytic pyrolysis of biomass by HZSM-5, Chin. J. Catal. 34 (2013) 641–650.
[23] D.A. Ruddy, J.A. Schaidle, J.R. Ferrell, J. Wang, L. Moens, J.E. Hensley, Recent advances in heterogeneous catalysts for bio-oil upgrading via "*ex situ* catalytic fast pyrolysis": catalyst development through the study of model compounds, Green Chem 16 (2014) 454.
[24] S. Boullosa-Eiras, R. Lødeng, H. Bergem, M. Stocker, L. Hannevold, E.A. Blekkan, Potential for metal-carbide, -nitride, and -phosphide as future hydrotreating (HT) catalysts for processing of bio-oils, Catalysis 26 (2014) 29–71.
[25] M. Asadieraghi, W.M. Ashri Wan Daud, H.F. Abbas, Heterogeneous catalysts for advanced bio-fuel production through catalytic biomass pyrolysis vapor upgrading: a review, RSC Adv 5 (2015) 22234–22255.
[26] Z. Ma, L. Wei, W. Zhou, L. Jia, B. Hou, D. Li, Y. Zhao, Overview of catalyst application in petroleum refinery for biomass catalytic pyrolysis and bio-oil upgrading, RSC Adv 5 (2015) 88287–88297.
[27] Y. Hong, A. Hensley, J.S. McEwen, Y. Wang, Perspective on Catalytic Hydrodeoxygenation of Biomass Pyrolysis Oils: Essential Roles of Fe-Based Catalysts, Catal. Lett. 146 (2016) 1621–1633.
[28] S. Cheng, L. Wei, X. Zhao, J. Julson, Application, Deactivation, and Regeneration of Heterogeneous Catalysts in Bio-Oil Upgrading, Catalysts 6 (2016).
[29] A.M. Robinson, J.E. Hensley, J. Will Medlin, Bifunctional Catalysts for Upgrading of Biomass-Derived Oxygenates: A Review, ACS Catal 6 (2016) 5026–5043.
[30] C. Kordulis, K. Bourikas, M. Gousi, E. Kordouli, A. Lycourghiotis, Development of nickel based catalysts for the transformation of natural triglycerides and related compounds into green diesel: a critical review, Appl. Catal. B Environment. (2016) 156–196.
[31] M.W. Nolte, B.H. Shanks, A Perspective on Catalytic Strategies for Deoxygenation in Biomass Pyrolysis, Energy Technol 5 (2017) 7–18.
[32] X. Li, G. Chen, C. Liu, W. Ma, B. Yan, J. Zhang, Hydrodeoxygenation of lignin-derived bio-oil using molecular sieves supported metal catalysts: A critical review, Renew. Sustain. Energy Rev. 71 (2017) 296–308.
[33] Y. Shi, E. Xing, K. Wu, J. Wang, M. Yang, Y. Wu, Recent progress on upgrading of bio-oil to hydrocarbons over metal/zeolite bifunctional catalysts, Catal. Sci. Technol. 7 (2017) 2385–2415.
[34] X. Hu, R. Gunawan, D. Mourant, M.D.M Hasan, L. Wu, Y. Song, C. Lievens, C.Z. Li, Upgrading of bio-oil via acid-catalyzed reactions in alcohols—A mini review, Fuel Process. Technol. 155 (2017) 5711–5750.
[35] M. Marafi, E. Furimsky, Hydroprocessing Catalysts Containing Noble Metals: Deactivation, Regeneration, Metals Reclamation, and Environment and Safety, Energy & Fuels 31 (2017) 5711–5750.
[36] A.N. Kay Lup, F. Abnisa, W.M.A. Wan Daud, M.K. Aroua, A review on reactivity and stability of heterogeneous metal catalysts for deoxygenation of bio-oil model compounds, J. Ind. Eng. Chem. 56 (2017) 1–34.
[37] M.M. Rahman, R. Liu, J. Cai, Catalytic fast pyrolysis of biomass over zeolites for high quality bio-oil–Areview, Fuel Process. Technol. 180 (2018) 32–46.
[38] S. Chen, G. Zhou, C. Miao, Green and renewable bio-diesel produce from oil hydrodeoxygenation: Strategies for catalyst development and mechanism, Renew. Sustain. Energy Rev. 101 (2019) 568–589.
[39] A.S. Ouedraogo, P.R. Bhoi, Recent progress of metals supported catalysts for hydrodeoxygenation of biomass derived pyrolysis oil, J. Clean. Prod. 253 (2020) 119957.
[40] R. Nishu, M.M. Liu, M. Rahman, M. Sarker, C. Chai, C. Li, J. Cai, A review on the catalytic pyrolysis of biomass for the bio-oil production with ZSM-5: Focus on structure, Fuel Process. Technol. 199 (2020), 106301.
[41] V. Balasundram, N. Ibrahim, R.M. Kasmani, R. Isha, M.K.A. Hamid, H. Hasbullah, Catalytic upgrading of biomass-derived pyrolysis vapour over metal-modified HZSM-5 into BTX: a comprehensive review, Biomass Conversion and Biorefinery 12 (2022) 1911–1938.
[42] J. Zhang, J. Sun, Y. Wang, Recent advances in the selective catalytic hydrodeoxygenation of lignin-derived oxygenates to arenes,, Green Chem 22 (2020) 1072–1098.
[43] M. Zhang, Y. Hu, H. Wang, H. Li, X. Han, Y. Zeng, C.C. Xu, A review of bio-oil upgrading by catalytic hydrotreatment: Advances, challenges, and prospects, Mol. Catal. 504 (2021) 111438.
[44] H. Zhang, S. Fu, X. Du, Y. Deng, Advances in Versatile Nanoscale Catalyst for the Reductive Catalytic Fractionation of Lignin, ChemSusChem 14 (2021) 2268–2294.
[45] A. de, R. Pinho, M.B.B. de Almeida, F.L. Mendes, L.C. Casavechia, M.S. Talmadge, C.M. Kinchin, H.L. Chum, Fast pyrolysis oil from pinewood chips co-processing with vacuum gasoil in an FCC unit for second generation fuel production, Fuel 188 (2017) 462–473.
[46] H. Aatola, M. Larmi, T. Sarjovaara, S. Mikkonen, Hydrotreated Vegetable Oil (HVO) as a Renewable Diesel Fuel: Trade-off between NO_x, Particulate Emission, and Fuel Consumption of a Heavy Duty Engine, SAE Int. J. Engines 1 (2009) 1251–1262.
[47] NIST Chemistry WebBook. https://webbook.nist.gov/.
[48] P. Arora, H. Ojagh, J. Woo, E. Lind Grennfelt, L. Olsson, D. Creaser, Investigating the effect of Fe as a poison for catalytic HDO over sulfided NiMo alumina catalysts, Appl. Catal. B Environ. 227 (2018) 240–251.
[49] M.A. Salam, D. Creaser, P. Arora, S. Tamm, E.L. Grennfelt, L. Olsson, Influence of Bio-Oil Phospholipid on the Hydrodeoxygenation Activity of NiMoS/Al_2O_3 Catalyst, Catalysts 8 (2018) 418.
[50] P. Arora, H. Abdolahi, Y.W. Cheah, M.A. Salam, E.L. Grennfelt, H. Rådberg, D. Creaser, L. Olsson, The role of catalyst poisons during hydrodeoxygenation of renewable oils, Catal. Today 367 (2021) 28–42.
[51] P. Zeuthen, H. Rasmussen, Future fuel, Digital Refin 327 (2017) 42–45.
[52] A.E. Coumans, E.J.M. Hensen, A model compound (methyl oleate, oleic acid, triolein) study of triglycerides hydrodeoxygenation over alumina-supported NiMo sulfide, Appl. Catal. B Environ. 201 (2017) 290–301.
[53] S. Brillouet, E. Baltag, S. Brunet, F. Richard, Deoxygenation of decanoic acid and its main intermediates over unpromoted and promoted sulfided catalysts, Appl. Catal. B Environ. 148–149 (2014) 201–211.
[54] W.K. Craig, D.W. Soveran, Production of Hydrocarbon with a relatively high cetane rating, United States Pat. 4,992,605, (1991).
[55] D. Valencia, L. Díaz-García, L.F. Ramírez-Verduzco, A. Qamar, A. Moewes, J. Aburto, Paving the way towards green catalytic materials for green fuels: impact of chemical species on Mo-based catalysts for hydrodeoxygenation, RSC Adv 9 (2019) 18292–18301.
[56] M.F. Wagenhofer, E. Baráth, O.Y. Gutiérrez, J.A. Lercher, Carbon−Carbon Bond Scission Pathways in the Deoxygenation of Fatty Acids on Transition-Metal Sulfides, ACS Catal 7 (2017) 1068–1076.
[57] B. Donnis, R.G. Egeberg, P. Blom, K.G. Knudsen, Hydroprocessing of Bio-Oils and Oxygenates to Hydrocarbons. Understanding the Reaction Routes, Top. Catal. 52 (2009) 229–240.
[58] S. Sharifvaghefi, Y. Zheng, Deoxygenation of Stearic Acid with a Novel Ni (Co)-MoS_2/Fe_3S_4 Catalyst, Can. J. Chem. Eng. 96 (2018) 231–240.
[59] P. Arora, E.L. Grennfelt, L. Olsson, D. Creaser, Kinetic study of hydrodeoxygenation of stearic acid as model compound for renewable oils, Chem. Eng. J. 364 (2019) 376–389.
[60] Z. Huang, S. Ding, Z. Li, H. Lin, F. Li, L. Li, Z. Zhong, C. Gao, C. Chen, Y. Li, Catalytic conversion of stearic acid to fuel oil in a hydrogen donor, Int. J. Hydrog. Energy 41 (2016) 16402–16414.
[61] R.W. Gosselink, S.A.W. Hollak, S.W. Chang, J. Van Haveren, K.P. De Jong, J. H. Bitter, D.S. Van Es, Reaction Pathways for the Deoxygenation of Vegetable Oils and Related Model Compounds, ChemSusChem 6 (2013) 1576–1594.
[62] O.İ. Şenol, T.-R. Viljava, A.O.I. Krause, Effect of sulphiding agents on the hydrodeoxygenation of aliphatic esters on sulphided catalysts, Appl. Catal. A Gen. 326 (2007) 236–244.
[63] E.M. Ryymin, M.L. Honkela, T.R. Viljava, A.O.I. Krause, Competitive reactions and mechanisms in the simultaneous HDO of phenol and methyl heptanoate over sulphided NiMo/Al_2O_3, Appl. Catal. A Gen. 389 (2010) 114–121.
[64] E. Laurent, B. Delmon, Study of the hydrodeoxygenation of carbonyl, carboxylic and guaiacyl groups over sulfided CoMo/γ-Al_2O_3 and NiMo/γ-Al_2O_3 catalysts: I. Catalytic reaction schemes, Appl. Catal. A Gen. 109 (1994) 77–96.
[65] O.I. Şenol, T.R. Viljava, A.O.I. Krause, Hydrodeoxygenation of methyl esters on sulphided NiMo/Al_2O_3 and CoMo/Al_2O_3 catalysts, Catal. Today 100 (2005) 331–335.
[66] O.I. Şenol, E.M. Ryymin, T.R. Viljava, A.O.I. Krause, Effect of hydrogen sulphide on the hydrodeoxygenation of aromatic and aliphatic oxygenates on sulphided catalysts, J. Mol. Catal. A Chem. 277 (2007) 107–112.
[67] A.E. Coumans, E.J.M. Hensen, A real support effect on the hydrodeoxygenation of methyl oleate by sulfided NiMo catalysts, Catal. Today 298 (2017) 181–189.
[68] P. Šimáček, D. Kubička, G. Šebor, M. Pospíšil, Fuel properties of hydroprocessed rapeseed oil,, Fuel 89 (2010) 611–615.
[69] P. Šimáček, D. Kubička, G. Šebor, M. Pospíšil, Hydroprocessed rapeseed oil as a source of hydrocarbon-based biodiesel, Fuel 88 (2009) 456–460.
[70] D. Kubička, L. Kaluža, Deoxygenation of vegetable oils over sulfided Ni, Mo and NiMo catalysts, Appl. Catal. A Gen. 372 (2010) 199–208.
[71] D. Kubička, J. Horáček, M. Setnička, R. Bulánek, A. Zukal, I. Kubičková, Effect of support active phase interactions on the catalyst activity and selectivity in deoxygenation of triglycerides, Appl. Catal. B Environ. 145 (2014) 101–107.
[72] M. Toba, Y. Abe, H. Kuramochi, M. Osako, T. Mochizuki, Y. Yoshimura, Hydrodeoxygenation of waste vegetable oil over sulfide catalysts, Catal. Today 164 (2011) 533–537.
[73] H. Wang, G. Li, K. Rogers, H. Lin, Y. Zheng, S. Ng, Hydrotreating of waste cooking oil over supported CoMoS catalyst – Catalyst deactivation mechanism study, Mol. Catal. 443 (2017) 228–240.
[74] J.M. Anthonykutty, J. Linnekoski, A. Harlin, A. Laitinen, J. Lehtonen, Catalytic upgrading of crude tall oil into a paraffin-rich liquid, Biomass Convers, Biorefinery 5 (2015) 149–159.

[75] J.M. Anthonykutty, J. Linnekoski, A. Harlin, J. Lehtonen, Hydrotreating reactions of tall oils over commercial NiMo catalyst, Energy Sci. Eng. 3 (2015) 286–299.
[76] B. Veriansyah, J.Y. Han, S.K. Kim, S.A. Hong, Y.J. Kim, J.S. Lim, Y.W. Shu, S. G. Oh, J. Kim, Production of renewable diesel by hydroprocessing of soybean oil: Effect of catalysts, Fuel 94 (2012) 578–585.
[77] I. Vázquez-Garrido, A. López-Benítez, A. Guevara-Lara, G. Berhault, Synthesis of NiMo catalysts supported on Mn-Al_2O_3 for obtaining green diesel from waste soybean oil, Catal. Today 365 (2021) 327–340.
[78] I. Sebos, A. Matsoukas, V. Apostolopoulos, N. Papayannakos, Catalytic hydroprocessing of cottonseed oil in petroleum diesel mixtures for production of renewable diesel, Fuel 88 (2009) 145–149.
[79] D. Kubička, M. Bejblová, J. Vlk, Conversion of Vegetable Oils into Hydrocarbons over CoMo/MCM-41 Catalysts, Top. Catal. 53 (2010) 168–178.
[80] H. Chen, Q. Wang, X. Zhang, L. Wang, Effect of support on the NiMo phase and its catalytic hydrodeoxygenation of triglycerides, Fuel 159 (2015) 430–435.
[81] A.A. Modenbach, S.E. Nokes, Enzymatic hydrolysis of biomass at high-solids loadings - A review, Biomass Bioenergy 56 (2013) 526–544.
[82] T. Dickerson, J. Soria, Catalytic Fast Pyrolysis: A Review, Energies 6 (2013) 514–538.
[83] D. Bourbiaux, J. Pu, F. Rataboul, L. Djakovitch, C. Geantet, D. Laurenti, Reductive or oxidative catalytic lignin depolymerization: An overview of recent advances, Catal. Today 373 (2021) 24–37.
[84] P. Mäki-Arvela, D. Murzin, Hydrodeoxygenation of Lignin-Derived Phenols: From Fundamental Studies towards Industrial Applications, Catalysts 7 (2017) 265.
[85] C. García-Mendoza, C.E. Santolalla-Vargas, L.G. Woolfolk, P. del Ángel, J.A. de los Reyes, Effect of TiO_2 in supported NiWS catalysts for the hydrodeoxygenation of guaiacol, Catal. Today 377 (2021) 145–156.
[86] Y.K. Hong, D.W. Lee, H.J. Eom, K.Y. Lee, The catalytic activity of *Sulfided* Ni/W/TiO_2 (anatase) for the hydrodeoxygenation of Guaiacol, J. Mol. Catal. A Chem. 392 (2014) 241–246.
[87] J.A. Tavizón-Pozos, V.A. Suárez-Toriello, P. Del Ángel, J.A. De Los Reyes, Hydrodeoxygenation of Phenol Over Sulfided CoMo Catalysts Supported on a Mixed Al_2O_3-TiO_2 Oxide, Int. J. Chem. React. Eng. 14 (2016) 1211–1223.
[88] M. Ferrari, S. Bosmans, R. Maggi, B. Delmon, P. Grange, CoMo/carbon hydrodeoxygenation catalysts: influence of the hydrogen sulfide partial pressure and of the sulfidation temperature, Catal. Today 65 (2001) 257–264.
[89] P.E. Ruiz, B.G. Frederick, W.J. De Sisto, R.N. Austin, L.R. Radovic, K. Leiva, R. García, N. Escalona, M.C. Wheeler, Guaiacol hydrodeoxygenation on MoS_2 catalysts: Influence of activated carbon supports, Catalysis Communications 27 (2012) 44–48.
[90] S. Mukundan, M. Konarova, L. Atanda, Q. Ma, J. Beltramini, Guaiacol hydrodeoxygenation reaction catalyzed by highly dispersed, single layered MoS_2/C, Catal. Sci. Technol. 5 (2015) 4422–4432.
[91] C.C. Templis, C.J. Revelas, A.A. Papastylianou, N.G. Papayannakos, Phenol Hydrodeoxygenation over a Reduced and Sulfided NiMo/γ-Al_2O_3 Catalyst, Ind. Eng. Chem. Res. 58 (2019) 6278–6287.
[92] M. Badawi, J.F. Paul, E. Payen, Y. Romero, F. Richard, S. Brunet, A. Popov, E. Kondratieva, J.P. Gilson, L. Mariey, A. Travert, F. Maugé, Hydrodeoxygenation of Phenolic Compounds by Sulfided (Co)Mo/Al_2O_3 Catalysts, a Combined Experimental and Theoretical Study, Oil Gas. Sci. Technol. 68 (2013) 829–840.
[93] A. Gutierrez, E.M. Turpeinen, T.R. Viljava, O. Krause, Hydrodeoxygenation of model compounds on sulfided CoMo/Al_2O_3 and NiMo/Al_2O_3 catalysts; Role of sulfur-containing groups in reaction networks, Catal. Today 285 (2017) 125–134.
[94] A.L. Jongerius, R. Jastrzebski, P.C.A. Bruijnincx, B.M. Weckhuysen, CoMo sulfide-catalyzed hydrodeoxygenation of lignin model compounds: An extended reaction network for the conversion of monomeric and dimeric substrates, J. Catal. 285 (2012) 315–323.
[95] Y. Romero, F. Richard, S. Brunet, Hydrodeoxygenation of 2-ethylphenol as a model compound of bio-crude over sulfided Mo-based catalysts: Promoting effect and reaction mechanism, Appl. Catal. B Environ. 98 (2010) 213–223.
[96] Y. Yang, A. Gilbert, C. (Charles) Xu, Hydrodeoxygenation of bio-crude in supercritical hexane with sulfided CoMo and CoMoP catalysts supported on MgO: A model compound study using phenol, Appl. Catal. A Gen. 360 (2009) 242–249.
[97] F.E. Massoth, P. Politzer, M.C. Concha, J.S. Murray, J. Jakowski, J. Simons, Catalytic Hydrodeoxygenation of Methyl-Substituted Phenols: Correlations of Kinetic Parameters with Molecular Properties, J. Phys. Chem. B 110 (2006) 14283–14291.
[98] A. Infantes-Molina, B. Pawelec, J.L.G. Fierro, C.V. Loricera, A. Jiménez-López, E. Rodríguez-Castellón, Effect of Ir and Pt Addition on the HDO Performance of RuS_2/SBA-15 Sulfide Catalysts, Top. Catal. 58 (2015) 247–257.
[99] K. Leiva, C. Sepúlveda, R. García, J.L.G. Fierro, N. Escalona, Effect of water on the conversions of 2-methoxyphenol and phenol as bio-oil model compounds over ReS_2/SiO_2 catalyst, Catal. Commun. 53 (2014) 33–37.
[100] K. Leiva, N. Martinez, C. Sepulveda, R. García, C.A. Jiménez, D. Laurenti, M. Vrinat, C. Geantet, J.L.G. Fierro, I.T. Ghampson, N. Escalona, Hydrodeoxygenation of 2-methoxyphenol over different Re active phases supported on SiO_2 catalysts, Appl. Catal. A Gen. 490 (2015) 71–79.
[101] C. Sepúlveda, R. García, P. Reyes, I.T. Ghampson, J.L.G. Fierro, D. Laurenti, M. Vrinat, N. Escalona, Hydrodeoxygenation of guaiacol over ReS_2/activated carbon catalysts. Support and Re loading effect, Appl. Catal. A Gen. 475 (2014) 427–437.
[102] C. Sepúlveda, N. Escalona, R. García, D. Laurenti, M. Vrinat, Hydrodeoxygenation and hydrodesulfurization co-processing over ReS_2 supported catalysts, Catal. Today 195 (2012) 101–105.
[103] P.E. Ruiz, K. Leiva, R. Garcia, P. Reyes, J.L.G. Fierro, N. Escalona, Relevance of sulfiding pretreatment on the performance of Re/ZrO_2 and Re/ZrO_2-sulfated catalysts for the hydrodeoxygenation of guayacol, Appl. Catal. A Gen. 384 (2010) 78–83.
[104] I.B. Adilina, N. Rinaldi, S.P. Simanungkalit, F. Aulia, F. Oemry, G.B.G. Stenning, I. P. Silverwood, S.F. Parker, Hydrodeoxygenation of Guaiacol as a Bio-Oil Model Compound over Pillared Clay-Supported Nickel−Molybdenum Catalysts, J. Phys. Chem. C. 123 (2019) 21429–21439.
[105] K. Wu, Y. Liu, W. Wang, Y. Huang, W. Li, Q. Shi, Y. Yang, Preparation of hydrophobic MoS_2, NiS_2-MoS_2 and CoS_2-MoS_2 for catalytic hydrodeoxygenation of lignin-derived phenols, Mol. Catal. 477 (2019) 110537.
[106] W. Song, S. Zhou, S. Hu, W. Lai, Y. Lian, J. Wang, W. Yang, M. Wang, P. Wang, X. Jiang, Surface Engineering of CoMoS Nanosulfide for Hydrodeoxygenation of Lignin-Derived Phenols to Arenes, ACS Catal 9 (2019) 259–268.
[107] W. Wang, L. Li, K. Wu, G. Zhu, S. Tan, Y. Liu, Y. Yang, Highly selective catalytic conversion of phenols to aromatic hydrocarbons on CoS_2/MoS_2 synthesized using a two step hydrothermal method, RSC Adv 6 (2016) 31265–31271.
[108] B. Yoosuk, D. Tumnantong, P. Prasassarakich, Unsupported MoS_2 and $CoMoS_2$ catalysts for hydrodeoxygenation of phenol, Chem. Eng. Sci. 79 (2012) 1–7.
[109] B. Yoosuk, D. Tumnantong, P. Prasassarakich, Amorphous unsupported Ni–Mo sulfide prepared by one step hydrothermal method for phenol hydrodeoxygenation, Fuel 91 (2012) 246–252.
[110] Y.Q. Yang, C.T. Tye, K.J. Smith, Influence of MoS_2 catalyst morphology on the hydrodeoxygenation of phenols, Catal. Commun. 9 (2008) 1364–1368.
[111] C.C. Tran, F. Stankovikj, M. Garcia-Perez, S. Kaliaguine, Unsupported transition metal-catalyzed hydrodeoxygenation of guaiacol, Catalysis Communications 101 (2017) 71–76.
[112] W. Wang, K. Zhang, L. Li, K. Wu, P. Liu, Y. Yang, Synthesis of Highly Active Co−Mo−S Unsupported Catalysts by a One-Step Hydrothermal Method for p-Cresol Hydrodeoxygenation, Ind. Eng. Chem. Res. 53 (2014) 19001–19009.
[113] W. Wang, K. Zhang, Z. Qiao, L. Li, P. Liu, Y. Yang, Hydrodeoxygenation of p-cresol on unsupported Ni–W–Mo–S catalysts prepared by one step hydrothermal method, Catal. Commun. 56 (2014) 17–22.
[114] C. Wang, D. Wang, Z. Wu, Z. Wang, C. Tang, P. Zhou, Effect of W addition on the hydrodeoxygenation of 4-methylphenol over unsupported NiMo sulfide catalysts, Appl. Catal. A Gen. 476 (2014) 61–67.
[115] C. Wang, Z. Wu, C. Tang, L. Li, D. Wang, The effect of nickel content on the hydrodeoxygenation of 4-methylphenol over unsupported NiMoW sulfide catalysts, Catal. Commun. 32 (2013) 76–80.
[116] V.M.L. Whiffen, K.J. Smith, Hydrodeoxygenation of 4-Methylphenol over Unsupported MoP, MoS_2, and MoO_x Catalysts, Energy & Fuels 24 (2010) 4728–4737.
[117] W. Wang, L. Li, K. Zhang, Z. Qiao, P. Liu, Y. Yang, Hydrodeoxygenation of p-cresol on MoS_2: the effect of adding hexadecyl trimethyl ammonium bromide during the catalyst synthesis, React. Kinet. Mech. Catal. 113 (2014) 417–429.
[118] W. Wang, L. Li, K. Wu, K. Zhang, J. Jie, Y. Yang, Preparation of Ni–Mo–S catalysts by hydrothermal method and their hydrodeoxygenation properties, Appl. Catal. A Gen. 495 (2015) 8–16.
[119] X. Guo, W. Wang, K. Wu, Y. Huang, Q. Shi, Y. Yang, Preparation of Fe promoted MoS_2 catalysts for the hydrodeoxygenation of p-cresol as a model compound of lignin-derived bio-oil, Biomass Bioenergy 125 (2019) 34–40.
[120] X. Liu, X. Hou, Y. Zhang, H. Yuan, X. Hong, G. Liu, In Situ Formation of CoMoS Interfaces for Selective Hydrodeoxygenation of p-Cresol to Toluene, Ind. Eng. Chem. Res. 59 (2020) 15921–15928.
[121] J. Cao, A. Li, Y. Zhang, L. Mu, X. Huang, Y. Li, T. Yang, C. Zhang, C. Zhou, Highly efficient unsupported Co-doped nano-MoS_2 catalysts for p-cresol hydrodeoxygenation, Mol. Catal. 505 (2021) 111507.
[122] K. Wu, W. Wang, H. Guo, Y. Yang, Y. Huang, W. Li, C. Li, Engineering Co Nanoparticles Supported on Defect MoS_{2-x} for Mild Deoxygenation of Lignin-Derived Phenols to Arenes, ACS Energy Lett 5 (2020) 1330–1336.
[123] W. Wang, L. Li, K. Wu, G. Zhu, S. Tan, W. Li, Y. Yang, Hydrothermal synthesis of bimodal mesoporous MoS_2 nanosheets and their hydrodeoxygenation properties, RSC Adv 5 (2015) 61799–61807.
[124] W. Wang, S. Tan, K. Wu, G. Zhu, Y. Liu, L. Tan, Y. Huang, Y. Yang, Hydrodeoxygenation of p-cresol as a model compound for bio-oil on MoS_2: Effects of water and benzothiophene on the activity and structure of catalyst, Fuel 214 (2018) 480–488.
[125] W. Wang, L. Li, S. Tan, K. Wu, G. Zhu, Y. Liu, Y. Xu, Y. Yang, Preparation of NiS_2//MoS_2 catalysts by two-step hydrothermal method and their enhanced activity for hydrodeoxygenation of p-cresol, Fuel 179 (2016) 1–9.
[126] S. Gillet, M. Aguedo, L. Petitjean, A.R.C. Morais, A.M. Da Costa Lopes, R. M. Łukasik, P.T. Anastas, Lignin transformations for high value applications: towards targeted modifications using green chemistry, Green, Chem 19 (2017) 4200.
[127] J. He, L. Lu, C. Zhao, D. Mei, J.A. Lercher, Mechanisms of catalytic cleavage of benzyl phenyl ether in aqueous and apolar phases, J. Catal. 311 (2014) 41–51.
[128] Z. Luo, C. Zhao, Mechanistic insights into selective hydrodeoxygenation of lignin-derived β-O-4 linkage to aromatic hydrocarbons in water, Catal. Sci. Technol. 6 (2016) 3476–3484.
[129] M. Koyama, Hydrocracking of lignin-related model dimers, Bioresour. Technol. 44 (1993) 209–215.
[130] L. Shuai, J. Sitison, S. Sadula, J. Ding, M.C. Thies, B. Saha, Selective C−C Bond Cleavage of Methylene-Linked Lignin Models and Kraft Lignin, ACS Catal 8 (2018) 6507–6512.
[131] M.A. Salam, P. Arora, H. Ojagh, Y.W. Cheah, L. Olsson, D. Creaser, NiMoS on alumina-USY zeolites for hydrotreating lignin dimers: Effect of support acidity and cleavage of C-C bonds, Sustain, Energy Fuels 4 (2019) 149–163.

[132] M.A. Salam, Y.W. Cheah, P.H. Ho, L. Olsson, D. Creaser, Hydrotreatment of lignin dimers over NiMoS-USY: effect of silica/alumina ratio, Sustain. Energy Fuels 5 (2021) 3445–3457.
[133] W. Song, W. Lai, Y. Lian, X. Jiang, W. Yang, Sulfated ZrO_2 supported CoMo sulfide catalyst by surface exsolution for enhanced hydrodeoxygenation of lignin-derived ethers to aromatics, Fuel 263 (2020) 116705.
[134] N. Ji, X. Wang, C. Weidenthaler, B. Spliethoff, R. Rinaldi, Iron(II) Disulfides as Precursors of Highly Selective Catalysts for Hydrodeoxygenation of Dibenzyl Ether into Toluene, ChemCatChem 7 (2015) 960–966.
[135] C. Zhang, J. Lu, X. Zhang, K. Macarthur, M. Heggen, H. Li, F. Wang, Cleavage of the lignin β-O-4 ether bond via a dehydroxylation–hydrogenation strategy over a NiMo sulfide catalyst, Green, Chem 18 (2016) 6545–6555.
[136] C. Zhang, H. Li, J. Lu, X. Zhang, K.E. Macarthur, M. Heggen, F. Wang, Promoting Lignin Depolymerization and Restraining the Condensation via an Oxidation−Hydrogenation Strategy, ACS Catal 7 (2017) 3419–3429.
[137] B. Shumeiko, M. Auersvald, P. Straka, P. Šimáček, D. Vrtiška, D. Kubička, Efficient One-Stage Bio-Oil Upgrading over Sulfided Catalysts, ACS Sustain. Chem. Eng. 8 (2020) 15149–15167.
[138] N. Priharto, F. Ronsse, W. Prins, I. Hita, P.J. Deuss, H.J. Heeres, Hydrotreatment of pyrolysis liquids derived from second-generation bioethanol production residues over NiMo and CoMo catalysts, Biomass Bioenergy 126 (2019) 84–93.
[139] S. Izhar, S. Uehara, N. Yoshida, Y. Yamamoto, T. Morioka, M. Nagai, Hydrodenitrogenation of fast pyrolysis bio-oil derived from sewage sludge on $NiMo/Al_2O_3$ sulfide catalyst, Fuel Process. Technol. 101 (2012) 10–15.
[140] H. Luo, M.M. Abu-Omar, Chemicals From Lignin, Encyclopedia of Sustainable Technologies, 3, (2017).
[141] P. Azadi, O.R. Inderwildi, R. Farnood, D.A. King, Liquid fuels, hydrogen and chemicals from lignin: A critical review, Renew. Sustain. Energy Rev. 21 (2013) 506–523.
[142] A.K. Deepa, P.L. Dhepe, Lignin Depolymerization into Aromatic Monomers over Solid Acid Catalysts, ACS Catal 5 (2015) 365–379.
[143] A. Wang, P. He, H. Song. Chapter 6. Lignin Valorization, Recent Advances in Bioconversion of Lignocellulose to Biofuels and Value-Added Chemicals within the Biorefinery Concept, 2020, pp. 133–152.
[144] M.P. Pandey, C.S. Kim, Lignin Depolymerization into Aromatic Monomers over Solid Acid Catalysts, Chem. Eng. Technol. 34 (2011) 29–41.
[145] N. Zhou, W.P.D.W. Thilakarathna, Q.S. He, H.P.V. Rupasinghe, A Review: Depolymerization of Lignin to Generate High-Value Bio-Products: Opportunities, Challenges, and Prospects, Front. Energy Res. 9 (2022) 1–18.
[146] X. Diao, N. Ji, Rational design of MoS_2-based catalysts toward lignin hydrodeoxygenation: Interplay of structure, catalysis, and stability, Journal of Energy Chemistry 77 (2023) 601–631.
[147] H. Wang, M. Tucker, Y. Ji, Recent Development in Chemical Depolymerization of Lignin: A Review, J. Appl. Chem. 2013 (2013) 1–9.
[148] C. Xu, R.A.D. Arancon, J. Labidi, R. Luque, Lignin depolymerisation strategies: towards valuable chemicals and fuels, Chem. Soc. Rev. 43 (2014) 7485–7500.
[149] C. Li, X. Zhao, A. Wang, G.W. Huber, T. Zhang, Catalytic Transformation of Lignin for the Production of, Chemicals and Fuels, Chem. Rev. 115 (2015) 11559–11624.
[150] Z. Sun, B. Fridrich, A. De Santi, S. Elangovan, K. Barta, Bright Side of Lignin Depolymerization: Toward New Platform Chemicals, Chem. Rev. 118 (2018) 614–678.
[151] R. Roy, M.S. Rahman, T.A. Amit, B. Jadhav, Recent Advances in Lignin Depolymerization Techniques: A Comparative Overview of Traditional and Greener Approaches, Biomass 2 (2022) 130–154.
[152] R.K. Chowdari, S. Agarwal, H.J. Heeres, Hydrotreatment of Kraft Lignin to Alkylphenolics and Aromatics Using Ni, Mo, and W Phosphides Supported on Activated Carbon, ACS Sustain. Chem. Eng. 7 (2019) 2044–2055.
[153] B.A. Vuori, J.B. Bredenberg, Liquefaction of Kraft Lignin, Holzforschung 42 (1988) 155–161.
[154] D. Raikwar, S. Majumdar, D. Shee, Effects of solvents in the depolymerization of lignin into value-added products: a review, Biomass Conversion and Biorefinery (2021).
[155] U. Schuchardt, O.A. Marangoni Borges, Direct liquefaction of hydrolytic eucalyptus lignin in the presence of sulphided iron catalysts, Catal. Today 5 (4) (1989) 523–531.
[156] B. Joffres, M.T. Nguyen, D. Laurenti, C. Lorentz, V. Souchon, N. Charon, A. Daudin, A. Quignard, C. Geantet, Lignin hydroconversionon MoS_2-based supported catalyst: Comprehensive analysis of products and reaction scheme, Appl. Catal. B Environ. 184 (2016) 153–162.
[157] B. Joffres, C. Lorentz, M. Vidalie, D. Laurenti, A.A. Quoineaud, N. Charon, A. Daudin, A. Quignard, C. Geantet, Catalytic hydroconversion of a wheat straw soda lignin: Characterization of the products and the lignin residue, Appl. Catal. B Environ. 145 (2014) 167–176.
[158] J. Horáček, F. Homola, I. Kubičková, D. Kubička, Lignin to liquids over sulfided catalysts, Catal. Today 179 (2012) 191–198.
[159] J. Pu, T.S. Nguyen, E. Leclerc, C. Lorentz, D. Laurenti, I. Pitault, M. Tayakout-Fayolle, C. Geantet, Lignin catalytic hydroconversion in a semi-continuous reactor: An experimental study, Appl. Catal. B Environ. 256 (2019) 117769.
[160] D. Meier, J. Berns, O. Faix, U. Balfanz, W. Baldauf, HYDROCRACKING OF ORGANOCELL LIGNIN FOR PHENOL PRODUCTION, Biomass and Bioenergy 7 (1994) 99–105.
[161] C.R. Kumar, N. Anand, A. Kloekhorst, C. Cannilla, G. Bonura, F. Frusteri, K. Barta, H.J. Heeres, Solvent free depolymerization of Kraft lignin to alkyl-phenolics using supported NiMo and CoMo catalysts, Green, Chem 17 (2015) 4921.
[162] A. Oasmaa, R. Alén, D. Meier, Catalytic hydrotreatment of some technical lignins, Bioresource Tech 45 (3) (1993) 189–194.
[163] N. Li, L. Wei, R. bibi, L. Chen, J. Liu, L. Zhang, Y. Zheng, J. Zhou, Catalytic hydrogenation of alkali lignin into bio-oil using flower-like hierarchical MoS_2-based composite catalysts, Fuel 185 (2016) 532–540.
[164] F.L. Pua, C.H. Chia, S. Zakaria, S.K. Neoh, T.K. Liew, Nano Transition Metal Sulfide Catalyst for Solvolysis Liquefaction of Soda Lignin, Sains Malaysiana 40 (2011) 221–226.
[165] Q. Tian, N. Li, J. Liu, M. Wang, J. Deng, J. Zhou, Q. Ma, Catalytic Hydrogenation of Alkali Lignin to Bio-oil Using Fullerene-like Vanadium Sulfide, Energy & Fuels 29 (2015) 255–261.
[166] A. Narani, R.K. Chowdari, C. Cannilla, G. Bonura, F. Frusteri, H.J. Heeres, K. Barta, Efficient catalytic hydrotreatment of Kraft lignin to alkylphenolics using supported NiW and NiMo catalysts in supercritical methanol, Green Chem 17 (2015) 5046.
[167] R.K. Sharma, M. Anand, B.S. Rana, R. Kumar, S.A. Farooqui, M.G. Sibi, A.K. Sinha, Jatropha-oil conversion to liquid hydrocarbon fuels using mesoporous titanosilicate supported sulfide catalysts, Catal Today 198 (2012) 314–320.
[168] B. Hočevar, M. Grilc, M. Huš, B. Likozar, Mechanism, *ab initio* calculations and microkinetics of straight-chain alcohol, ether, ester, aldehyde and carboxylic acid hydrodeoxygenation over Ni-Mo catalyst, Chem. Eng. J. 359 (2019) 1339–1351.
[169] B.S. Gevert, J.-E. Otterstedt, F.E. Massoth, Kinetics of the HDO of methyl-substituted phenols, Appl. Catal. 31 (1987) 119–131.
[170] K. Leiva, C. Sepulveda, R. García, D. Laurenti, M. Vrinat, C. Geantet, N. Escalona, Kinetic study of the conversion of 2-methoxyphenol over supported Re catalysts: Sulfide and oxide state, Appl. Catal. A Gen. 505 (2015) 302–308.
[171] V.O.O. Gonçalves, S. Brunet, F. Richard, Hydrodeoxygenation of Cresols Over Mo/Al_2O_3 and $CoMo/Al_2O_3$ Sulfided Catalysts, Catal. Lett. 146 (2016) 1562–1573.
[172] G. Liu, A.W. Robertson, M.M.J. Li, W.C.H. Kuo, M.T. Darby, M.H. Muhieddine, Y. C. Lin, K. Suenaga, M. Stamatakis, J.H. Warner, S.C.E. Tsang, MoS_2 monolayer catalyst doped with isolated Co atoms for the hydrodeoxygenation reaction, Nat. Chem. 9 (2017) 810–816.
[173] Y.W. Cheah, M.A. Salam, P. Arora, O. Öhrman, D. Creaser, L. Olsson, Role of transition metals on MoS_2-based supported catalysts for hydrodeoxygenation (HDO) of propylguaiacol, Sustain Energy Fuels 5 (2021) 2097–2113.
[174] J. Pu, D. Laurenti, C. Geantet, M. Tayakout-Fayolle, I. Pitault, Kinetic modeling of lignin catalytic hydroconversion in a semi-batch reactor, Chem. Eng. J. 386 (2020) 122067.
[175] M. Grilc, B. Likozar, J. Levec, Hydrodeoxygenation and hydrocracking of solvolysed lignocellulosic biomass by oxide, reduced and sulphide form of NiMo, Ni, Mo and Pd catalysts, Appl. Catal. B Environ. 150–151 (2014) 275–287.
[176] M. Grilc, G. Veryasov, B. Likozar, A. Jesih, J. Levec, Hydrodeoxygenation of solvolysed lignocellulosic biomass by unsupported MoS_2, MoO_2, Mo_2C and WS_2 catalysts, Appl. Catal. B Environ. 163 (2015) 467–477.
[177] M. Grilc, B. Likozar, J. Levec, Simultaneous Liquefaction and Hydrodeoxygenation of Lignocellulosic Biomass over $NiMo/Al_2O_3$, Pd/Al_2O_3, and Zeolite Y Catalysts in Hydrogen Donor Solvents, ChemCatChem 8 (2016) 180–191.
[178] C.H. Bartholomew, Mechanisms of catalyst deactivation, Appl. Catal. A Gen. 212 (2001) 17–60.
[179] M. Badawi, J.F. Paul, S. Cristol, E. Payen, Y. Romero, F. Richard, S. Brunet, D. Lambert, X. Portier, A. Popov, E. Kondratieva, J.M. Goupil, J. El Fallah, J. P. Gilson, L. Mariey, A. Travert, F. Maugé, Effect of water on the stability of Mo and CoMo hydrodeoxygenation catalysts: A combined experimental and DFT study, J. Catal. 282 (2011) 155–164.
[180] P.M. Mortensen, D. Gardini, C.D. Damsgaard, J.D. Grunwaldt, P.A. Jensen, J. B. Wagner, A.D. Jensen, Deactivation of Ni-MoS_2 by bio-oil impurities during hydrodeoxygenation of phenol and octanol, Appl. Catal. A Gen. 523 (2016) 159–170.
[181] F. Pedraza, S. Fuentes, M. Vrinat, M. Lacroix, Deactivation of MoS_2 catalysts during the HDS of thiophene, Catal. Lett. 62 (1999) 121–126.
[182] B. Guichard, M. Roy-Auberger, E. Devers, C. Legens, P. Raybaud, Aging of Co(Ni) MoP/Al_2O_3 catalysts in working state, Catal. Today 130 (2008) 97–108.
[183] M. Badawi, J.F. Paul, S. Cristol, E. Payen, Guaiacol derivatives and inhibiting species adsorption over MoS_2 and CoMoS catalysts under HDO conditions: A DFT study, Catal. Commun. 12 (2011) 901–905.
[184] P.M. Train, M.T. Klein, Hydroprocessing lignin and lignin model compounds: Products, Kinetics, and Catalyst aging, Fuel Science and Technology 9 (2) (1991) 193–227.
[185] D. Kubička, J. Horáček, Deactivation of HDS catalysts in deoxygenation of vegetable oils, Appl. Catal. A Gen. 394 (2011) 9–17.
[186] G.H.C. Prado, Y. Rao, A. De Klerk, Nitrogen Removal from Oil: A Review, Energy & Fuels 31 (2017) 14–36.
[187] A. Pimerzin, A. Savinov, A. Vutolkina, A. Makova, A. Glotov, V. Vinokurov, A. Pimerzin, Transition Metal Sulfides- and Noble Metal-Based Catalysts for N-Hexadecane Hydroisomerization: A Study of Poisons Tolerance, Catalysts 10 (2020) 594.
[188] M. Meena, S. Antony, F. Edward, Chapter 4 - Catalyst Deactivation, Handbook of Spent Hydroproessing Catalysts, 2010.
[189] A. Pinheiro, D. Hudebine, N. Dupassieux, C. Geantet, Impact of Oxygenated Compounds from Lignocellulosic Biomass Pyrolysis Oils on Gas Oil Hydrotreatment, Energy & Fuels 23 (2009) 1007–1014.
[190] J.H. Koh, J.J. Lee, H. Kim, A. Cho, S.H. Moon, Correlation of the deactivation of $CoMo/Al_2O_3$ in hydrodesulfurization with surface carbon species, Appl. Catal. B Environ. 86 (2009) 176–181.
[191] M. Guisnet, P. Magnoux, Organic chemistry of coke formation, Appl. Catal. A Gen. 212 (2001) 83–96.

[192] C. Glasson, C. Geantet, M. Lacroix, F. Labruyere, P. Dufresne, Beneficial Effect of Carbon on Hydrotreating Catalysts, J. Catal. 212 (2002) 76–85.
[193] K.H. Kang, G.T. Kim, S. Park, P.W. Seo, H. Seo, C.W. Lee, A review on the Mo-precursors for catalytic hydroconversion of heavy oil, J. Ind. Eng. Chem. 76 (2019) 1–16.
[194] G. Berhault, A. Mehta, A.C. Pavel, J. Yang, L. Rendon, M.J. Yácaman, L.C. Araiza, A.D. Moller, R.R. Chianelli, The Role of Structural Carbon in Transition Metal Sulfides Hydrotreating Catalysts, J. Catal. 198 (2001) 9–19.
[195] A. Ochoa, J. Bilbao, A.G. Gayubo, P. Castaño, Coke formation and deactivation during catalytic reforming of biomass and waste pyrolysis products: A review, Renew. Sustain. Energy Rev. 119 (2020) 109600.
[196] S. Eijsbouts, On the flexibility of the active phase in hydrotreating catalysts, Appl. Catal. A Gen. 158 (1997) 53–92.
[197] B.M. Vogelaar, P. Steiner, A. Dick van Langeveld, S. Eijsbouts, J.A. Moulijn, Deactivation of Mo/Al_2O_3 and $NiMo/Al_2O_3$ catalysts during hydrodesulfurization of thiophene, Appl. Catal. A Gen. 251 (2003) 85–92.
[198] C. Leyva, J. Ancheyta, A. Travert, F. Maugé, L. Mariey, J. Ramírez, M.S. Rana, Activity and surface properties of $NiMo/SiO_2–Al_2O_3$ catalysts for hydroprocessing of heavy oils, Appl. Catal. A Gen. 425–426 (2012) 1–12.
[199] E. Furimsky, F.E. Massoth, Deactivation of hydroprocessing catalysts, Catalysis Today 52 (1999) 381–495.
[200] A. Popov, E. Kondratieva, L. Mariey, J.M. Goupil, J. El Fallah, J.P. Gilson, A. Travert, F. Maugé, Bio-oil hydrodeoxygenation: Adsorption of phenolic compounds on sulfided (Co)Mo catalysts, J. Catal. 297 (2013) 176–186.
[201] A. Popov, E. Kondratieva, J.P. Gilson, L. Mariey, A. Travert, F. Maugé, IR study of the interaction of phenol with oxides and sulfided CoMo catalysts for bio-fuel hydrodeoxygenation, Catal. Today 172 (2011) 132–135.
[202] T. Cordero-Lanzac, R. Palos, I. Hita, J.M. Arandes, J. Rodríguez-Mirasol, T. Cordero, J. Bilbao, P. Castaño, Revealing the pathways of catalyst deactivation by coke during the hydrodeoxygenation of raw bio-oil, Appl. Catal. B Environ. 239 (2018) 513–524.
[203] X. Liu, X. Fan, Q. Wei, Y. Zhou, Theoretical investigation of the edge substitution of Co-(Ni-)MoS_2 by water during hydrodeoxygenation, Appl. Catal. A Gen. 648 (2022) 118919.
[204] X. Diao, N. Ji, X. Li, Y. Rong, Y. Zhao, X. Lu, C. Song, C. Liu, G. Chen, L. Ma, S. Wang, Q. Liu, C. Li, Fabricating high temperature stable $Mo-Co_9S_8/Al_2O_3$ catalyst for selective hydrodeoxygenation of lignin to arenes, Appl. Catal. B Environ. 305 (2022) 121067.
[205] L.I. Al-Ali, O. Elmutasim, K. Al Ali, N. Singh, K. Polychronopoulou, Transition Metal Phosphides (TMP) as a Versatile Class of Catalysts for the Hydrodeoxygenation Reaction (HDO) of Oil-Derived Compounds, Nanomaterials 12 (2022) 1435.
[206] F. Morteo-Flores, A. Roldan, Mechanisms and Trends of Guaiacol Hydrodeoxygenation on Transition Metal Catalysts, Front. Catal. 2 (2022) 1–12.
[207] C. Liu, H. Tao, C. Lian, H. Liu, Molecular Insights into Guaiacols Hydrodeoxygenation on Nickel Nanoparticle Surfaces, J. Phys. Chem. C. 126 (2022) 9724–9735.
[208] J.N.D. de León, C.R. Kumar, J. Antúnez-García, S. Fuentes-Moyado, Recent Insights in Transition Metal Sulfide Hydrodesulfurization Catalysts for the Production of Ultra Low Sulfur Diesel: A Short Review, Catalysts 9 (2019) 87.
[209] 'Fit for 55': delivering the EU's 2030 Climate Target on the Way to Climate Neutrality European Comission 2021."Fit for 55″: Delivering the EU's 2030Climate Target on the Way to Climate Neutrality, 2021.
[210] S. Jin, Z. Xiao, C. Li, X. Chen, L. Wang, J. Xing, W. Li, C. Liang, Catalytic hydrodeoxygenation of anisole as lignin model compound over supported nickel catalysts, Catal. Today 234 (2014) 125–132.
[211] K. Kohli, R. Prajapati, S.K. Maity, B.K. Sharma, Effect of Silica, Activated Carbon, and Alumina Supports on NiMo Catalysts for Residue Upgrading, Energies 13 (2020) 1–16.
[212] L. Wang, F.S. Xiao, Nanoporous catalysts for biomass conversion, Green Chem 17 (2015) 24–39.
[213] S. Eijsbouts, S.W. Mayo, K. Fujita, Unsupported transition metal sulfide catalysts: From fundamentals to industrial application, Appl. Catal. A, Gen. 322 (2007) 58–66.
[214] F.L. Plantenga, R. Cerfontain, S. Eijsbouts, F. Van Houtert, G.H. Anderson, S. Miseo, S. Soled, K. Riley, K. Fujita, Y. Inoue, NEBULA": A Hydroprocessing Catalyst with Breakthrough Activity, Science and Technology in Catalysis 89 (2002) 846–849.
[215] G. Bellussi, G. Rispoli, A. Landoni, R. Millini, D. Molinari, E. Montanari, D. Moscotti, P. Pollesel, Hydroconversion of heavy residues in slurry reactors: Developments and perspectives, J. Catal. 308 (2013) 189–200.
[216] P. Raybaud, Understanding and predicting improved sulfide catalysts: Insights from *first principles* modeling, Appl. Catal. A Gen. 322 (2007) 76–91.
[217] X. Liu, Q. Wei, W. Huang, Y. Zhou, P. Zhang, Z. Xu, DFT insights into the stacking effects on HDS of 4,6-DMDBT on Ni-Mo-S corner sites, Fuel 280 (2020) 118669.
[218] C. Sattayanon, S. Namuangruk, N. Kungwan, M. Kunaseth, Reaction and free-energy pathways of hydrogen activation on partially promoted metal edge of CoMoS and NiMoS: A DFT and thermodynamics study, Fuel Process. Technol. 166 (2017) 217–227.
[219] P. Zheng, T. Li, K. Chi, C. Xiao, J. Fan, X. Wang, A. Duan, DFT insights into the formation of sulfur vacancies over corner/edge site of Co/Ni-promoted MoS_2 and WS_2 under the hydrodesulfurization conditions, Appl. Catal. B Environ. 257 (2019) 117937.
[220] M. Ruinart De Brimont, C. Dupont, A. Daudin, C. Geantet, P. Raybaud, Deoxygenation mechanisms on Ni-promoted MoS_2 bulk catalysts: A combined experimental and theoretical study, J. Catal. 286 (2012) 153–164.
[221] N. Bergvall, L. Sandström, Y.W. Cheah, O.G.W. Öhrman, Slurry Hydroconversion of Solid Kraft Lignin to Liquid Products Using Molybdenum- and Iron-Based Catalysts, Energy & Fuels 36 (2022) 10226–10242.
[222] M. Abdus Salam, Y. Wayne Cheah, P. Hoang Ho, D. Bernin, A. Achour, E. Nejadmoghadam, O. Öhrman, P. Arora, L. Olsson, D. Creaser, Elucidating the role of NiMoS-USY during the hydrotreatment of Kraft lignin, Chem. Eng. J. 442 (2022) 136216.
[223] A. Achour, D. Bernin, D. Creaser, L. Olsson, Evaluation of kraft and hydrolysis lignin hydroconversion over unsupported NiMoS catalyst, Chem. Eng. J. 453 (2022) 139829.